UNIVERSITAT DE BARCELONA

Effects of CO2 and long day length on primary productivity in the Arctic Ocean: a perspective on climate change

Efectos del CO2 y largos fotoperiodos en la productividad primaria del Océano Ártico: una perspectiva sobre el cambio climático

Marina Sanz Martín

Effects of CO_2 and long day length on primary productivity in the Arctic Ocean: a perspective on climate change

Marina Sanz Martín

Thesis 2018

UNIVERSITAT DE BARCELONA

Effects of CO_2 and long day length on primary productivity in the Arctic Ocean: a perspective on climate change

Efectos del CO_2 y largos fotoperiodos en la productividad primaria del Océano Ártico: una perspectiva sobre el cambio climático

A dissertation presented by Marina Sanz Martín, BSc, MSc
to fulfill the requirements for the degree of Doctor of Philosophy (Ph.D) in the Marine Science Program

Thesis supervisor:
Carlos M. Duarte,
King Abdullah University of Science and Technology

Thesis co-supervisor:
Paul F. Wassmann,
The Arctic University of Norway

Thesis tutor: Miquel Canals, University of Barcelona

Marina Sanz Martín

15 January 2018

Cover image credit: Maria L. Paulsen.
Broken sea ice at the NW Svalbard shelf.
Printed in Palma de Mallorca, Spain. January 2018.

To Johnna, Iris and Aurore

Take a breath.

Half of the oxygen that you have just taken is
produced by marine plants: phytoplankton,
macroalgae, and seagrasses.

– Prof. John Beardall

Scientific environment

This Ph.D. was funded by 'Fundación La Caixa' (2013-2017) and was carried out at Department of Global Change in the Mediterranean Institute of Advanced Studies (IMEDEA-CSIC/UIB). The work was mainly part of the project 'Carbon Bridge' funded by the Norwegian Research Council (RCN 226415), the project 'Efecte del canvi global sobre els ecosistemes marins' funded by the University of Balearic Islands in cooperation with the Greenland Institute of Natural Resources (GINR) and the Danish Environmental Protection Agency within the Danish Cooperation for Environment in the Arctic program.

Obra Social
Fundación "la Caixa"

Bridging productivity regimes in the Arctic Ocean
CarbonBridge
UiT - The Arctic University of Norway

IMEDEA
CSIC UIB

EFECTE DEL CANVI GLOBAL SOBRE ELS ECOSISTEMES MARINS

Grønlands Naturinstitut

Danish Ministry of the Environment
Environmental Protection Agency

Contents

Abstract

Climate change, caused by anthropogenic emissions of carbon dioxide (CO_2) and other greenhouse gasses into the atmosphere, is producing profound impacts on ecosystems. The Arctic Ocean is one of the most vulnerable regions of the world and is experiencing the most substantial effects of climate change. This region is characterized by strong seasonality with highly productive episodes, called phytoplankton blooms, that together with the entrance of ice-melt, reduce the CO_2 concentration in seawater (from about 370 to 130 μatm). During spring and summer, the low CO_2 concentrations might limit the photosynthesis of marine plants and algae. However, during these periods the increase of atmospheric and oceanic CO_2 may stimulate the primary productivity in the Arctic Ocean.

Increased atmospheric CO_2 is directly related with Arctic warming and the consequent acceleration of glaciers and sea-ice melting. During spring and summer, the ice cover retreat increases the light irradiance in submersed areas and ice-free areas become more frequent. An increase of ice-free waters may probably favour the expansion of marine vegetation into the Arctic and the migration of subarctic species to northern regions, characterized by long day length in summer.

Since pelagic and benthic ecosystems contribute largely to the primary productivity of the Arctic Ocean, in this thesis I investigate the experimental effects of two abiotic factors: increased CO_2 and long day length. These effects have been tested on planktonic communities in surface waters and benthic macrophytes in subarctic and Arctic ecosystems. In parallel, I investigate the relationship between planktonic primary production rates estimated with three different methods: the O_2 mass balance, the ^{18}O method and the ^{14}C method. This comparison of methods has been carried out for the first time in the Arctic Ocean, specifically in the north and northwest of the Svalbard shelf, and we conclude that the ^{14}C method, with incubations of 24 h, underestimate the gross primary productivity measured with the O_2-based methods, although the relationships change seasonally. In spring, the O_2-based methods are the most appropriate methods to estimate the gross primary productivity while in summer both C and O_2-based method are adequate. Therefore, the O_2-based methods were applied to investigate the possible

limitation of CO_2 in planktonic communities in two regions of the Arctic Ocean. With this aim, we carried out experiments of CO_2 additions in spring and summer in the west and northwest of the Svalbard shelf and observed that the stimulation was restricted to highly productive episodes, when CO_2 concentrations were already low and nutrients concentrations were low but still present in seawater.

To determine the periods of CO_2 limitation, I carried out weekly experiments of increased CO_2 during the development of a phytoplankton bloom, from March to late May in 2016 in Godthåbsfjord, southwestern of Greenland. We observed that during approximately two weeks after the bloom reached its maximum production, called the *peak bloom stage*, the phytoplankton community was limited by the low CO_2 concentrations. During this window of time the net primary production rates increased with increasing CO_2 concentrations in presence of dissolved inorganic nutrients.

Additionally, we experimentally evaluated the effects of long day length, characteristic of Arctic summers, and the effect of increased CO_2. on three subarctic macrophytes species: *Ascophyllum nodosum*, *Fucus vesiculosus* and *Zostera marina*. We observed that their photosynthetic activity, measured as the electron transport rate, were highest at long day length. Increased CO_2 also had a positive, though non-significant effect on the macroalgae species *A. nodosum* and on the seagrass *Z. marina*. Therefore, these species will benefit from increased day length as they expand in the Arctic and migrate poleward with decreasing ice cover.

The results of the present thesis suggest that present and future increases of CO_2 concentrations are likely to enhance the contribution of the spring bloom to the annual primary production budget in Arctic and subarctic waters. Moreover, long day length will benefit the expansion and poleward migration of the subarctic species investigated. In this thesis, I present experimental evidence of the effects of climate change in pelagic and benthic ecosystems in two regions of the Arctic Ocean, contributing to the field of climate change ecology in the marine environment. Besides, the comparative study of primary production methodologies contributes to the field of Arctic oceanography by which aids in developing further investigation and expectations conducive to forming conclusions on how climate change will affect the Arctic Ocean in the future.

Resumen

El cambio climático, causado por la emisión antropogénica de dióxido de carbono (CO_2) y otros gases de efecto invernadero a la atmósfera, está produciendo grandes cambios en los ecosistemas. El Océano Ártico es una de las regiones más vulnerables del mundo y por ello en esta región se están produciendo cambios sustanciales. El Ártico se caracteriza por una fuerte estacionalidad con episodios altamente productivos, llamados floraciones o *blooms* de fitoplancton, que, junto con la entrada de agua de deshielo, reducen la concentración de CO_2 en el agua de mar (de 370 a 130 µatm aproximadamente). Durante primavera y verano, las bajas concentraciones de CO_2 pueden limitar la fotosíntesis de plantas y algas marinas. Sin embargo, durante estos periodos, el aumento global de CO_2 atmosférico y oceánico podría estimular la producción primaria en aguas árticas y subárticas.

El aumento de CO_2 atmosférico está directamente relacionado el calentamiento del Ártico y la consecuente aceleración de la pérdida de glaciares y hielo marino. El retroceso de la cubierta de hielo en primavera y en verano está aumentado la entrada de luz en zonas sumergidas, y las zonas libres de hielo son más frecuentes. El aumento de aguas sin hielo marino podría favorecer la expansión de vegetación marina en el Ártico y la migración de especies subárticas hacia el norte, donde las horas de luz diaria alcanzan las 24 h.

Debido a la importante contribución de ecosistemas pelágicos y bentónicos a la productividad primaria del Océano Ártico, en esta tesis he investigado los efectos experimentales de dos factores abióticos: el aumento de CO_2 y largos fotoperiodos. Estos efectos han sido evaluados en comunidades planctónicas de aguas superficiales y en macrófitos bentónicos de ecosistemas subárticos y Árticos. De forma paralela, he investigado la relación de las tasas de producción primaria planctónica estimadas a través de tres métodos diferentes: el método de balance de oxígeno, el método de ^{18}O y el método de ^{14}C. Esta comparación se ha realizado por primera vez en el Océano Ártico y concluimos que el método de ^{14}C, con incubaciones de 24 h, subestima la producción primaria bruta medida con los métodos basados en oxígeno, aunque las relaciones cambian estacionalmente. En primavera, periodo de alta producción, los métodos basados en oxígeno son los más apropiados para estimar de la producción primaria bruta mientras que en

verano ambos métodos, basados en carbono y en oxígeno, son adecuados. Por ello, estos métodos se emplearon para investigar la posible limitación de CO_2 en comunidades planctónicas del Océano Ártico. Con este objetivo realizamos experimentos de adición de CO_2 en primavera y en verano en el oeste y noroeste de Svalbard y observamos que la estimulación estaba restringida a episodios de alta productividad, cuando las concentraciones de CO_2 ya habían bajado y los nutrientes inorgánicos seguían presentes en el agua a bajas concentraciones.

Para determinar el periodo de limitación de CO_2, realicé experimentos semanales de aumento de CO_2 durante el desarrollo de una floración de fitoplancton, desde Marzo hasta finales de Mayo de 2016 en Godthåbsfjord, al suroeste de Groenlandia. En estos experimentos, observamos que durante dos semanas aproximadamente y después de que la floración alcanzase su máxima producción, el llamado *peak bloom stage*, la comunidad fitoplanctónica está limitada por las bajas concentraciones de CO_2. Durante este periodo de tiempo, las tasas de producción primaria neta aumentaron con el aumento de la concentración de CO_2 en presencia de nutrientes inorgánicos disueltos.

Además, hemos evaluado experimentalmente el efecto de largos fotoperiodos, característicos de la temporada de verano en el Océano Ártico, y el efecto del aumento de CO_2 en tres especies de macrófitos subárticos: *Ascophyllum nodosum*, *Fucus vesiculosus* y *Zostera marina*. Hemos observado que la actividad fotosintética, medida como la tasa de transporte de electrones, era mayor en el fotoperiodo de luz continua. El aumento de CO_2 también tuvo un efecto positivo, pero no significativo, en la especie de macroalga *A. nodosum* y en la fanerógama *Z. marina*. Por ello, estas tres especies se beneficiarán del aumento de horas de luz a medida en que se expandan y migren hacia el norte, siguiendo el retroceso de la cubierta de hielo.

Los resultados de esta tesis sugieren que el presente y el futuro aumento de las concentraciones de CO_2 incrementan la contribución de la floración de fitoplancton primaveral al balance de la producción primaria anual en aguas Árticas y subárticas. Además, el fotoperiodo de luz continua favorecerá la expansión y la migración hacia el norte de tres especies de macrófitos subárticos. En esta tesis presento evidencias experimentales sobre los efectos del cambio climático en comunidades planctónicas superficiales y en tres especies de macrófitos bentónicos en dos regiones del Océano Ártico, contribuyendo al conocimiento de la disciplina de la ecología del cambio climático en el medio marino y contribuyendo a la disciplina de la oceanografía ártica con el estudio comparativo de las metodologías de producción primaria en esta región, fomentando el desarrollo de futuros estudios y predicciones de los efectos del cambio climático en el Océano Ártico.

Image 1: Frazil ice and coastline at the NW of the Svalbard Archipelago aboard the R/V Helmer Hanssen. Photo credit: M. Sanz-Martín.

1. Introduction

1.1 Global climate change in the Arctic Ocean

Anthropogenic greenhouse gases (GHGs) emission has increased since the beginning of the industrial revolution due to the large economic and population growth (IPCC, 2014). Concentrations of carbon dioxide (CO_2), methane (CH_4) and nitrous oxide (N_2O) have risen (Canadell *et al.*, 2007; IPCC, 2014) with larger increases between 2000 and 2010, in spite of the growth of climate change mitigation policies (IPCC, 2014) (Figure 1). GHGs are affecting the climate system and are causing the increase of global temperatures, the retreat of glaciers and sea-ice melting as well as the rise of global mean sea level during the last decades (IPCC, 2014). Atmospheric CO_2 concentrations have increased from 240 ppm in 1750 (Zeebe, 2012) to more than 400 ppm in 2017 (http://scrippsco2.ucsd.edu). Between 1750 and 2011, 2040 ± 310 $GtCO_2$ have been emitted (IPCC, 2014). About 55 % of these emissions has been transferred to land and oceans and 45 % have remained in the atmosphere (Ballantyne *et al.*, 2012; IPCC, 2014). Oceans have absorbed ~30 % of the anthropogenic CO_2 emitted, although predictions about how the ocean CO_2 sink will change as the earth warms are not accurate (Sarmiento & Gruber, 2004).

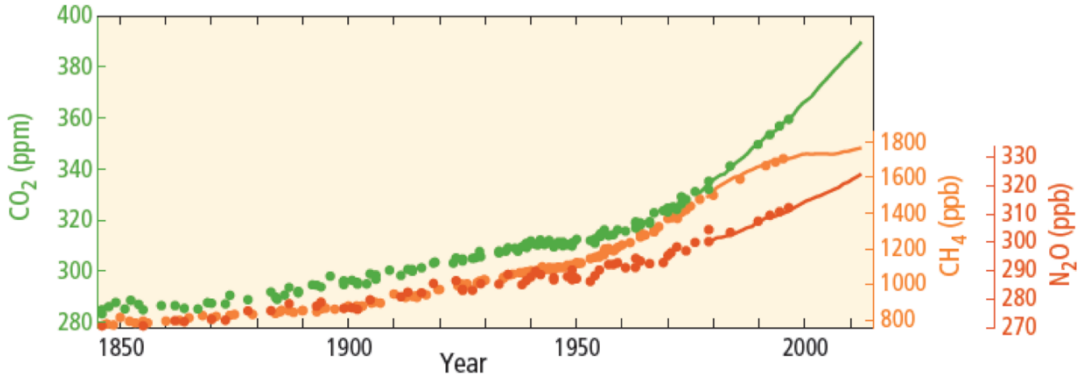

Figure 1: Atmospheric concentrations of the greenhouse gases carbon dioxide (CO_2, green), methane (CH_4, orange) and nitrous oxide (N_2O, red) determined from ice core data (dots) and from direct atmospheric measurements (line) (IPCC, 2014).

Surface temperature on land and ocean has increased 0.85 °C on average from 1880 to 2012 and further increases are predicted by the end of the 21st century (IPCC, 2014). In the Arctic atmosphere, temperature has increased almost two times more than the global average in the last 100 years (ACIA, 2004; Trenberth *et al.*, 2007) and will continue to warm more rapidly than global mean (IPCC, 2014). Arctic warming is causing accelerated sea-ice and glacier melting, particularly in spring and summer (Maslanik *et al.*, 2007; Duarte *et al.*, 2012b). The Arctic region is experiencing the most substantial effects of climate change and for that, it is one of the most vulnerable regions (Duarte *et al.*, 2012a,b).

The European Sector of the Arctic Ocean is characterized by a warm Atlantic current call the West Spitsbergen Current (WSC) which flows northward through the Fram Strait (more details in section 3.1 Study areas). The warming of this region is causing the reduction of the transport of sea ice from the Arctic Ocean into the Barents Sea, probably promoting an effect of "atlantification" that leads to changes in heat transport and vertical mixing (Sundfjord *et al.*, 2008). The intense warming across the Arctic has lead into a decreased annual sea-ice extent and the reduction of its thickness at a rate of 3.5-4.1 % per decade (Vaughan *et al.*, 2013). In some Arctic regions, the period of ice-free waters has increased around 90 days between 1972 and 2011 (Vaughan *et al.*, 2013). Climate models suggest reductions in Arctic sea ice but the worst scenario forecasts a high Arctic largely free of sea ice for the summer of 2037 (Wang & Overland, 2009; IPCC, 2014). Increased temperatures, reductions of sea ice and increased global mean sea level, among other factors, are expected to cause declines and redistribution of global rates of the net primary production (NPP) by 2100 in the open ocean, while increases in NPP are expected at high latitudes (IPCC, 2014). In the Arctic Ocean annual NPP, estimated based on satellite chlorophyll concentrations, has increased by 30 % since 1998 (Arrigo & van Dijken, 2015) and further increases are predicted across much of the Arctic Ocean with regional contrasts (Arrigo *et al.*, 2008; Arrigo & van Dijken, 2015; Slagstad *et al.*, 2015).

1.2 The role of CO_2 in Arctic waters

The increase of atmospheric CO_2 is producing oceanic CO_2 absorption due to the air-sea imbalance (Wolf-Gladrow *et al.*, 2007; Zeebe, 2012; IPCC, 2014). When the partial pressure of a gas is increased in the atmosphere, the gas enters by diffusion in the water mass through the air-water interface, producing an input flux into the water until both partial pressures are equilibrated. After the equilibrium between partial pressures is stablished (Eq. 1), seawater has about the same concentration of CO_2 as the atmosphere:

$$CO_2 \text{ (atmospheric)} \rightleftharpoons CO_2 \text{ (dissolved)} \qquad \text{(Eq. 1)}$$

Most of the carbon (C) in seawater is dissolved in four inorganic forms: free CO_2 (hereafter CO_2), bicarbonate ion (HCO^-_3) and carbonate ion (CO_2^{-3}). The sum of the dissolved carbonate species is usually expressed as total dissolved inorganic carbon (DIC). HCO_3^- is the major component of DIC in the ocean, at a typical pH of 8-8.1. DIC consists of 90 % HCO_3^-, 9 % CO_2^{-3} while only 1 % is CO_2 (Wolf-Gladrow *et al.*, 2007; Zeebe, 2012). Carbonic acid (H_2CO_3) concentration is commonly included in the measurements of CO_2 since it is less than 1 % of the CO_2 pool.

The equilibrium of DIC is also called the carbonate buffering system:

$$CO_2 + H_2O \rightleftharpoons H_2CO_3 \rightleftharpoons HCO_3^- \rightleftharpoons CO_3^{2-} \quad \text{(Eq. 2)}$$

By increasing the CO_2 concentration (Eq. 2), the concentration of HCO_3^- and protons (H^+) will increase and the concentration of CO_3^{2-} will decrease, causing a decrease in pH, generally called acidification. According to predictions, after 2100, the pH in the surface ocean will approach 7.8 although this pH is above 7, which is not technically "acidic (Wolf-Gladrow *et al.*, 1999). During photosynthesis, CO_2 and HCO_3^- are consumed and the DIC levels decrease, yielding CO_3^{2-} as a by-product and increasing the pH. Respiration increases CO_2, which binds with CO_3^{2-} lowering its concentrations, forming HCO_3^- and lowing the pH. Henry's law in thermodynamic equilibrium relates gaseous CO_2 and CO_2 concentrations trough the following equation:

$$K_0 = [CO_2]/CO_2(g) \quad \text{(Eq. 3)}$$

Where K_0 is the solubility coefficient of CO_2 in seawater, which is highly dependent on temperature and, to a lesser extent, on salinity (Weiss, 1974). The solubility coefficient increases with decreasing temperature and increasing salinity (Eq. 3). For instance, the solubility of CO_2 is practically double when the temperature decreases from 20°C to 0°C (Sakshaug *et al.*, 2009). The cooling of Atlantic waters flowing into the Arctic Ocean increases CO_2 solubility and decreases pCO_2 (Kaltin; *et al.*, 2002). Together with the biological CO_2 uptake, that decreases further pCO_2 in the surface, the capacity of the Arctic Ocean to absorb large quantities of gaseous CO_2 increases (Kaltin; *et al.*, 2002). In this thesis, the capacity of the Arctic Ocean as CO_2 sink has been evaluated through the relationship between air-sea fluxes and the productivity of the planktonic community in during certain periods within the sections Results 4.2 & 4.3.

1.3 Primary productivity and its methods in the Arctic Ocean

Photosynthesis is the basic process that produces energy for all the organisms of the food web and the rate at which the photosynthesis occurs is called primary production (PP) or primary productivity rate (Beer *et al.*, 2014). Marine vegetation provides approximately half of the global PP (Woodward, 2007; Falkowski & Raven, 2013). Phytoplankton is responsible for nearly all the PP that occurs in the pelagic ecosystems of the Arctic Ocean while macrophytes have a fundamental role as primary producers in the Arctic coastline (Sakshaug *et al.*, 2009). In near-shore areas of the high Arctic, the photosynthetic activity of phytoplankton contributes 65 % to the primary productivity, benthic macrophytes contributes 21 %, benthic microphytes 13 % and the contribution of sea-ice algae is less than 1 % (Glud & Rysgaard, 2007). Although recent studies indicate that the contribution of sub-ice

phytoplankton might double previous annual estimates in some regions of the Arctic Ocean (Fernández-Méndez *et al.*, 2015) and they seem to become more common in a future Arctic (Assmy *et al.*, 2017). Nevertheless, this thesis focuses on the productivity of plankton communities and benthic macrophytes, excluding the study of benthic microphytes and sea-ice algae.

During photosynthesis, the photosynthetic-pigment molecules, principally chlorophyll *a*, absorbs part of the radiant energy from sunlight providing chemical energy to reduce CO_2 to carbohydrates, hydrolyse water, release O_2 and create organic matter. Chlorophyll reaction centres become chemically excited and electrons are moved to a higher energy state from photosystem (PS) I to II by absorption of light quanta, resulting in a photosynthetic electron transport rate (ETR) that leads consequently to rates of O_2 production and C assimilation during photosynthesis in the light (Ralph & Gademann, 2005; Falkowski & Raven, 2013).

Because photosynthesis is a fundamental process, affecting either directly or indirectly the functioning of marine ecosystems, from their capacity to take up atmospheric CO_2 to the distribution and breeding success of higher trophic levels, quantification of PP has long been a core measurement in biological oceanography (Robinson *et al.*, 2009; Regaudie-de-Gioux *et al.*, 2014). Measurements of PP over the last decades, both remote and *in situ*, have provided critical insight into the spatial and temporal variability of phytoplankton growth in the Arctic. Although the Arctic Ocean is strongly seasonal, some of its regions rank among the most productive in the oceans (Gosselin *et al.*, 1997; Tremblay *et al.*, 2002; Vaquer-Sunyer *et al.*, 2013), directly related with pelagic and benthic higher trophic levels (Grebmeier & Mcroy, 1989; Grebmeier *et al.*, 2006, 2013). While recent modelling and remote sensing studies have also suggested climate-driven changes in Arctic PP (Pabi *et al.*, 2008; Slagstad *et al.*, 2015), methodological differences in PP measurements nevertheless introduce uncertainty in these future projections. To evaluate PP responses, appropriate estimations and evaluations of PP based on comparable methods are fundamental.

Three primary methods have historically been used to estimate planktonic PP, each with different underlying assumptions and shortcomings. However, the reporting of method is often unspecific. Gross photosynthesis or gross primary production (GPP) is an estimate of total photosynthetic rate before any losses, like respiration, take place. GPP has been quantified using two oxygen-based methods as the photosynthetic production of ^{18}O from ^{18}O-labelled water additions (GPP-^{18}O) (Bender *et al.*, 1987) as well as using the O_2 mass balance method (Carpenter, 1995). The determination of GPP-^{18}O through mass spectrometry measures the O_2 produced during 24-h incubation (Bender *et al.*, 1987) and has been identified as the best approach to estimate GPP-^{18}O (Regaudie-de-Gioux *et al.*, 2014). However, not all the oxygen-producing metabolic processes measured with the ^{18}O method are directly related to carbon assimilation (i.e. the Mehler reaction,

photorespiration and mitochondrial respiration) (Bender *et al.*, 1999; Laws *et al.*, 2000; Dickson *et al.*, 2001; Marra, 2002), potentially leading to biased estimates. The O_2 mass balance method (Carpenter, 1995), on the other hand, measures the change in dissolved oxygen in light/dark incubations over 24 h subject to a natural photoperiod. GPP, (hereafter GPP-DO) is derived by summing the rate of change of oxygen in dark bottles (an estimate of community respiration, CR) and that in clear bottles subject (an estimate of net community production, NCP) (Carritt & Carpenter, 1966; Duarte *et al.*, 2011). However, this procedure assumes that respiration in the dark is the same as that in the light. Recently, this has been shown to be particularly incorrect in the Arctic Ocean during spring and summer, with 24-h daylight increasing respiration rates (Mesa *et al.*, 2017).

The third and most widely used method to resolve planktonic PP is the ^{14}C method (Steemann-Nielsen, 1952) which traces the incorporation of inorganic carbon into particulate organic carbon (^{14}C-POC), and can also be used to track the release of ^{14}C incorporated as dissolved organic carbon (^{14}C-DOC), by subtracting the total organic carbon production (^{14}C-TOC) from ^{14}C-POC. Whereas estimates based on O_2 mass balance consistently incubate the communities over 24 h in estimating GPP, high variability in incubation times have resulted of significant uncertainty as to how to interpret ^{14}C rate measurements. If incubations are long enough to account for CO_2 losses due to algal respiration, then this method reflects net primary production (NPP) (Marra, 2002, 2009), which may account for a minimum of ~35 % of GPP (Bender *et al.*, 1996; Duarte & Cebrián, 1996). As a consequence of losses due to algal respiration and DOC production, particulate C-based production (^{14}C-POC) underestimates GPP by about 48 % (Del Giorgio & Duarte, 2002).

Comparison of estimates derived from these various methods have led to conflicting results. In previous studies in the North Pacific (Grande *et al.*, 1989b), the O_2 mass balance and the ^{18}O methods provided similar estimates of productivity, while the ^{18}O estimates were higher than O_2 estimates for the Arctic Ocean (Mesa *et al.*, 2017), similar to large-scale comparisons (Robinson *et al.*, 2009; Regaudie-de-Gioux *et al.*, 2014). In contrast, ^{18}O values can be significantly lower than O_2 rates in nutrient-rich areas with low oxygen concentration (Gazeau *et al.*, 2007). This large variability indicate that the performance of the methods to estimate PP are based on environmental conditions and the use of multiple methods to estimate PP is recommended (Robinson *et al.*, 2009).

In turn, comparisons between the C-based method and the O_2-based methods have indicated lower rates of ^{14}C incorporation than O_2 production (Robinson *et al.*, 2009; Regaudie-de-Gioux *et al.*, 2014). These discrepancies are likely due to variability in the assumed photosynthetic quotient (PQ), a critical parameter quantifying the amount of oxygen evolved per unit of photosynthetically carbon fixed into organic matter. PQ values range widely, from 1.0 to 1.8, with values 1.0

to 1.4 in non-polar oceanic areas (e.g. Bender *et al.*, 1987; Grande *et al.*, 1989a; Laws *et al.*, 2000; Dickson *et al.*, 2001) and from 1.1 to 1.8 in the Southern Ocean surrounding Antarctica (i. e. Williams *et al.*, 1979; Aristegui *et al.*, 1996; Robinson *et al.*, 1999). No PQ value has been derived for the Arctic Ocean, so the most widely applied PQ, 1.25 proposed by Williams *et al.* (1979), has been applied in this region (i. e. Vaquer-Sunyer *et al.*, 2013).

Historically, ^{14}C-PP measurements have primarily been collected across the Arctic Ocean, with O_2-based rates collected only in select regions (Matrai *et al.*, 2013). Average ^{14}C-PP rates in surface waters derived from estimates compiled over 50 years (1954 to 2007) across this region in summer are 70 and 21 mg C m^{-3} d^{-1} in spring and summer, respectively (Matrai *et al.*, 2013). O_2-based estimates, collected in the European sector of the Arctic between 2007 and 2011, report average rates of GPP-DO in surface waters of 168 and 55 mg C m^{-3} d^{-1} in spring and summer, respectively (Vaquer-Sunyer *et al.*, 2013), two-fold higher than those derived for ^{14}C-PP rates measured in summer across all the Arctic regions (Matrai *et al.*, 2013). Whether these differences are due to spatial gradients or temporal changes in the system, or a result of bias in the methods of measurement remains unknown due to a lack of comparison between concurrent C-based and O_2-based measurements of PP in Arctic waters.

An appropriate understanding of gross and net PP measurements is fundamental for marine biogeochemical research but a definitive estimate of PP remains uncertain in oceans globally given the differences between methods and their underlying assumptions. This is particularly relevant in the Arctic Ocean, where recent modelling and remote sensing studies suggest changes in rates of PP (Arrigo *et al.*, 2008; Pabi *et al.*, 2008; Arrigo & van Dijken, 2015; Slagstad *et al.*, 2015) although estimations with different methods are sparse (Matrai *et al.*, 2013). In order to reconcile PP estimations and facilitate future studies in this rapidly changing region, my co-authors and I have assessed the relationships between C and O_2-based PP rates in the Arctic Ocean (Results 4.1).

1.4 Arctic seasonality: drawdown of CO_2 and reduced ice cover

The Arctic Ocean is characterized by extreme seasonal changes in solar radiation and sea-ice cover. During spring and summer, the sun is above the horizon from 21 h to 24 h of daylight depending on the latitude. In winter and early spring, the sun is under or low over the horizon following the same pattern of hours of darkness. The presence of snow and ice cover in this region has prevented vegetation growth in both pelagic and benthic ecosystems (Krause-Jensen & Duarte, 2014). However, current reductions in ice cover particularly in spring and summer will have important consequences in these ecosystems (Krause-Jensen *et al.*, 2016). During

this period, the increase of day length and increased irradiance stimulate photosynthesis of both pelagic and benthic autotrophs, consuming DIC and leading to low CO_2 levels that might become limiting in coastal and shelf areas. In this thesis, I focussed on the community-level responses of plankton in pelagic ecosystems (Results 4.2 & 4.3) and physiological-level responses of macrophytes in benthic ecosystems in the Arctic Ocean (Results 4.4) to increased CO_2 concentrations and increased day length.

1.4.1 Planktonic productivity in the Arctic Ocean

The deep Arctic Ocean basin is poorly productive along the whole year due to the presence of ice while the surrounding seas are highly productive in spring and summer (Wassmann, 2008), such as the western and central European Arctic Corridor, that currently supports the highest GPP, and also in the Chuckchi Sea and the Bering Strait GPP is relatively higher (Slagstad *et al.*, 2015). On an annual scale, the European Arctic is likely net autotrophic, given the high productivity of intense blooms of phytoplankton while in winter and summer it is likely net heterotrophic (Vaquer-Sunyer *et al.*, 2013). The Arctic spring blooms are generally triggered by increased solar radiation from longer days together with increased temperature, melting ice and the consequent stratification (Sakshaug & Skjoldal, 1989; Niebauer, 1991), along with increased underwater irradiance due to the large sea-ice loss (Reigstad *et al.*, 2002; Hodal *et al.*, 2012; Juul-Pedersen *et al.*, 2015). In presence of abundant nutrients, the stabilization of the water column from melting induced stratification, and high pCO_2, blooms of phytoplankton develop across the Arctic

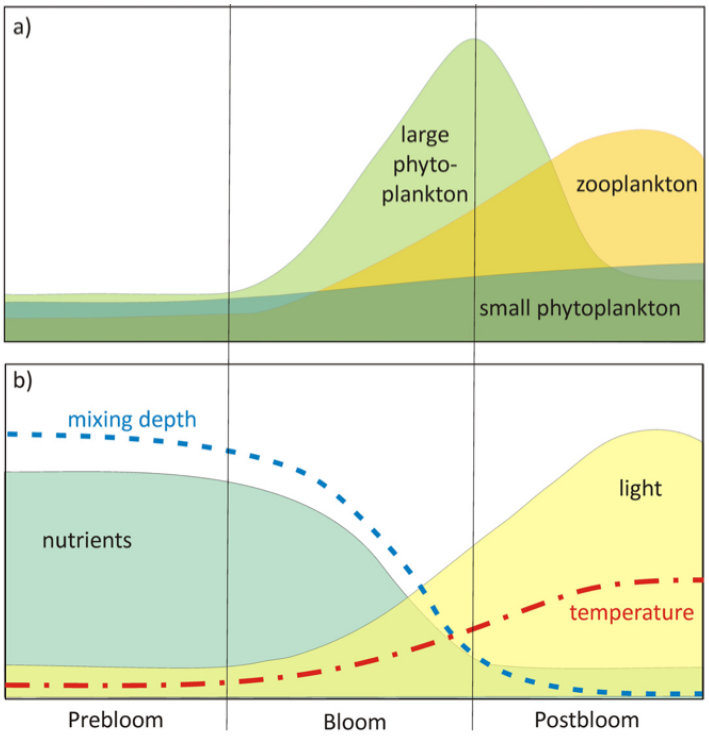

Figure 2: Development of biotic (a) and abiotic (b) factors from the prebloom to the postbloom phase of a theoretical high-latitude ecosystem (Berreville *et al.*, 2008; Seuthe, 2011).

Ocean following three stages: prebloom, bloom and postbloom phases (Figure 2) (Sakshaug & Skjoldal, 1989; Platt *et al.*, 1991; Berreville *et al.*, 2008). A spring bloom of phytoplankton depletes dissolved inorganic nutrients (Figure 2) and draws down CO_2 in surface waters (Rysgaard *et al.,* 1999, 2009; Tremblay *et al.*, 2006; Bates & Mathis, 2009; Meire *et al*., 2015). Spring blooms are usually considered to be terminated by nutrient depletion and grazing with the export of particulate organic matter, but secondary blooms can be produced by wind-driven events that break down the weak stratification and supply nutrients to the euphotic zone (Sakshaug & Skjoldal, 1989; Niebauer, 1991; Wassmann *et al.*, 1999; Tremblay *et al.*, 2006; Fransson *et al.*, 2017).

The strength of the Arctic plankton bloom in spring results not only from high primary production, but also from the very low respiratory demand of the plankton community due to the low temperatures, among other factors (Vaquer-Sunyer *et al.*, 2013), resulting in low biological CO_2 recycling. The biological CO_2 uptake in shallow stratified layers (Chierici *et al.*, 2011; Yasunaka *et al.*, 2016) results in surface values as low as 100 µatm of partial pressure of CO_2 (pCO_2) at the end of the spring bloom (Fransson *et al.*, 2009), which are among the lowest pCO_2 values reported across the open ocean (Takahashi *et al.*, 2009). As a consequence, several regions of the Arctic Ocean play the role of a CO_2 sink, such as the Eurasian shelves and the Barents Sea (Fransson *et al.*, 2001, 2009) and the Bering-Chukchi shelves (Kaltin & Anderson, 2005), rendering it as a sink of atmospheric CO_2 of approximately 66 to 199 Tg C yr^{-1} during spring and summer (Bates & Mathis, 2009). Although these estimates are based on very limited data and near absence of wintertime data (Bates & Mathis, 2009).

Spring blooms are key biological events that make the Arctic Ocean responsible for about 5-14 % of the annual atmospheric CO_2 uptake (Bates & Mathis, 2009). During these episodes as much as 60 % of the total annual NCP can take place (Vaquer-Sunyer *et al.*, 2013). However, the growth of phytoplankton might be limited not only by low levels of nutrients but also by episodes of low levels of CO_2 in highly productive waters (Mercado & Gordillo, 2011), such as those produced in Arctic spring blooms. Nevertheless, the limitation by CO_2 in the Arctic Ocean has hardly been evaluated. Changes in NCP in general and specifically during the spring bloom could influence the oceans capacity to take up atmospheric CO_2 thus creating a potential feedback mechanism in climate change (Slagstad *et al.*, 2015; Tremblay *et al.*, 2015). Previous experimental studies of CO_2 increases in Arctic plankton communities suggest positives NPP responses using the ^{14}C method (Engel *et al.*, 2013) as well as increases in GPP using the O_2-based methods, but the greatest CO_2 effect was observed only at low temperatures and the phenology of the phytoplankton was inferred (Coello-Camba *et al.*, 2014; Holding *et al.*, 2015). However, decreases in NPP of planktonic communities are also found with high irradiance (Hoppe *et al.*, 2017). Experimental evidence of CO_2 limitation has been

observed in sub-ice blooms in the Baltic Sea (Spilling, 2007) and in the Atlantic Ocean (Hein & Sand-Jensen, 1997).

The rate of PP attained during the spring blooms might be limited by CO_2, as PP can depend on the CO_2 influx by diffusion, in presence of nutrients (Engel *et al.*, 2014; Holding *et al.*, 2015). Thus, there may be a window of time of CO_2 limitation of PP that might also slow down the development of a bloom after the decline of CO_2 concentration. This hypothesis has been tested in the section Results 4.2, where the CO_2 limitation was evaluated along different seasons in the Arctic Ocean as well as in Results 4.3, where a time window of CO_2 limitation has been identified a subarctic spring bloom.

1.4.2 Benthic macrophytes in the Arctic Ocean

Benthic macroalgae in the Arctic region grow in assemblages at shallow depths forming intertidal belts (e.g. *Ascophyllum nodosum*, *Fucus* sp.) and subtidal kelps (e.g. *Saccharina latissima*) (Wulff *et al.*, 2009). Most habitat-forming Arctic macrophytes have a origin in the North Atlantic and North Pacific regions (Wulff *et al.*, 2009; Wilce & Dunton, 2014). Only one seagrass species, *Zostera marina*, is present forming in eelgrass meadows with a limit at 70° N (Olesen *et al.*, 2015).

The presence of macroalgae assemblages in the Arctic is often limited by extended sea-ice cover that reduces submersed light penetration (Wulff *et al.*, 2009; Krause-Jensen *et al.*, 2012; Krause-Jensen & Duarte, 2014). However, a predicted Arctic largely free of sea ice in summer (Wang & Overland, 2009; IPCC, 2014) may favor the entrance of new species into the Arctic and the expansion of existing Arctic vegetation (Krause-Jensen and Duarte, 2014). Arctic warming has already led to increased Arctic cod fishery due to the poleward expansion of cod habitat (Kjesbu *et al.*, 2014).

The ice cover prevents the availability of suitable habitat such as soft sediments for seagrass and rocky bottoms for most macroalgae, present along the Arctic coast (Krause-Jensen & Duarte, 2014). Increasing ice melting in this region is expected to have large impacts associated with ice as habitat (Duarte *et al.*, 2012a,b). Reduction of ice cover might facilitate the colonization of subarctic vegetation into northern regions and the expansion of existing arctic species (Krause-Jensen & Duarte, 2014).

Marine macrophytes are often limited by CO_2 because the boundary layers formed around the blades limit the entrance of CO_2 by diffusion due to its thicknesses (Hendriks *et al.*, 2017), which together with high primary productivity rates in dense vegetated areas result in low CO_2 levels close to the blade surface (Holbrook *et al.*, 1987; Bowes & Salvuci, 1989; Hurd *et al.*, 2009), which may cause CO_2

limitation, with the risk being particularly likely in vegetated coastal habitats that represent hot spots of productivity and CO_2 draw down. Krause-Jensen *et al.* (2016) concluded that day lengths longer than 21 h, characteristic of Arctic summers, were conducive to sustained up-regulation of pH by photosynthesis of macrophytes. They also concluded that experimental increase in CO_2 concentration stimulated the capacity of macrophytes to deplete CO_2 but they did not explore the species-specific responses. In Results 4.4, we have analyzed the photosynthetic responses of three subarctic species (*A. nodosum*, *F. vesiculosus* and *Z. marina*) to longer photoperiods and increased CO_2 in order to predict the ecological consequences as they expand into the Arctic region.

1.5 Marine physiological responses to CO_2 variations

In the 1980s, Badger *et al.*, (1980) and Kaplan *et al.*, (1980) demonstrated that cultures of phytoplankton accumulated inorganic C in photosynthetic cells. The enzyme ribulosa-1, 5-biphosphate carboxylase/oxygenase (Rubisco) can only use CO_2 as inorganic carbon substrate for the carboxylase reaction. CO_2 can diffuse passively through the cell membrane however, Rubisco shows low-affinity for CO_2 (Badger *et al.*, 1998). In seawater there is very little CO_2 and the most available source of dissolved carbon is HCO^-_3, thus the photosynthetic process of phytoplankton may suffer from CO_2-limitation (Rost *et al.*, 2006). To avoid CO_2-limitation, many autotrophic organisms developed Carbon Concentrating Mechanisms (CCMs) to increase their intracellular CO_2 concentration relative to external concentrations (Rost *et al.*, 2006). Some of these mechanisms involve active uptake of CO_2 and/or HCO^-_3 and the conversion HCO^-_3 to CO_2 catalyzed by the secretion of the enzyme carbonic anhydrase (Giordano *et al.*, 2005). There is no consensus in tracing the origin of CCMs despite the general assumption is that CCMs evolved in response to low CO_2 availability and maintained in the following periods of high CO_2 levels (Raven *et al.*, 2011).

Most of autotrophs present different types of CCMs (Giordano *et al.*, 2005; Raven *et al.*, 2005, 2011; Reinfelder, 2010; Raven & Beardall, 2014) and the presence of CCMs is most widespread in environments with low CO_2 concentrations and high light availability (Maberly & Gontero, 2017). The response of photosynthetic organisms to increased CO_2 seems to depend on the efficiency of CCMs, tending to species-specific responses (Tortell *et al.*, 2002; Rost *et al.*, 2003; Riebesell, 2004; Sobrino *et al.*, 2008, 2009). The expression degree of CCMs appears to be a response to the external DIC concentrations with higher values of DIC leading to a greater degree of suppression of CCMs activity (Giordano *et al.*, 2005). However, the use of these mechanisms is energetically expensive and their partial deactivation or downregulation at increased CO_2 concentrations could decrease the energetic demand, reducing the incorporation and synthesis of new metabolic

components as it has been shown in different algal species (Gordillo *et al.*, 2001; Sobrino *et al.*, 2008, 2009). At very high DIC, stronger responses such as the complete loss of CCMs expression have been observed in some eukaryotic autotrophs (Giordano *et al.*, 2005; Falkowski & Raven, 2013), although some macroalgae do not show any deactivation of CCMs in response to increased CO_2 (Zou & Gao, 2009; Zou *et al.*, 2011). Other environmental factors, such as temperature, have also been proposed to regulate the efficiency of the CCMs. In cold waters, such as Arctic waters, the need for CCMs seems to be reduced due to the increased solubility of CO_2 and the consequent greater availability of CO_2 (Raven, 1991; Raven *et al.*, 2002). Although the efficiency of CCMs has not been researched in this thesis, species-specific responses that might depend on CCMs have been taken into account in the section Results 4.2, where the effect of increased CO_2 has been researched in Arctic plankton communities, in Results 4.3 where the effects of increased CO_2 and long day length were addressed also plankton community level in subarctic waters, and in the section Results 4.4, where both effects were studied in three species of subarctic macrophytes, in order to fulfill the general objective of this thesis.

Image 2: Crossing the Godthåbsfjord in August 2016, Greenland. Photo credit: F. Ugarte.

2. Objectives

Goals and specific objectives

The general goals of this thesis are to assess the effects of increased CO_2 and long day length on planktonic communities and macrophytes, and to evaluate the relationship between gross primary production estimates measured with three different methods in the Arctic Ocean.

The specific objectives are three-fold:

1) To assess estimates of planktonic primary production rates in the Arctic Ocean using three methods and reconcile C and O_2-based rates, taking into account their underlying assumptions. By realizing this goal through the section Results 4.1, we contribute to the field of Arctic oceanography by facilitating future studies on primary productivity in this region.

2) To evaluate the planktonic community response to experimental increases of CO_2 at different seasonal periods, spring and summer, along the section Results 4.2, and during the development of a spring bloom in Results 4.3, using in both cases O_2-based rates of primary productivity in order to identify a windows of time of CO_2 limitation episodes in the Arctic Ocean. Thus, we contribute to field of climate change ecology by providing experimental evidence of the effects of climate change in the Arctic Ocean.

3) To study the photosynthetic responses of three macrophytes species to increased day length as a consequence of reduced ice cover and increased CO_2 in order to evaluate an expansion of subarctic macrophytes species into the Arctic. With the accomplishment of this goal in the section Results 4.4, we contribute to the field of climate change ecology by providing the experimental response of subarctic macroalgae species in a future Arctic Ocean.

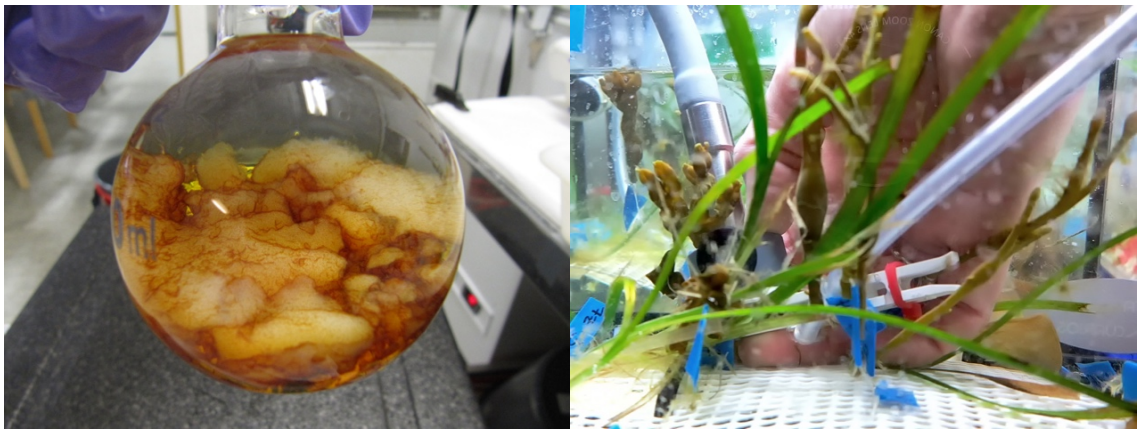

Image *3*: Dissolution of the precipitated formed for Winkler titration using the O_2 mass balance method (left). Photo credit: M. Sanz-Martín. Photosynthetic activity analysis on Z. marina in aquaria, in presence of F. vesiculosus and A. nodosum (right). Photo credit: I. Hendriks.

3. Methodologies

3.1 Study areas

The warm Gulf Stream enters into the Arctic Ocean through the North Atlantic current, which flows along the west coast of Norway and splits into the North Cape current heading towards the Barents Sea, and into the West Spitsbergen Current (WSC) (Figure 3), going across the Fram Strait (Rudels *et al.*, 1996, 2000). The Fram Strait, situated between Greenland and the Svalbard Archipelago, is the only deep gateway between the Arctic and subarctic seas. As the Atlantic water flows, it melts southwards-drifting ice and keeps the water ice free in the north of Svalbard (Rudels *et al.*, 2000), being the major heat advection of the Arctic Ocean (Spielhagen *et al.*, 2011). The study areas of Results 4.1 & 4.2 are located in this region, in the shelf and shelf break of the west and northwest of the Svalbard Archipelago from 77°N to 81°N (Figure 3).

Figure 3: Map of the Arctic Ocean circulation and the study areas of the NW of the Svalbard shelf (Results 4.1 & 4.2) and the Godthåbsfjord (Results 4.3) and the Kobbefjord (Results 4.4) in SW Greenland (adapted with permission of Woods Hole Oceanographic Institute, 2017).

The North Atlantic current brings warm water much further north than reaches around Canada and Greenland. The Transpolar current brings cold water from the Arctic Ocean to the Atlantic Ocean through the Greenland Sea, in the east coast of Greenland, and through the Davis Strait between the west of Greenland and Canada (Figure 3). The study area of Results 4.3 is located in the southwestern of

Greenland, at 64°N below the Arctic Circle (Figure 3), specifically in the fjord Nuup Kangerlua, known by its colonial name Godthåbsfjord. It is a large fjord system with a length of ~190 Km, influenced by three tidewater outlet glaciers located in the innermost part of the fjord (Mortensen *et al.*, 2011, 2013). Sea-ice conditions show interannual variability and ice floes and glacier icebergs are present during spring and summer with variable sizes along the fjord, which were originated from sea and glacier ice in the inner part of the fjord (Mortensen *et al.*, 2011). Macrophyte samples used in Results 4.4 were taken from this region, specifically from Kangerluarsunnguaq, whose Danish name is Kobbefjord (Figure 3). This fjord is smaller with 17 Km long and from 0.8 to 2 Km wide, reaches 100 m depth and the innermost part is usually covered by sea ice (Mikkelsen *et al.*, 2008).

3.2 Sampling sites and experimental set-ups

3.2.1 Multi-method assessment of primary production at the NW Svalbard shelf

Two cruises were conducted in the northwestern part of the Svalbard shelf during May and August 2014 aboard the R/V Helmer Hanssen (Figure 4). Five stations were sampled at different depths within the euphotic zone using a rosette sampler system fitted with Niskin bottles and a calibrated Seabird 911plus CTD (conductivity, temperature and depth). Samples to measure primary production (PP) were collected from thirty CTD casts and the results are located in the section Results 4.1.

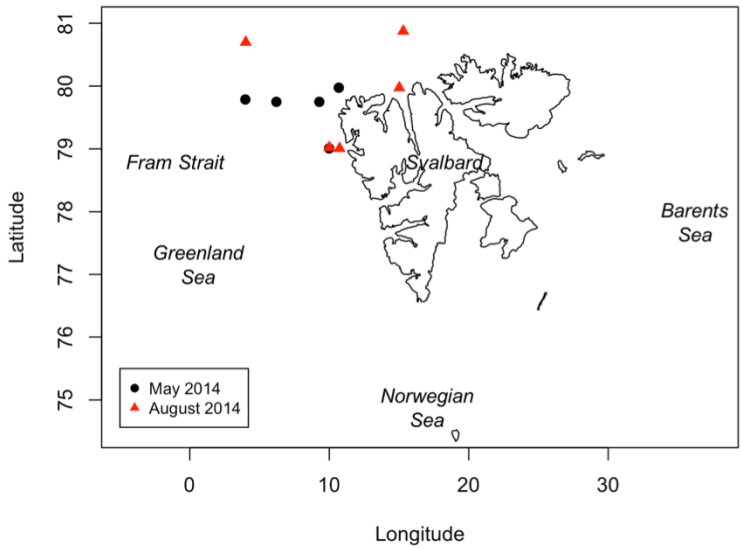

Figure 4: Location of samplings at the N and NW Svalbard shelf in May and August in 2014.

PP rates were measured using three methods: the O_2 mass balance (Carpenter, 1995), the ^{18}O method (Bender *et al.*, 1987) and the ^{14}C method (Steemann-Nielsen, 1952). Seawater for O_2–based PP determination was sampled at the surface (1 or 3 m), at the deep chlorophyll maximum layer depth (DCM, 20 to 30 m

depending on stations) and at an intermediate depth (10 or 15 m). Seawater for ^{14}C–based PP determination method was sampled at 1 or 3 m, 10 m, 15 or 20 m, 25 or 30 m, with exact sampling depths varying depending on the vertical fluorescence distribution. Due to sampling limitations, water for the C-based and O_2-based methods was sampled from non-consecutive CTD casts, introducing a time lag between CTD casts. We suspect this may have contributed to differences between rates derived here (see Results 4.1 for more details).

Samples measured with the ^{14}C method were incubated *in situ* for some of the stations: light and dark bottles were hung from a line anchored to an ice floe, and deployed for approximately 22 h and later converted into 24 h rates. In other stations, ^{14}C-labelled samples were incubated on deck for 24 h with UVA/B opaque methacrylate incubator with *in situ* water temperatures maintained with flow-through surface seawater baths to maintain samples close to the *in-situ* temperature. All of the samples measured with the O_2-based methods were also incubated for 24 h on deck in methacrylate tubes with surface seawater baths.

To simulate light attenuation in the water column, screens covered the methacrylate tubes holding the bottles inside the incubators. Light attenuation inside each methacrylate incubator was estimated with a Photosynthetically Available Radiation (PAR) radiometer (Biospherical Instruments Inc. QSL-101). Light attenuation was simulated using screens as a % of the on-deck PAR with 0 screen, 2 screens, 3 screens, and/or 4 screens, simulating 100 %, 50 %, 25 % and/or 12 % of surface PAR respectively for the ^{14}C samples. And using 0 screen, 2 screens, 3 screens, simulating 60 %, 33 % and 25 % of surface PAR respectively for the O_2-based samples. Light attenuation by the methacrylate incubator (0 screen) was higher in this case.

3.2.2 Episodic Artic CO_2 limitation at W Svalbard shelf

Three cruises were conducted in west and northwest of the Svalbard shelf on board R/V Helmer Hanssen in 2014 and 2015. The localization of the experiments was heterogeneous, four of the experiments where located in the path of the West Spitsbergen Current (WSC), that flows northward along the shelf edge at the west of the Svalbard Archipelago and carried out in May and August 2014, and two of the experiments were located in the mouth of two western fjords in May 2015 (Figure 5). Results of the experiments were analyzed in Results 4.2. The first experiment in May 2014 was previously analyzed in Holding *et al.* (2015).

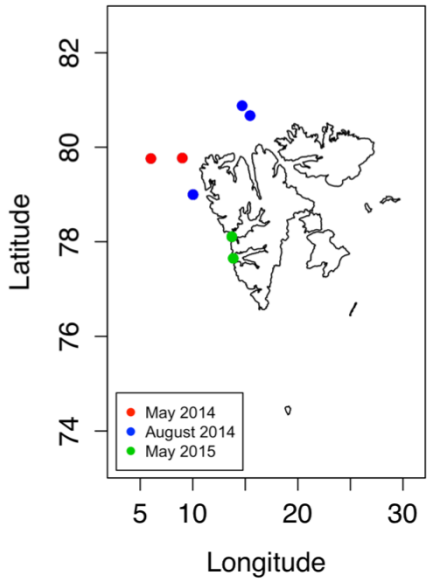

Figure 5: Study area at W and NW of the Svalbard shelf. Sampled stations of the experiments May 2014 (red), August 2014 (blue) and May 2015 (green).

In the stations of Figure 5, a sample of 50 L of subsurface seawater (3 m) was collected using a Rosette sampler system fitted with Niskin bottles and a calibrated CTD profiler (Seabird 911plus). The seawater was located in two closed tanks of 25 L using Tygon tubing. Samples for chlorophyll *a* concentration (Chl *a*) analysis were taken and measured 24 h later and samples for dissolved inorganic nutrients were taken and preserved for further analysis.

To simulate possible scenarios of elevated CO_2 in the Arctic Ocean, 25 L of seawater was stored in a closed tank and the remaining 25L were bubbled with CO_2 until ~1000 ppm was reached using a PP-Systems Environmental Gas Monitor (EGM-3) to measure pCO_2 while a water pump ensured proper mixing. The treated and untreated water was gently mixed in 10-L carboys to produce a gradient of pCO_2. This gradient included three pCO_2 levels in 2014, and was simplified, based on the results obtained, to experiments with only three pCO_2 levels in 2015, shifting the effort to be able to conduct experiments with a greater number of communities within the time available (pCO_2 of each treatment is detailed in Table A1). After every treatment reached the targeted pCO_2 (45 min), two sets of samples were collected. The first set was immediately preserved to determinate the initial dissolved O_2 concentration, $\delta^{18}O$ (in dissolved O_2), total alkalinity (TA) and total dissolved inorganic carbon (DIC) and the second set of samples was incubated for 24 h an subsequently preserved to determinate the GPP-^{18}O and CO_2 removal rates. The second set of samples was incubated in transparent methacrylate tubes during the 2014 cruises which allowed the 60 % transmittance of photosynthetically active radiation surface (PAR), with flow-through surface seawater baths to maintain samples close to the *in situ* temperature during the cruises of 2014. Incubations were on deck, as the incubations for O_2-based analysis of Results 4.1. In May 2015, samples were incubated in a 40-L tank with circulation of surface seawater and neutral screens that allowed the 70 % transmittance of surface PAR.

3.2.3 CO_2 limitation of subarctic spring bloom production

Weekly sampling was conducted in the central part of Godthåbsfjord, SW Greenland (Station GF7, Figure 3, Figure 13), in station GF7 from the 29th of February to the 27th of May 2016. The station was sampled 14 times during this period, in order to quantify the seasonal development in physical and chemical parameters of the water column. We also conducted 14 experiments of CO_2 additions to quantify net community production (NCP) of the planktonic community) using the O_2 mass balance method. Results of the water column and the experiments are located in Results 4.3. The spring bloom phenology has been well studied in the fjord based on 7 years of monthly samplings (Krawczyk *et al.*, 2015; Meire *et al.*, 2016).

Vertical profiles from 0 to 50 m were recorded using a CTD instrument (Sea-Bird SBE19plus), equipped with additional sensors for photosynthetically active radiation (PAR, LI-COR 190SA quantum Q PAR sensor) and fluorescence (Seapoint chlorophyll fluorometer). pCO_2 was measured *in situ* using HydroC™ CO_2 sensor (Contros, Germany; yearly calibrated by the company) that provides a relative standard deviation of 1 %. At each depth (1, 5, 10, 20, 30, 40 and 50 m), the sensor was equilibrated for 3-5 min until a stable reading was available. At 5 m depth, 50 L of seawater was collected using a 10-L Niskin bottle into 10-L polyethylene carboys. The experimental set-up used to simulate two predicted scenarios of elevated atmospheric CO_2 was already described in the previous section and resulted in three levels of pCO_2: control, treatment 1 and treatment 2. The *in situ* conditions of the experiments, pCO_2 of each treatment and the resulting NCP and DIC removal rates are shown in Table A2 of the Appendices section.

Each treatment was incubated for 24 h and samples were collected at the start and the end of the incubations. Samples for the start point were fixed immediately and stored in cold and darkness to determinate the initial conditions of dissolved O_2 concentration, TA and DIC with three replicates each. The samples were incubated in 6 narrow-mouth, borosilicate Winkler bottles for 24 h in a cold room at 0.4 to 1 °C illuminated with two bulb lamps providing PAR (photosynthetically active radiation) at 160 to 240 µmol photons m^{-2} s^{-1}, measured with a spherical radiometer. The average PAR at station GF7 at 5 m depth recorded in 2012 and 2013 was 108, 167 and 200 µmol photons m^{-2} in March, April and May, respectively (L. Meire, pers. com.). The photoperiod increased from 9.5 h on February 28th to 21 h on May 27th, increasing the daylight by 45 min per week. At the end of the incubation, seven replicated samples for dissolved O_2 concentration, three replicates for TA and DIC and two replicated samples for nutrients concentration (NO_2 + NO_3, PO_4, SiO_4) were collected. Dissolved O_2 samples were measured between 5 and 24 h later. *In situ* conditions at 5 m depth, pCO_2 of each treatment and the resulting NCP and DIC removal rates are shown in Table A2.

3.2.4 Long day length and increased CO_2 in subarctic macrophytes

Brown macroalgae (*A. nodosum*, *F. vesiculosus*) fronds and seagrass (*Z. marina*) shoots were collected from shallow waters in the central part of Kobbefjord (64°10'N and 51°29'W, Greenland) in early June 2014 (Figure 3). They were stored in cold, wetted in seawater and quickly transported by airplane to the laboratories of the Mediterranean Institute for Advanced Studies (IMEDEA, Mallorca, Spain), where they were held in a cold-room at 4 ^{o}C to test the effect of long day length and increased CO_2. The plants were then transferred into six aquaria of 6 L with controlled photoperiod, temperature and pCO_2 levels. The total biomass of algae in each aquarium was 2.7-3.7 g dry weight (DW), yielding a biomass density of 0.45-0.61 g DW L^{-1}, mimicking dense vegetation. The aquaria were exposed to three pCO_2 levels (200, 400 and 1000 ppm in the absence of macrophytes) with two replicated aquaria per level. 200 ppm reflected contemporary pCO_2 levels in subarctic surface waters in spring/summer (Meire *et al.*, 2015). Results of this experiment are located in Results 4.4. The highest CO_2 manipulation (1000 ppm) was set to the predicted scenario of atmospheric pCO_2 by 2100 (IPCC Panel, 2014), and 400 ppm represented an intermediate level. To mimic the photosynthetic active radiation (PAR) within *in situ* canopies, the aquaria were illuminated with 111 ± 5 mmol photons m^{-2} s^{-1} of PAR at the water surface using 2 lamps with 54 W fluorescent tubes. This light level is close to maximum PAR (204-289 mmol photons m^{-2} s^{-1}) reported in Greenland fjords close to the Godthåbsfjord at 2m depth during May and June 2013 (Olesen *et al*., 2015).

The aquaria were filled with 200-L artificial seawater made from distilled water, Reef Crystals® and NaCl to obtain experimental salinity (30.2 ± 0.42, subarctic range: 28.9-31.7) and alkalinity (2241 µmol kg SW^{-1} ± 31.3, measured in the sampled area: 1980-2240 µmol kg_{SW}^{-1}) conditions similar to those in the field. The artificial seawater was pre-exposed to UV to limit the growth of microorganisms during the experiment. To reach targeted pCO_2 levels, air was circulated through soda lime tubes to remove the CO_2 present and it was mixed with pure CO_2 gas in a bottle with marbles to maximize the mixing surface area. The concentration of air and pure CO_2 in the mixing bottle was regulated with mass flow controllers (MFCs, AALBORG GFC-17, US). The targeted pCO_2 concentration was continuously supplied to the aquaria through porous bubbling curtains. pH was measured *in continuum* with pH electrodes (Omega, PHE-1411) and recorded at 15 min intervals (IKS Aquastar, Germany) (for more details see Krause-Jensen *et al*., 2016). When seawater in the aquaria had reached a stabilized target pH, the same number of tips of *A. nodosum* and *F. vesiculosus* and shoots of *Z. marina* (6 individuals of each species) were attached to the base of the aquaria, with every individual identified with a label. The plants in each of the six aquaria were cycled through a series of alternated photoperiods (12:12 h, 15:9 h, 18:6 h, 21:3 h and 24:0 h, light:dark hours), maintained 4 days at each photoperiod treatment.

3.3 Overview of methods

To provide a general overview of the methods applied along the Results section, Table 1 summarizes samplings, experimental set-ups, studied responses and parameters analyzed.

Table 1: Summary of methodologies applied in each Results section. The acronyms of the statistical analysis are RMA (Reduced Major Axis), GLM (Generalized Linear Models) and GLMM (Generalized Linear Mixed Models).

Methods and analysis applied			Results			
			4.1	4.2	4.3	4.4
Area	Arctic region		✔	✔		
	Subarctic region				✔	✔
Sampling or set-up	Sampling water column		✔	✔	✔	
	Experimental CO_2 addition			✔	✔	✔
	Experimental increase of daylength				✔	✔
Incubation	Situation	*In situ*	✔			
		On deck	✔	✔		
		In cold room			✔	✔
	Time	24h	✔	✔	✔	
		4 days				✔
Responses	Plankton community	GPP-^{18}O	✔	✔		
		GPP - DO	✔			
		NCP - DO		✔	✔	
		GPP-^{14}C	✔			
		DIC removal rate		✔	✔	
		CO_2 removal rate		✔	✔	
	Macrophytes	$rETR_{max}$				✔
Measured parameters	Chlorophyll *a*		✔	✔	✔	
	Carbonate system	DIC	✔	✔	✔	✔
		TA		✔	✔	
		pH				✔
	pCO_2			✔	✔	✔
	Dissolved inorganic nutrients			✔	✔	
	Air-sea CO_2 flux			✔	✔	
	Phytoplankton community			✔	✔	
Period			May 2014 August 2014	May 2014 August 2014 May 2015	March to May 2016	June 2014
Statistical analysis			RMA, Two sample t-test, GLM	Ln Effect Size	Student t-test	GLMM

3.4 Primary production and photosynthetic activity

3.4.1 The ^{18}O method

GPP-^{18}O was measured as the photosynthetic production of $^{18}O_2$ following the addition of $H_2{}^{18}O$ after 24-h incubations on deck, according to (Bender *et al.*, 1987). The samples were carefully distributed into eight 12-ml borosilicate vials, which are ultraviolet A and B (UVA/B) opaque, allowing them to overflow to avoid contamination with atmospheric O_2. Four of the vials were immediately preserved with 100 µl of saturated mercury chloride ($HgCl_2$) solution for further analysis of initial $\delta^{18}O$ (in dissolved O_2) and stored in darkness upside down. The other four vials, containing glass beads to provide mixing, were labeled with 80 µl of 98 % $H_2{}^{18}O$ and shaken to ensure mixing. The labelled samples were incubated for 24 h on deck in methacrylate tubes with flow-through surface seawater baths and screens to attenuate light, as previously mentioned in sections 3.2.1 and 3.2.2. After 24-h incubation, vials were spiked with 100 µl of saturated $HgCl_2$ solution and stored for further analysis.

Samples were analyzed two weeks later at the Stable-Isotope Laboratory (IACT-CSIC, Armilla, Spain). A headspace of 100 % Helium of 4 mL was generated in each vial and left for 24 h at room temperature letting the dissolved gases in water equilibrate with the headspace. After 24 h, the $\delta^{18}O$ of dissolved oxygen in the headspace was measured in a Finnigan GasBench II attached to a Finnigan DeltaPlusXP isotope ratio mass spectrometer, with precision of 0.2 ‰ (A. Delgado, pers. com.). The flow was passed through a liquid nitrogen trap to remove water vapor before entering into the GasBench II. Molecules of O_2 and N_2 were separated in a Molecular Sieve 5Å chromatographic column. Corrected data with atmospheric air was reported as $\delta^{18}O$ value (‰) relative to V-SMOW (Vienna Standard Mean Ocean Water) standard. The $\delta^{18}O(H_2O)$ composition of labelled samples was measured in a liquid water isotope analyzer (Los Gatos Research), with precision of 0.2 ‰. In order to avoid contamination of the analyzer with highly ^{18}O-enriched H_2O (≈ 3000 ‰), the labeled sample was diluted (approximately 1:20) with a laboratory standard of known isotopic composition. GPP-^{18}O was calculated using the following equation from Bender *et al.*, 1999:

$$GPP\text{-}^{18}O = [(\delta^{18}O_{final} - \delta^{18}O_{initial}) \div (\delta^{18}O_{water} - \delta^{18}O_{initial})] \times [O_2]_{initial} \quad \text{(Eq. 4)}$$

Where $\delta^{18}O_{initial}$ and $\delta^{18}O_{final}$ are the initial and final $\delta^{18}O$ of dissolved O_2 (‰) respectively, $\delta^{18}O_{water}$ is the $\delta^{18}O$ of the labelled seawater (‰) and $[O_2]_{initial}$ is the initial O_2 concentration (µmol O_2 L^{-1}) measured by high-precision Winkler titration (see more details in section 3.4.2).

3.4.2 The O_2 mass balance method

Samples were carefully distributed into 14 borosilicate Winkler bottles of 100 mL, which are UVA/B opaque. Seven replicates were used to determine the initial oxygen concentration, and seven replicates were incubated in dark and seven in light for 24 h on deck. The bottles were incubated on deck in the same methacrylate tubes as the GPP-^{18}O samples. O_2 concentrations were determined using an automatic titrator (808 Tritando, Metrohm) (Carritt and Carpenter, 1966; Carpenter, 1995), using a potentiometric electrode and automated endpoint detection (Oudot *et al.*, 1988). Values that reported O_2 production in darkness were considered unviable and discarded from the database. Gross primary production measured with the O_2 mass balance method (GPP-DO) was calculated by the difference between the mean final oxygen concentration of light incubated bottles and the mean final oxygen concentration of dark incubated bottles.

The O_2 mass balance method has been used in the sections Results 4.1, 4.2 & 4.3 (Table 1). Results of NCP and community dark respiration (R) in the water column were included in Results 4.2 to calculate the gross primary production/respiration ratio (GPP/R ratio). NCP and R was determined at 3 different depths on the euphotic layer: at the surface (1 or 3 m), at the DCM (20 to 30 m) and at an intermediate depth (10 or 15 m). This method measures NCP and R (NCP + R = GPP), allowing, the calculation of the GPP/R ratio in which autotrophic communities have GPP/R ratios greater than 1 (i.e., NCP > 0) and heterotrophic communities have GPP/R ratios less than 1 (i.e., NCP < 0).

In Results 4.3, NCP was measured at 5 m, which was used as the control treatment, and in the CO_2 treatments (level 1 and level 2), using a first set of five replicates samples to determine the initial oxygen concentration and other five replicates to determine the final oxygen concentration after 24 h incubation in light. Standard errors among five replicates sampled for each oxygen measurement varied between 0.05 and 3.4 mmol O_2 L^{-1}.

3.4.3 The ^{14}C method

Primary production using the ^{14}C method included the estimation of particulate (^{14}C-POC) and total (^{14}C-TOC) organic carbon production. Seawater samples were distributed in four UVA/B opaque 150-mL polycarbonate bottles. Treatments included 2 light bottles, 1 dark and one Time Zero. Ten µCuries of ^{14}C-labelled bicarbonate were dispensed into each bottle, and the Time Zero was preserved as explain below. In addition, for each depth (1-3 m, 5 m, 10 m, 15-20 m, 25-30 m) a 100 µL aliquot was sampled into a 6-mL scintillation vial containing 0.1 mL 6N NaOH in order to estimate the initial ^{14}C-bicarbonate concentration. Samples were

incubated for 24 h *in situ* and on deck, as mentioned in section 3.2.1. After 24-h incubations, bottles were recovered and sampled, keeping the bottles refrigerated. Two hundred µL of 20 % HCl was dispensed into each 6-mL scintillation vial containing either a Whatman GF/F filter (for particulate, ^{14}C-POC) or 2 mL of seawater (for total production, ^{14}C-TOC) in order to release any inorganic ^{14}C remaining in the sample. After 24 h, 5 ml of Ultima Gold (Perkin Elmer, USA) was added and the samples stored in the dark for further analysis. One week later, each vial was shaken and the ^{14}C activity measured in a Perkin Elmer scintillation counter at the University of Tromsø. Primary production was calculated as ^{14}C incorporation into the sample that is measured in units of disintegration per minute (DPM). The intensity of the signal is proportional to the beta particle emission from the ^{14}C incorporated into the cells. PP (units mg C m^{-3} d^{-1}) was calculated following the equation:

^{14}C-PP = [(DPM in the light bottle – DPM in the dark bottle) ÷ (Volume sample filtered × DIC in the samples × 1.05 × (24 ÷ h of incubation))] ÷ (specific activity in the sample ÷ volume specific activity) (Eq. 5)

where ^{14}C-PP is production, total DIC was measured in every sample, and 1.05 is the discrimination factor between incorporation of ^{14}C and ^{12}C. The ^{14}C incorporation in the light bottle is considered to account both for biotic (i.e., photosynthesis and $CaCO_3$ incorporation) and for abiotic (i.e., adsorption) processes (Banse, 1993). Thus, ^{14}C incorporation rates are corrected by subtracting the ^{14}C incorporation in the dark bottle, accounting for biological ^{14}C uptake that can occur outside photosynthesis and adsorption. The incorporation of ^{14}C into $CaCO_3$ is corrected by conversion to CO_2 following acidification. Finally, a time-zero determination corrects for abiotic processes. The PP estimates derived from this method were only analyzed in the section Results 4.1 (Table 1).

3.4.4 Photosynthetic activity

The photosynthetic activity of the three macrophyte species was measured through photosynthesis-irradiance curves (PI curves), also known as rapid light curves (RLC), showing the response of the chlorophyll *a* fluorescence to a range of light intensities (Ralph & Gademann, 2005; Falkowski & Raven, 2013). The measurements were done at the end of each photoperiod-incubation on two individuals of each species using Pulse Amplitude Modulation, with a diving-PAM fluorometer (Walz, Germany). The measurements were always done on the same individuals. To avoid excessive manipulation of macrophytes, the measurements were done inside the aquaria. Using a PAM leaf-clip, the tissue, dark-adapted for 5 min, was illuminated with a series of nine increasing actinic light intensities (from 0 to maximum 616 µmol PAR m^{-2} s^{-1}) at intervals of 10 s to produce a RLC. The

maximum relative electron transport rate ($rETR_{max}$, n = 12 per species and per photoperiod) was calculated by fitting the RLC data with the non-linear model (Platt *et al.*, 1982; Harrison & Platt, 1986; Ralph & Gademann, 2005):

$$rETR = rETR_{max} \times (1 - e^{(-\alpha \times \text{incident PAR} \div rETR_{max})}) \qquad \text{Eq. 6}$$

The photosynthetic parameters $rETR_{max}$, photosynthetic or quantum efficiency (α) and saturating irradiance (Ik, $Ik = rETR_{max}/\alpha$) were estimated by fitting the data of the RLC to Eq. 6 using R version 1.0.44 (R Development Core Team 2009). Even though *A. nodosum* and *Z. marina* showed no asymptotic approximation to the $rETR_{max}$ in some cases due to the limited range of actinic light intensities above light saturation (Figure A2, Figure A4) $rETR_{max}$ could still be estimated from the curvature of the RLCs. The results of this method have been analyzed in the section Results 4.4 (Table 1).

3.5 Oceanographic parameters

3.5.1 Chlorophyll a analysis

Samples for Chl *a* analysis were collected and determined fluorometrically by filtering a volume of the sampled seawater (200 mL for Results 4.2 and 50 mL for Results 4.3) through GF/F filters (Whatmanm 0.7 µm pore size). Samples were extracted in 90 % acetone (for Results 4.2) or in 96 % ethanol (for Results 4.3) during 24 h. Chl *a* fluorescence was analyzed using a Shimadzu RF-5301PC fluorometer (Results 4.2) or using the fluorometer TD-700 Turner Designs (Results 4.3) before and after the addition of 200 µL of 1M HCl solution, following Parsons *et al*., (1984) in both cases.

3.5.2 Carbonate system analysis

Seawater was sampled and distributed into 100 mL borosilicate bottles, which were then preserved with 20 µL of $HgCl_2$ and stored in dark and cold until analysis of DIC and total alkalinity (TA). DIC was determined using gas extraction of the acidified sample followed by coulometric titration and photometric detection using a Versatile Instrument for the Determination of Titration carbonate (VINDTA 3C, Marianda, Germany). TA was determined using potentiometric titration in closed cell using a using a Versatile Instrument for the Determination of Titration Alkalinity (VINDTA 3C, Marianda). The standard operating procedures from Dickson *et al.*, (2007) were followed and certified reference material provided by Dr. Andrew Dickson (Scripps Institution of Oceanography, University of California) was used to control accuracy of the analyses. The program CO2SYS (Pierrot *et al.*,

2006) was used to calculate the carbonate system parameter values; output parameters were standardized to standard pressure and *in situ* water temperature. The limit of detection is estimated at approximately 1.0 mg C m^{-3} d^{-1}.

Samples from 1 to 30 m were collected and DIC was measured for the section Results 4.1 (Table 1) at the Norwegian Polar Institute (M. Chierici PI). Water for DIC analysis was taken from the same CTD casts as the water for C-based estimates. TA and DIC was analyzed in the CO_2 experiments and included in the section Results 4.2 (Table 1). Here, seawater samples were collected from each treatment carboy in two borosilicate bottles per treatment. Initial samples were preserved and analyzed aboard and the final samples were preserved after 24 h of incubation and analyzed onboard. The CO_2 removal rates were calculated as the difference in CO_2 concentration during 24-h incubation.

In Results 4.3, triplicate water samples were collected at each depth (from 1 to 50 m) using a 5 L Niskin bottle and Tygon tubing to fill 12.5-mL vials for analysis of TA and DIC (Table 1). Samples were preserved and stored until further analysis as previously mentioned. DIC was analyzed using an infrared DIC analyzer (AS-C3, Apollo SciTech) and TA was analyzed using an alkalinity titrator (AS-ALK2 from Apollo SciTech). Results were verified against certified reference material. The average numerical deviation from the reference material (accuracy) was 5.8 µmol kg^{-1} for DIC and 7.2 µmol kg^{-1} for TA. The precision (average standard deviation of triplicates) was 2.7 and 5.1 µmol kg^{-1} for DIC and TA respectively. The CO_2 and DIC removal rates were calculated.

In Results 4.4, TA was measured at the start and end of each photoperiod and interpolated linearly over the four-day period. pH was measured *in continuum* as described in the experimental set-up of this section. TA and pH were used to calculate the CO_2 concentrations using CO2SYS (Table 1). In-between photoperiod treatments, seawater was changed and replaced by seawater pre-treated with CO_2 gas at the targeted pCO_2 levels.

3.5.3 Inorganic nutrients analysis

Samples of a volume of seawater was collected in vials or bottles for analysis of inorganic nutrients (nitrate and nitrite, phosphate and silicate) and were kept frozen at -20 °C until analysis using standard seawater methods. In Results 4.2 (Table1), 50 mL of seawater was sampled at the same depth of the experiments conducted in May 2015; and nutrients concentrations of the experiments conducted in May and August 2014 were analyzed in a previous vertical profile from the same station. Samples were analyzed using a Flow Solution IV analyzer from O.I. Analytical, USA. In Results 4.3 (Table 1), samples were filtered through

0.45 µm filters into 25 mL polyethylene bottles and were measured on a Scalar auto-analyzer with flow injection as detailed in (Hansen & Koroleff, 1999). In both cases the analyzers was calibrated using reference seawater from Ocean Scientific International Ltd. UK.

3.5.4 Air-sea CO_2 flux

The air-sea CO_2 exchange (ASE) flux was calculated using the following equation:

$$ASE = K_{av} \times \alpha \times \Delta pCO_2 \qquad \text{Eq. 7}$$

Where α is the solubility of CO_2 in seawater (mol m^{-3} atm^{-1}), calculated according to Weiss (1974) using the measured at the SST and salinity values. ΔpCO_2 is the difference in pCO_2 at the surface (1 m water depth) and the atmospheric pCO_2 with negative values implying an uptake by the ocean. K_{av} (m s^{-1}) is the gas transfer coefficient (Wanninkhof & McGillis, 1999). In Results 4.2 (Table 1), wind speed data used to calculate K_{av}, was obtained from monthly and daily average data from the meteorological station in Ny-Ålesund (Norwegian Institute for Air Research). In Results 4.3 (Table 1), the air-sea CO_2 flux equally calculated and the wind speed data was obtained from the meteorological station in Nuuk (Asiaq Greenland Survey).

3.5.5 Phytoplankton community composition

Samples of 100 mL were collected from untreated plankton community (3 or 5 m depth) and fixed with glutaraldehyde (at 1-1.5 %) in the section Results 4.2 and with 1.5 mL of 2 % formaldehyde in Results 4.3 (Table 1). Samples were concentrated using sedimentation chambers for 24 h prior to analysis. The cells were counted in a transmitted-light inverted microscope (Zeiss Axiovert 200) at 200x or 400x magnification. Phytoplankton cells were differentiated into genus or major taxonomic groups.

3.6 Statistical analysis

The statistical analysis applied in each study of the Results sections is summarized in Table 1. In Results 4.1, we compared volumetric rates of PP from three different methods using Reduced Major Axis (RMA) (e.g. model II regression) since each method is subject to measurement error (Legendre & Legendre, 1998). RMA regression analysis was applied on PP data log (x+1) - transformed to satisfy the

assumptions of linear regression analysis. Significance tests for slope equal to 1 from RMA equations were performed (Clarke, 1980; McArdle, 1988). Equality of means has been tested using a two-sample t-test, without assuming equality of variances. We propagated the standard error (SE) for the average PP rates taking into account the SE associated to the replicated rates. The effect of time lag between CTD casts was tested using generalized linear models (GLM) using dependent variable GPP-^{18}O and independent variables ^{14}C-TOC or ^{14}C-POC and time lag. As the incubations were done at different depths (see above), the ^{14}C and O_2-based methods were compared only for samples taken at the same depths (maximum of ~3 m difference in depth), resulting in two to three depths per station. Statistical analyses were made using the lmodel2 package (Legendre, 2014), implemented in R software version 1.0.44 (R Development Core Team 2009).

In the section Results 4.2, the response of GPP to increased CO_2 was compared among experiments in the section using the Ln-transformed effect size:

$$\text{Ln effect size GPP} = \text{Ln GPP}_E - \text{Ln GPP}_C \qquad \text{(Eq. 8)}$$

Where GPP_E and GPP_C are the mean response in the experimental and control treatments, respectively (n = 3 to 4). The effect size is frequently used in experimental ecology to quantify the proportional effect of a treatment and to facilitate the interpretation of biological results (Hedges *et al*., 1999) across experiments. An Ln effect size of GPP of zero is interpreted as having no effect on GPP, whereas a positive value indicates a positive effect of CO_2 on GPP and a negative value indicates a negative effect of CO_2. The variance in the Ln effect size was calculated following Kroeker *et al.* (2010). Moreover, comparisons based on the Ln effect size GPP did not assume normality and were heterogeneous because the experiments encompassed distinct phases of blooms, which occur rapidly and yield extreme data (i.e., very low pCO_2 and high GPP). The analyses were carried out using RStudio 0.98.945 and the "Metafor package" designed for meta-analyses (Viechtbauer, 2010).

In the section Results 4.3, the NCP response in the control was compared with the NCP response in two CO_2 treatments (Treatment 1: 576 ± 48 ppm; Treatment 2: 916 ± 34 ppm, on average) and evaluated following Student t-test ($p < 0.025$). Significant differences between the control response and the CO_2 treatment are indicated in Figure 15.

In Results 4.4, we evaluated if CO_2 (3 levels) and photoperiod (5 levels) had an effect on photosynthetic responses, as represented by $rETR_{max}$, α and Ik, and if such effects were similar or different for the three macrophyte species tested. The experiment was a split-plot design due to restricted randomization for photoperiod, i.e. each level of photoperiod was run separately (whole plot) and

without replication. Experimental units (whole plots) consisted of six aquaria that were grouped into three levels of CO_2 with two replicates for each CO_2 treatment at each photoperiod. The experimental units were sub-divided or split into different periods (sub-plots) to test the effects of varying photoperiod. However, aquaria were nested within CO_2 treatment, as the same CO_2 treatment was applied to the same aquarium for all photoperiods. All three species were randomly sampled for each sub-plot and, consequently, species variation was a factor fully crossed with the two treatment factors. Finally, individual macrophyte specimens within each aquarium were not replaced between different photoperiod levels and constituted a random factor nested within CO_2 treatment and aquarium. The following split-plot model (using capital letters for random factors) was employed for the three photosynthesis variables separately ($rETR_{max}$ and Ik were log-transformed):

$$Y_{ijkl} = \mu + \underbrace{c_i + A_l(C_j) + I_m\left(A_l(C_j)\right)}_{whole-plot} + \underbrace{p_j + p_j \times c_i + P_j \times A_l(C_j) + P_j \times I_m\left(A_l(C_j)\right)}_{split-plot}$$

$$+ \underbrace{s_k + s_k \times c_i + s_k \times p_j + s_k \times p_j \times c_i}_{species\ variations\ fixed\ effects} \qquad \text{(Eq. 9)}$$

Where μ is the overall mean, c_j= CO_2 treatment, p_i= photoperiod, s_k=species, A_l= aquarium and I_m= individual macrophyte specimen. The three main effects (p_i, c_j, and s_k) and their interaction were fixed effects, whereas variation among aquaria (A_l) and macrophyte individuals (I_m) and interactions derived from these were random. Marginal means were calculated for all the fixed effects and back-transformed to the geometric mean for the two log-transformed response variables.

The split-plot model is a generalized linear mixed model (GLMM) and was analyzed using PROC MIXED in SAS version 9.3. Statistical testing for fixed effects (F-test with Satterthwaite approximation for denominator degrees of freedom) and random effects (Wald Z-test) were carried out at a 5 % significance level. The F-test for fixed effects was partial, i.e. considering the specific contribution of the given effect in addition to all other factor

Image 4: Seawater sampling from a rosette system fitted with Niskin bottles aboard the R/V Helmer Hansen. Photo credit: R. Caeyers.

4. Results

4.1 Multi-method assessment of primary production at the NW Svalbard shelf

Aim

Here we report on rates of primary production derived using ^{14}C, O_2 mass balance and ^{18}O methods in the NW Svalbard shelf in the European Arctic and focus on comparing the rates to reconcile these three sets of measurements. We consider the pathways of carbon and oxygen within the microbial food web and provide a methodological assessment of their underlying assumptions to promote their use in the Arctic Ocean and facilitate future primary production studies in the region.

Results

While seawater for the O_2-based methods (the O_2 mass balance and the ^{18}O method) were sampled from the same CTD cast, time lags between O_2-based and ^{14}C casts ranged from 0 to 32 h. The effect of the time lag on the GLMs between GPP-^{18}O and ^{14}C-TOC and ^{14}C-POC was not statistically significant ($p = 0.14$ and $p = 0.07$, respectively). O_2 and C-based rates were on average an order of magnitude higher in May during the episodes of intense spring blooms than in August (Figure 6, Table 2). However, O_2-based estimates of PP were overall much higher than C-based estimates, particularly in spring (Table 2).

Table 2: Average volumetric rates of GPP-DO, GPP-^{18}O, ^{14}C-TOC and ^{14}C-DOC with standard errors (mean ± SE) with units mmol O_2 m^{-3} d^{-1} or mmol C m^{-3} d^{-1}. Seasonal means as well as an overall mean are reported. Results of comparisons of means with GPP-^{18}O (in grey) using a two-sample t-test are indicated (not significantly different, * for $p > 0.01$ and ** for $p > 0.05$).

	GPP-DO	GPP-^{18}O	^{14}C-TOC	^{14}C-POC
May	24.3 ± 0.9**	25 ± 2.5	13.0 ± 1.2**	6.6 ± 0.3*
August	2.8 ± 0.6**	2.0 ± 0.2	3.5 ± 0.3**	3.2 ± 0.3**
Total	15.1 ± 0.7 **	15.1 ± 1.5	9.0 ± 0.9**	5.2 ± 0.3*

Mean GPP-DO and GPP-^{18}O estimates were overall not significantly different ($p > 0.01$, Table 2), the RMA regression equation was highly correlated ($R^2 = 0.92$, , Figure 6a, Table 3) and the slope was not significantly different than 1 ($p > 0.05$, Table 3).

Table 3: Statistical parameters of RMA linear regressions on log (x+1) - transformed volumetric rates of GPP-DO, GPP-^{18}O, ^{14}C-TOC and ^{14}C-POC and the standard errors (SE). RMA linear regressions are shown in Figure 5 and Figure 6. Angle indicated between the regression line and the abscissa.

Y vs. X	Slope	2.5% Slope	97.5% Slope	Intercept	2.5% Intercept	97.5% Intercept	Angle	N	p-value	R^2	Slope diff. from 1
GPP-DO vs. GPP-^{18}O	0.98	0.85	1.14	0.08	-0.23	0.35	45	21	9E-12	0.92	p = 0.46
^{14}C-TOC vs. ^{14}C-POC	1.19	1.00	1.41	0.01	-0.26	0.24	50	25	2E-11	0.87	p = 0.16
^{14}C-POC vs. GPP-^{18}O	0.78	0.34	2.87	0.05	-3.11	0.72	38	25	0.02	0.20	p = 0.28
^{14}C-POC vs. GPP-DO	0.53	0.24	1.19	0.71	-0.46	1.23	28	21	0.01	0.31	p = 0.08
^{14}C-TOC vs. GPP-^{18}O	0.93	0.32	2.55	-0.26	-3.29	0.87	43	25	0.02	0.20	p = 0.43
^{14}C-TOC vs. GPP-DO	0.74	0.31	1.64	0.20	-1.38	0.97	37	21	0.01	0.30	p = 0.25

Mean ^{14}C-TOC and ^{14}C-POC were not significantly different (p = 0.46, Table 2), although ^{14}C-TOC rates were higher than ^{14}C-POC particularly in the spring due to the contribution of ^{14}C-DOC (Table 2), with ^{14}C-TOC and ^{14}C-POC highly correlated by the RMA regression (R^2 = 0.87, Figure 6b, Table 3) and a slope not significantly different than 1 (p = 0.16, Table 3).

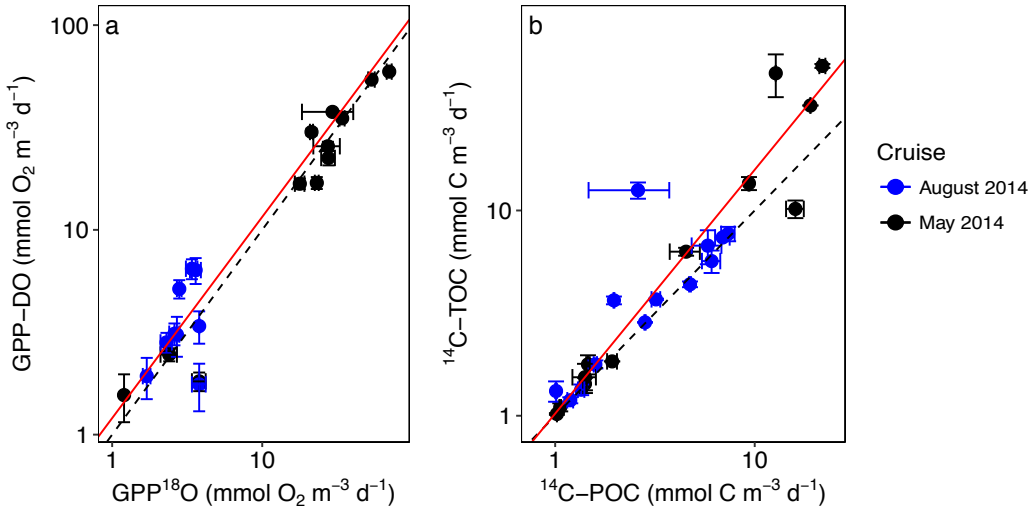

Figure 6: Relationships between the log (x+1) - transformed volumetric rates of (a) GPP-DO and GPP-^{18}O during May (in black, mean ± standard error, SE) and August (in blue, mean ± SE) of (a) and (b) ^{14}C-TOC and ^{14}C-POC within the euphotic zone (b). Dashed-lines represent the 1:1 line and red solid lines represent the RMA linear regressions whose statistical parameters are indicated in Table 3.

The slopes of the RMA regression equations between O_2-based and C-based rates were also not significantly different than 1 (p > 0.05, Table 3) and their means were not significantly different (p > 0.01, Table 2), however correlation were significantly weaker (R^2 = from 0.20 to 0.31, Figure 7, Table 3) relative to correlation within methods (R^2 = from 0.87 to 0.92, Figure 6, Table 3). C-based rates increased as the averaged 0.37 power of the O_2-based rates, thereby resulting in a relevant difference in rates (Figure 6, Figure 7, Table 2 and Table 3).

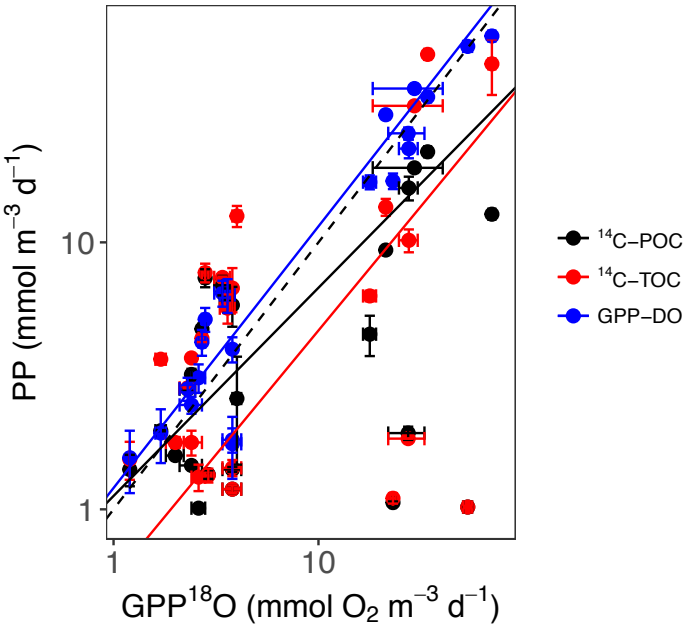

Figure 7: Relationships between the log (x+1) - transformed volumetric rates of GPP-^{18}O and GPP-DO (in blue, mean ± SE), ^{14}C-TOC (in red, mean ± SE) and ^{14}C-POC (in black, mean ± SE). Dashed-line represents the 1:1 line and the solid lines represent the RMA linear regression whose statistical parameters are included in Table 3.

These results indicate that ^{14}C-PP measurements underestimate GPP in the European Arctic Ocean, with average ^{14}C-PP estimates 40 % lower than both GPP-^{18}O and GPP-DO (59 ± 6 %). However, significant seasonal variability is also apparent. In the spring, during the phytoplankton bloom, ^{14}C-PP rates equally 54 ± 5 % and 52 ± 5 % of GPP-DO and GPP-^{18}O estimates, respectively, leading to underestimation of C-based rates. These results support previous studies that found lower rates with ^{14}C method during productive periods (Matrai *et al.*, 2013; Vaquer-Sunyer *et al.*, 2013). However, in August, when recycling processes dominated primary production and overall rates were low, ^{14}C-PP was 27 ± 13 % higher than the GPP-DO and 79 ± 18 % higher than the GPP-^{18}O estimates. For the North Atlantic, Robinson *et al.* (2009) highlighted that the difference between these methods depended on the magnitude of respiration. However, respiration rates in European Arctic communities are characteristically low (i. e. Vaquer-Sunyer *et al.*, 2013), suggesting that other processes involved caused the differences observed in Arctic plankton communities.

The 24-h photoperiod in the Arctic helps support the rapid growth and primary production of phytoplankton, but may impose higher respiratory loss such as in the Beaufort Sea, in the western Arctic, than in temperate regions (Nguyen *et al.*, 2012), as respiration is higher for phytoplankton during periods of high light availability (Bender *et al.*, 1987; Grande *et al.*, 1989a). A recent study showed that elevated phytoplankton respiration rates during periods of long day length in the high Arctic accounted for reported differences between light and dark respiration (Mesa *et al.*, 2017).The time lag between casts could be a factor impacting GPP estimates at low productivity rates, but this effect was apparently not statistically significant in our study.

GPP-^{18}O rates were also expected to exceed GPP-DO rates by upwards of 20 % greater than GPP-DO, as GPP-^{18}O has been reported to overestimate GPP due to the O_2-produced not related with C-assimilation through the Mehler reaction and photorespiration (Grande *et al.*, 1989b; Laws *et al.*, 2000), both reactions related with high irradiances (Grande *et al.*, 1989a). In the Mehler reaction, a molecule of labelled O_2 is produced and a molecule of unlabeled O_2 is consumed, being recorded as GPP by the ^{18}O method (Falkowski & Raven, 1997). Photorespiration results when O_2 binds Rubisco that leads to the excretion of glycolate (Falkowski & Raven, 1997; Beardall *et al.*, 2009). However, this was not the case in the Arctic communities studied, with GPP-^{18}O and GPP-DO rates were comparable and highly correlated in both May and August.

Daily ^{14}C uptake into particulate carbon using 24-h incubation provides an estimate of NPP (Marra, 2002; Robinson *et al.*, 2009; Regaudie-de-Gioux *et al.*, 2014). The difference between GPP-^{18}O and ^{14}C-POC rates can be assumed to represent the losses of PP due to respiration by autotrophs and heterotrophs (Grande *et al.*, 1989b). In our study, these losses accounted for 73 ± 2 % (18.3 mmol O_2 or C m^{-3} d^{-1}) and -63 ± 3 % (-1.2 mmol O_2 or C m^{-3} d^{-1}) in May and August respectively. The rapid growth of phytoplankton would raise metabolic demands, accounting for the increasing gap between methods in highly-productive Arctic communities at this time of the year. In August, when low abundance of large phytoplankton and recycling processes are dominating, average ^{14}C-PP was higher than the O_2-based estimates. Our results are agreement to observations in a recent multi-regional study where C-based rates were closer to O_2-based rates however in the study the effect of seasonality in the linearity of PP rates was not researched (Regaudie-de-Gioux *et al.*, 2014).

In addition to respiration losses, which are higher in the light than in the dark at continuous daylight (Mesa *et al.*, 2017), the C-based method includes losses due to dissolved organic carbon excretion (Bender *et al.*, 1987). In our study, ^{14}C-DOC was higher in May due to high C and O_2-based PP rates in spring, accounting for 6.4 ± 0.2 mmol C m^{-2} d^{-1} or 49 ± 2 % of the ^{14}C-TOC and 0.3 ± 0.1 % mmol C m^{-2} d^{-1} or 9 ± 2 % of the ^{14}C-TOC in August. These values compare well with previous estimates of DOC production in the Arctic (Vernet *et al.*, 1998).

Our results agree with the notion that the ^{14}C method underestimates GPP due to processes of respiration, grazing and DOC excretion (Marra, 2002; Regaudie-de-Gioux *et al.*, 2014). This was particularly notable in spring, confirming that in 24-h incubations ^{14}C approximates net primary production (NPP-^{14}C, Table 3) (Grande *et al.*, 1989b; Laws *et al.*, 2000). The main benefit of the widely-used ^{14}C method is its high sensitivity when both ^{14}C-TOC and ^{14}C-POC are measured, including the contribution of the DOC pool and allowing for the determination of photosynthesis in low-productive oceans.

In our study, this sensitivity resulted in higher ^{14}C-TOC rates than GPP-^{18}O in summer, a season characterized by low productivity rates in the Nordic and Barents seas (Matrai *et al.*, 2013). However, ^{14}C-TOC does not account for the newly incorporated organic carbon that has been respired by the predominant microbial plankton community. Short incubation times (<4h) are recommended to minimize the loss of ^{14}C-DOC that is consumed by heterotrophic prokaryotes, a process that underestimates ^{14}C-DOC in long incubations, as in this study (Steemann-Nielsen, 1952; Marra, 2002). The ^{14}C method also underestimates the C-assimilation due to release of organic ^{14}C by photorespiration (Peterson, 1980; Laws *et al.*, 2000). In contrast, the O_2 mass balance method is inaccurate to estimate GPP in the Arctic with 24-h daylight (Mesa *et al.*, 2017) and the ^{18}O method measures all O_2-producing metabolic process, including also those not related with C-assimilation, such as photorespiration (~10 % of the GPP-^{18}O) and the Mehler reaction (~10 % of the GPP-^{18}O) among other less studied processes that might have overestimated GPP (Bender *et al.*, 1999; Laws *et al.*, 2000; Dickson *et al.*, 2001; Marra, 2002). Thus, differences in the underlying assumptions of the methods yield significant uncertainty in the reported PP values, complicating comparisons.

The O_2-based methods and the ^{14}C method provide understanding of different processes critical to describe ecosystem function such as *gross and net primary production* and *respiration* at phytoplankton or community level. The choice of either method should be guided by the specific question being addressed. In this way, the methods are complementary. For Arctic waters, we recommend the use of O_2-based methods for GPP estimation, ^{14}C-TOC for NPP and ^{14}C-POC for phytoplankton carbon production when the focus is in quantifying the food available for higher trophic levels. The combination of ^{14}C-TOC and ^{14}C-POC provides information of food supply (as DOC) for the microbial food web. According to our results and the marked seasonality of the Arctic, the use of O_2-based methods during the productive period is preferable, as the C-based method involves underestimations due to respiratory processes. During low production periods, as in non-blooms conditions or under the ice locations, the use of both C and O_2-based methods is adequate.

4.2 Episodic Arctic CO_2 limitation at the W Svalbard shelf

Aim

Here we test the hypothesis that the characteristically low concentrations of CO_2 in Arctic waters during spring and summer limit the primary productivity of plankton communities, before dissolved inorganic nutrients have been fully consumed. To test this hypothesis we conducted a series of seven experiments of elevated CO_2 to study the response of planktonic GPP at the W and NW of the Svalbard shelf located in the European Arctic sector in May and August. The communities sampled experienced a range of conditions in terms of net and gross primary production and nutrient conditions. We evaluated the net biological demand of CO_2, as the NCP measured with the O_2 mass balance method, and compared this to the atmospheric supply of CO_2 through air-sea exchange. The response to elevated CO_2 of GPP measured with the ^{18}O method, was evaluated experimentally.

Results

Community metabolism and CO_2 demand

GPP-O_2 in the euphotic layer increased with increasing Chl *a* concentration ($p < 0.0001$, $R^2 = 0.81$, Figure A1), resulting in low *in situ* CO_2 concentration waters (ranging from 281 to 128 µatm pCO_2, Table 4) in all the experiments.

Table 4: *In situ* conditions and results of the experiments.

Variables		Experiments						
		May2014-1	**May2014-2**	**Aug2014-1**	**Aug2014-2**	**Aug2014-3**	**May2015-1**	**May2015-2**
Date	(d)	23/5/14	25/5/14	7/8/14	12/8/14	14/8/14	2/5/15	4/5/15
Depth	(m)	2.4	3.2	5.7	2.9	3.0	5.0	5.0
Temperature	(°C)	-0.8	-1.2	7.0	-0.4	-0.1	-1.0	-1.3
Salinity	(psu)	33.9	33.6	34.3	31.5	31.6	34.2	34.2
GPP ± SE	($\mu molO_2\ L^{-1}\ d^{-1}$)	6.2 ± 0.1	5.8 ± 0.6	1.4 ± 0.1	0.4 ± 0.03	0.8 ± 0.1	46.0 ± 6.0	82.4 ± 11.4
Avg. LN ES GPP	($\mu molO_2\ L^{-1}\ d^{-1}$)	0.5	-0.5	-1.5	-0.1	-0.6	0.2	0.2
pCO_2	(μatm)	142.5	127.9	281.2	170.8	185.7	167.5	192.5
Chl a	($\mu g\ L^{-1}$)	7.9	1.8	1.1	0.3	0.4	10.6	13.0
NO_3 + NO_2 ± SE	($\mu molN\ L^{-1}$)	0.7 ± 0.0	0 ± 0.0	10.3 ± 0.6	0.7 ± 0.0	0.5 ± 0.0	0.0	1.7
PO_4 ± SE	(μmolP L-1	0.1 ± 0.0	0.0 ± 0.0	0.7 ± 0.0	0.1 ± 0.0	0.1 ± 0.0	0.1	0.3
SiO_4 ± SE	μmolSi L-1	0.9 ± 0.1	na	4.8 ± 0.6	0.6 ± 0.0	0.7 ± 0.0	0.4	1.5
Total	(cell L^{-1})	47300	19400	870	1870	2910	10180	147302
Phaeocystis spp.	%	99.4	79.2	0.0	8.2	26.2	0	0
Diatoms	%	0.6	11.6	97.3	90.5	69.9	68.6	80.28
No identified	%	0.0	9.2	0.0	0.0	2.4	31.0	19.7
Air-sea CO_2 flux	($\mu molC\ m^{-2}\ d^{-1}$)	1504	37927	12613	33655	14823	8450	13224
Integrated NCP ± SE	($\mu molO_2\ m^{-2}\ d^{-1}$)	236302 ± 4097	290586 ± 11732	41755 ± 7814	191310 ± 17888	44962 ± 10460	nd	nd
Integrated NCP/ Air-sea CO_2 flux	No units	157.1	7.7	3.3	5.7	3.0	nd	nd
Integrated NCP/ Air-sea CO_2 flux	%	0.6	13.1	30.2	17.6	33.0	nd	nd
Ice conditions		Very open drif ice	Open drift ice	Open waters	Open drift ice	Open drift ice	Fjord mouth/ no ice	Fjord mouth/ no ice

GPP, measured with the ^{18}O method, of these low-CO_2 communities ranged from 82.4 to 5.8 µmol O_2 L^{-1} d^{-1} in spring, under blooming conditions, while in summer GPP was much lower (1.4 to 0.4 and µmol O_2 L^{-1} d^{-1}), reflecting a non-blooming and recycling nutrients period. The GPP/R ratio (between GPP-DO and dark respiration, measured with the O_2 mass balance method) was extremely high in the euphotic layer in May (43.4 ± 0.85 µmol O_2 L^{-1} d^{-1}, with a maximum value of 244.6) compared with low values in August (2.67 ± 0.73 µmol O_2 L^{-1} d^{-1}). As a result, the waters sampled were consistently undersaturated in CO_2, with the *in situ* pCO_2 range (128 to 281 µatm, Table 4) and with a broad range of primary productivity rates. Consistent with the role of biota as a CO_2 sink, there was oceanic uptake of atmospheric CO_2 at the stations sampled, which increased with increasing integrated NCP (Figure 8, Table 4). However, the input of atmospheric CO_2 was much smaller than the net demand by the plankton community, accounting for 19 % on average of the net biological removal, assuming 1:1 ratio between O_2 and C (Figure 8, Table 4).

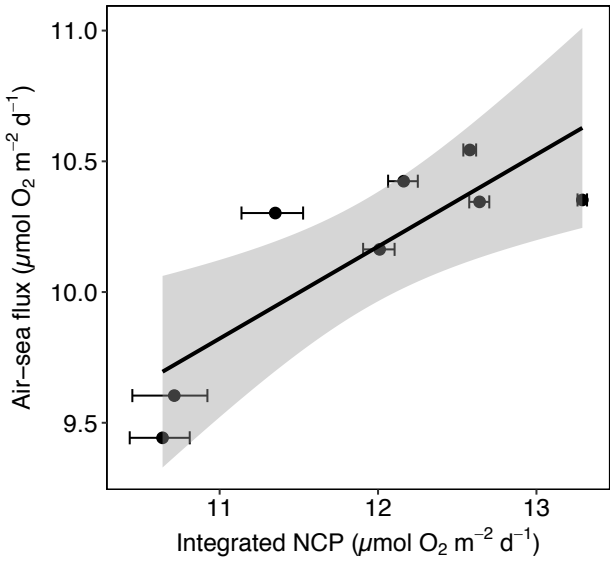

Figure 8: Oceanic uptake of CO_2 shown by the relationship between the air-sea CO_2 flux and the NCP integrated (p = 0.01, R^2 = 0.64, df = 6). The grey area represents the confidence interval (CI).

Response to experimental CO_2 additions

The range of experimentally elevated pCO_2 (178 to 1096 µatm, Table A1) was much greater than of the *in situ* pCO_2 range (128 to 281 µatm, Table 4), but it was consistent with the range reported across the Arctic Ocean (78 to 765 µatm, Bakker *et al.*, 2016). The experimentally tested plankton communities represented variable biogeochemical parameters, from low-productivity communities supported by nutrient recycling sampled in August 2014, to pre-bloom, blooming and decay phases, sampled in May 2014 and 2015.

Three of the experiments showed a positive response to CO_2 additions, all of them for communities sampled in May (May 2014-1, May 2015-1, 2) characterized by

the highest *in situ* GPP (6.2, 46 and 82.4 µmol O_2 L^{-1} d^{-1}, respectively), high Chl *a* concentration (7.9, 10.6 and 13 µg L^{-1}), low pCO_2 (< 193 µatm) and generally low nutrient concentrations but present in seawater (0.7 µmol N L^{-1}, 0.1 µmol P L^{-1} and 0.9 µmol Si L^{-1}, in May 2014-1), depleted in nitrite and nitrate and in presence of phosphate and silicate (0 µmol N L^{-1}, 0.1 µmol P L^{-1}, 0.4 µmol Si L^{-1}, in May 2015-1) and slightly higher nitrate, phosphate and silicate (1.7 µmol N L^{-1}, 0.3 µmol P L^{-1}, 1.5 µmol Si L^{-1}, in May 2015-2) (Table 4).

In these three experiments the phytoplankton communities supported high cell density, with a dominance of diatoms in May 2015-1 and 2 and a community dominated by *Phaeocystis sp.* in May 2014-1 (Table 4). The GPP yield of every community tested was calculated as the slope of the fitted regression equations between GPP and the concentration of added CO_2 (Figure 9, Table A1). The GPP yield per µmol added CO_2 increased with increased GPP at *in situ* CO_2 concentration, being 10-fold times higher in spring than in summer (Figure 9).

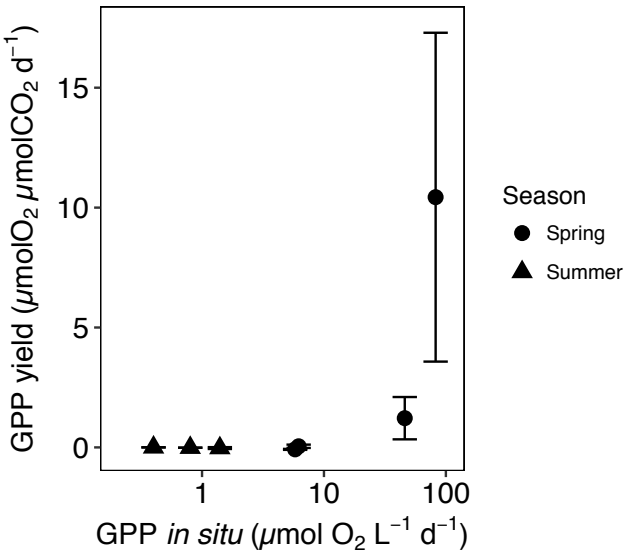

Figure 9: The relationship between the average (± SE) GPP yield per µmol of added CO_2 in each community tested and the GPP at *in situ* pCO_2. The shape corresponds with the communities tested in spring (circles) and summer (triangles).

The response of GPP to CO_2 addition was negative in four of the seven experiments, including all of the experiments conducted in August and the experiment of May 2014-2, with communities generally characterized by low GPP (from 5.8 to 0.4 µmol O_2 L^{-1} d^{-1}), low Chl *a* concentration (1.8 to 0.3 µg L^{-1}), low pCO_2 (ranging from 128 to 281 µatm) and low abundance of phytoplankton, dominated by diatoms (Table 4). Dissolved inorganic nutrients concentrations were generally low in nitrite and nitrate (~ 0.7 µmol N L^{-1}), phosphate (~ 0.1 µmol P L^{-1}) and silicate (~ 0.6), except for the August 2014-1experiment, which showed high nitrate concentrations (10.3 µmol N L^{-1}) and high silicate concentrations (4.8 µmol Si L^{-1}) although *in situ* GPP did not respond to CO_2 addition at high nutrient levels (1.4 µmol O_2 L^{-1} d^{-1}). All of the stations had low salinity (< 34.3) and low temperatures (< 0.1 °C), except in the experiment August 2014-1 that the temperature was 7 °C, probably due to the proximity of surface waters to the WSC that transports warm Atlantic water mass.

A meta-analysis of the experimental results showed patterns in the range of responses observed. In particular, the response to CO_2 enrichment, measured as the Ln effect size of GPP, increased significantly with the biomass of communities tested ($p = 0.002$, $R^2 = 0.36$, Figure 10a). The Ln effect size of GPP became positive, indicative of an increase in GPP under elevated CO_2, during dense blooms in which the Chl *a* concentration was in excess of about 7 µg Chl *a* L^{-1} (Figure 10a). The Ln effect size of GPP declined with increasing *in situ* pCO_2 and became positive when the *in situ* pCO_2 was below 150 µatm (Figure 10b).

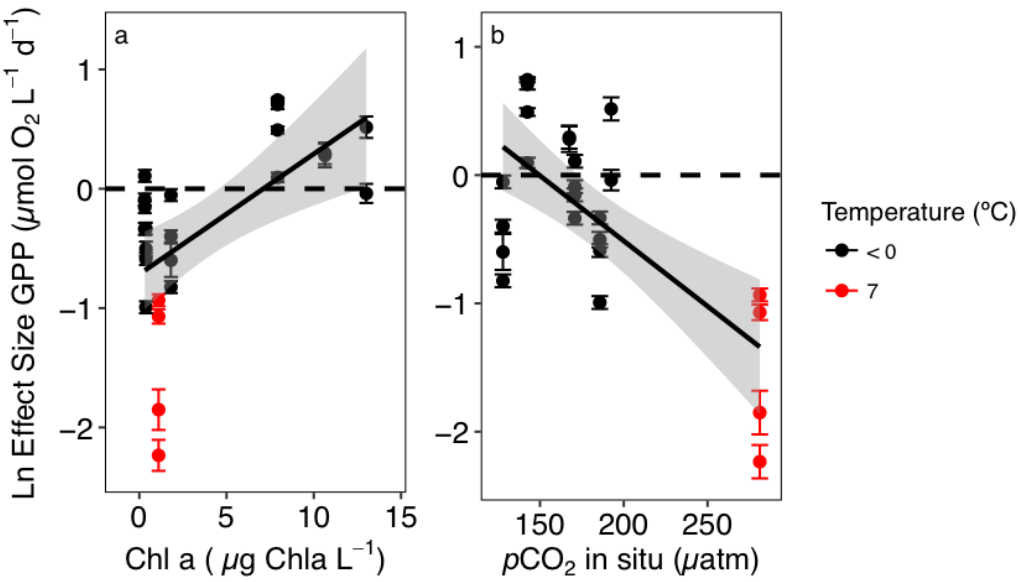

Figure 10: The relationship between the Ln Effect Size of GPP (± SE) and: a) *in insitu* Chl *a* concentration in the communities tested and the regression equation (Ln Effect Size of GPP = -0.7 (±0.17) + 0.10 (±0.3) Chl *a*; $R^2 = 0.36$, p-value = 0.002); and b) the *in situ* pCO_2 and the regression equation (Log Effect Size of GPP = 1.52 (±0.43) - 0.01 (±0.00) *in situ* pCO_2; $R^2 = 0.50$, p-value = 0.0001) at temperature < 0°C in black and 7°C in red. The grey area represents the CI.

The strongest GPP stimulation was found in a community with intermediate GPP (6.2 ± 0.1 µmol O_2 L^{-1} d^{-1}, May 2014-1) and dominated by *Phaeocystis sp.* (99.4% of the biovolume, Figure 11, Table 4, Table A1). Two diatom-dominated communities (51.5% and 76.6% of the microphytoplankton biovolume) with high GPP (46 ± 6 and 82.4 ± 11.4 µmol O_2 L^{-1} d^{-1}) were also stimulated by CO_2 enrichment (May 2015-1 and May 2015-2 respectively, Table 4, Table A1).

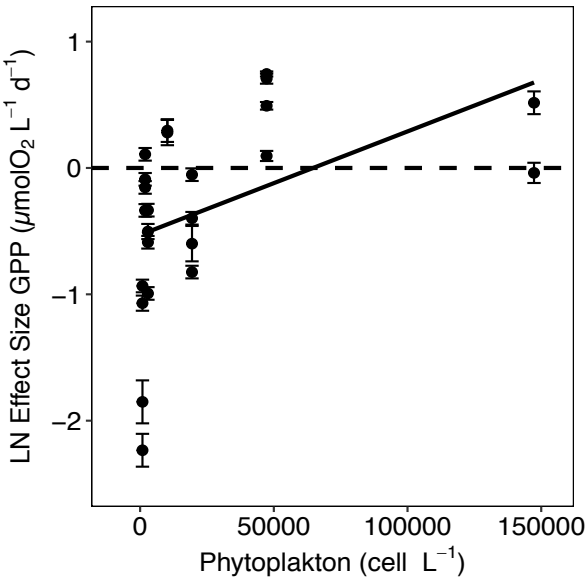

Figure 11: The Ln Effect Size of GPP (± SE) in relation to the total abundance of phytoplankton. The solid line represents the regression equation (p-value < 0.05, R^2 = 0.20).

As a result of CO_2-unsaturated waters and the low atmospheric CO_2 input (Figure 8), the turnover of CO_2 in the communities tested, calculated as the slopes of fitted regression equations between the CO_2 removal rates (in units of µmol CO_2 L^{-1} d^{-1}) and the concentration of added CO_2 increased with increasing *in situ* GPP (Figure 12, Table A1).

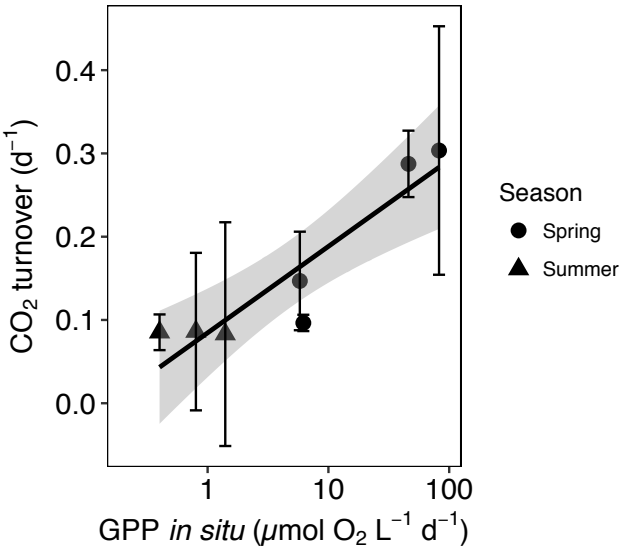

Figure 12: The relationship between CO_2 turnover (± SE) and GPP at *in situ* pCO_2 and the regression equation (CO_2 turnover = 0.10 (±0.02) + 0.003 (±0.0005) GPP *in situ*, R^2 = 0.87, p-value = 0.001), the shaded area indicates the 95 % confidence interval (CI) of the regression equation. The shape corresponds with the communities tested in spring (circles) and summer (triangles).

The atmospheric resupply of CO_2 was far too slow to compensate for the observed biological drawdown of CO_2 (19 %, Figure 8), resulting in low CO_2 waters during the Arctic spring bloom (Kaltin *et al.*, 2002; Bates *et al.*, 2006; Bates and Mathis, 2009; Fransson *et al.*, 2009, 2017). Upward CO_2 flux from deeper layers was also likely to be low due to the seasonal stratification produced by sea-ice melting in the same area leads to small upward nitrate fluxes (Randelhoff *et al.*, 2016). The large imbalances that we observed between net biological CO_2 consumption and atmospheric CO_2 resupplies explain the sensitivity of the Arctic phytoplankton community to CO_2 limitation. The time for photosynthetic removal of the CO_2 pool, in the absence of recycling mechanisms, ranged from more than 10 days for the

least productive communities in summer to 3 days for communities in an active phase of the spring bloom (Figure 12). Respiratory remineralization of CO_2 was characteristically low during the spring bloom (40-fold lower than photosynthetic uptake, i.e., GPP/R = 43) as is the atmospheric input of CO_2, leading to CO_2 depletion and creating the conditions for CO_2 limitation during the spring bloom. The peak of the spring Arctic bloom was characterized by autotrophic communities with high net biological CO_2 demand and high GPP/R ratios on average (43 ± 0.8) as previous studies showed (Vaquer-Sunyer *et al.*, 2013), acting as CO_2 sinks during the spring. In August, when recycling processes drive primary production, the GPP/R ratios on average were more than 10-fold lower (3 ± 0.7).

Accordingly, increased GPP with CO_2 enrichment was generally observed (3 of 4 experiments) in spring (May 2014-1, May 2014-2 and May 2015), along with a very high GPP yield per unit CO_2 added, whereas suppression was observed in the summer experiments. The plankton communities tested spanned a range of bloom stages according to the season and the location and yielded a broad diversity of responses to increased CO_2, from increased GPP, generally observed in the spring, to suppression of GPP in the summer. This is consistent with expectations, as high net biological demand for CO_2 in spring, along with low resupply from respiration rates and air-sea exchange, lead to a rapid CO_2 depletion; whereas there is a closer balance between community production and respiration during the recycling mode, in summer, when communities are strongly nutrient-limited, releases them from CO_2 limitation. The finding of a prevalence of suppression of GPP with CO_2 enrichment in the summer is surprising, as we expected no effect, but not a negative effect. The broad diversity of responses observed further allowed us, through a meta-analysis approach, to explore the conditions associated with CO_2 limitation. In particular, we found that these divergent results were dependent on the biological demand of CO_2 and the extent of CO_2 depletion in the water column and the biological demand for CO_2, all of which are related to the seasonal development of Arctic phytoplankton supporting the hypothesis of episodes of CO_2 limitation during highly productive periods in spring, such as the spring blooms.

We observed the most negative effect size (i.e., suppression of GPP with addition of CO_2) in a community sampled in warm surface water and slightly influenced by sea-ice melting (with 7°C temperature and 34.3 salinity), likely indicating the proximity of the WSC, transporting warm Atlantic water mass. This community was supported a low Chl *a* concentration and the highest *in situ* pCO_2 (281 µatm) relative to the communities sampled in the rest of the experiments (Figure 10). This negative result is consistent with the temperature dependence of the experimental CO_2 effect on GPP reported by Holding *et al.* (2015) as well as with the temperature threshold of 4°C at which Arctic plankton communities have been shown to shift from autotrophic to heterotrophic (Holding *et al.*, 2013). However, the mechanism through which added CO_2 suppresses GPP is unclear. It may

involve indirect effects of changes in pH on cellular composition (Taraldsvik & Myklestad, 2000) or the availability of other nutrients, such as trace metals (Saito & Goepfert, 2008; Shi *et al.*, 2010; Xu *et al.*, 2010, 2012). No or little response is expected in waters with pCO_2 near atmospheric equilibrium (Mercado & Gordillo, 2011) and increases in GPP were expected in cold waters with depleted CO_2 relative to atmospheric equilibrium but still containing enough dissolved inorganic nutrients to support production (Holding *et al.*, 2015).

Our results showed that GPP increased by 32 to 72 % (Table A1) on average when CO_2 was added during a phytoplankton bloom (Chl *a* > 7 μg L^{-1}) with high CO_2 demand (GPP > 6 μmol O_2 L^{-1} d^{-1}), low pCO_2 (< 150 μatm) and in presence of low nutrients concentrations, conditions that approximately define episodes of CO_2 limitation during Arctic spring blooms. It was previously found that the CO_2 concentration limits photosynthesis of phytoplankton bloom episodes in semi-enclosed systems (Mercado & Gordillo, 2011), but the environmental conditions for CO_2 limitation in Arctic communities have not yet been defined. Moreover, previous experimental results showed that increased CO_2 concentrations may increase primary production in nutrient-poor communities (Hein & Sand-Jensen, 1997) and nutrient-depleted conditions resulted in carbon-overconsumption (Taucher *et al.*, 2015). Such carbon-overconsumption has been observed (Sambrotto *et al.*, 1993; Banse, 1994) and has been associated with experimental nutrient stress (Taucher *et al.*, 2012, 2015), suggesting that episodes of CO_2 limitation could extend into the later phases of a bloom.

Positive responses of GPP with elevated CO_2 were observed in highly productive communities (Figure 11), one of them dominated by *Phaeocystis sp*. and two dominated by diatoms. The strongest enhancement was observed in the community controlled by *Phaeocystis sp.* (Table 4, Table A1), which is an important Arctic haptophyte that is highly concentrated close to drifting ice (Wassmann *et al.*, 1999). *Phaeocystis sp*. is considered to have less-efficient CCMs than diatoms have (Rost *et al.*, 2008). Elevated CO_2 produces a decrease in inorganic carbon affinity and leads to strong downregulation in the expression of CCMs in some eukaryotic algae such that the diffusive entry of CO_2 can be facilitated (Giordano *et al.*, 2005; Reinfelder, 2010; Raven *et al.*, 2011). This suggests a possible mechanism through which the GPP of *Phaeocystis sp.* and diatoms are stimulated during CO_2-enriched conditions. Besides, in our study the abundance of *Phaeocystis sp*. was observed to increase when pCO_2 concentrations were lower than 150 ppm, which can potentially influence competitions among phytoplankton species (Tortell *et al.*, 2002). *Phaeocystis sp.* replaces diatoms when the growth of diatoms is limited by the availability of silicic acid while other nutrients remain available to support growth of non-diatom taxa (Lasternas & Agustí, 2010). Recently, an under ice bloom in the Arctic dominated by *Phaeocystis pouchetii* was detected earlier than expected with subsequent decline of DIC (Assmy *et al.*, 2017). Our results indicate

that both *Phaeocystis sp.* and diatoms are sensitive to CO_2 limitation during highly productive periods in W of the Svalbard shelf although *Phaeocystis sp.* might be more sensitive than diatoms when CO_2 resupply is scarce. Although our results may be apply only to the area tested, they are relevant because the European sector of the Arctic contributes 50 % of the annual Arctic Ocean plankton production (Arrigo, 2007).

Our results add to those of Holding *et al.*, (2015) and suggest that increased atmospheric CO_2 and the resulting increased air-sea CO_2 supply may stimulate Arctic spring algal blooms at certain conditions (high biomass, presence of nutrients and low pCO_2). However, this expectation assumes that the nutrient supply will not be affected by concurrent changes. Increased stratification, due to Arctic warming and freshening may reduce vertical nutrient supplies from deeper layers (Sarmiento *et al.*, 2004; Wassmann, 2011; Randelhoff *et al.*, 2017), possibly reducing the intensity and timing of the spring algal bloom and, therefore, reducing its carbon demand and potential CO_2 limitation. In contrast, areas currently covered by ice would, as the extent of ice continues to decline, support stronger algal spring blooms (Arrigo *et al.*, 2008), during which episodes of CO_2 limitation, such as those demonstrated in this study, may persist.

4.3 CO_2 limits subarctic spring bloom production

Aim

Here we experimentally identify a window of time of CO_2 limitation in a subarctic phytoplankton bloom, after the peak bloom stage. During this time, the net productivity of the spring bloom, estimated with the O_2 mass balance method, was stimulated by CO_2 additions. Data was collected weekly from late February to late May in 2016 producing a time series on the bloom development coupled with experiments of added CO_2 additions in Godthåbsfjord in West Greenland.

Results

Phenology of CO_2 limitation of the Arctic spring bloom

The central part of the Godthåbsfjord showed a marked seasonality: in late February, the pCO_2 in the surface water (370 µatm) was close to atmospheric equilibrium, temperature was low (-0.8 °C) and salinity was relatively high (33.1, at 5m depth). During March and in early April, the pCO_2 decreased to 355 µatm, temperature slightly increased, on average (-0.2 °C) as well as salinity (33.3, Figure 13, Table A2). The spring plankton bloom was initiated in the last week of April and reached a maximum chlorophyll a concentration of 8 µg Chl *a* L^{-1} on May 2nd at 1m, with a surface temperature of 1.1 °C. This resulted in a decrease of the pCO_2 to 305 µatm and depletion of the dissolved inorganic nutrients in the surface waters. Nitrate and nitrite declined from 9.6 to 2.5 µmol N L^{-1}in one week, with similar declines observed for phosphate (0.8 to 0.3 µmol P L^{-1}) and silicic acid (6 to 3.7 µmol Si L^{-1}) concentrations (Figure 13). Plankton NCP increased 32-fold from low winter values of 1.2 ± 0.4 µmol O_2 L^{-1} d^{-1} prior to bloom development to 38.8 ± 1.0 µmol O_2 L^{-1} d^{-1} on May 2nd.

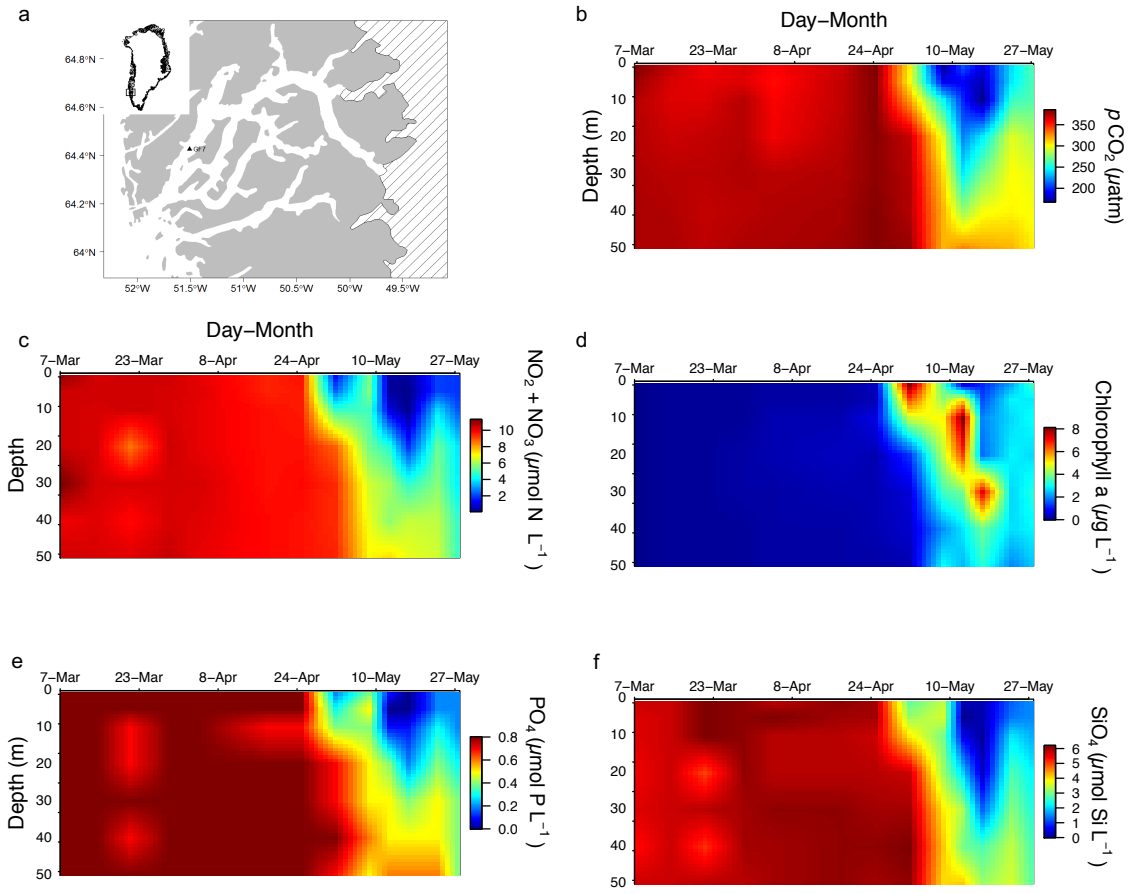

Figure 13: Seasonal development of the spring bloom in the upper 50 m of the water column for a) map showing the Godthåbsfjord system in West Greenland; b) pCO_2; c) nitrate and nitrite concentration; d) chlorophyll *a* concentration; e) phosphate concentration and f) silicic acid concentration on the sampling station sampled for March 7th to May 27th.

The phytoplankton abundance also increased from low cell abundance of about 273 cells L^{-1} prior to bloom development to a maximum abundance of $2.8 \cdot 10^5$ cells L^{-1}, mostly consisting of diatoms (Figure 14, Table A2). As a consequence, the removal rate of dissolved inorganic carbon (DIC) reached a maximum value of 29.9 ± 0.7 µmol C L^{-1} d^{-1} Table A2). One week later, May 9th, the nutrient concentrations increased slightly (5.6 µmol N L^{-1}, 0.5 µmol P L^{-1} and 4 µmol Si L^{-1}, Figure 13), the pCO_2 declined further (171 µatm at 1 m depth), the DIC removal rate remained high (23.6 ± 4 µmol C L^{-1} d^{-1}). However, the Chl *a* concentration, the NCP and the phytoplankton abundance at the sea surface were already decreasing relative to the maximum values attained on May 2nd (Figure 13, Table A2). On day 13th May, the maximum Chl *a* of 8.1 µg L^{-1} was found deeper (at 10 m depth) and the pCO_2 remained low at 191 µatm, temperature increased (1.8 °C) and salinity decreased (32.3) at 5 m depth (Figure 13). The minimum pCO_2 (168 µatm) was observed four days later (May 17th), the maximum Chl *a* was found even deeper, at 20 m depth, temperature continued to increase (2.1 °C) and salinity decreased slightly (32). Calculations of air-sea exchange indicated that the maximum air-sea CO_2 supply

rate (-147.7 mmol CO_2 m^{-2} d^{-1}, Table A2) during the bloom episode was insufficient to resupply the CO_2 removed by NCP, since the atmospheric input only supplied 22 % of that removed with NCP (1:1 ratio assumed).

The phytoplankton abundance increased with NCP (Figure 14) and the community was entirely dominated by diatoms from late February to late May, consisting mostly of *Navicula pelagica*, *Thalassiosira* spp. and pennate diatoms during the bloom. Diatoms such as *Chaetoceros* spp. and *Fragilariopsis oceanica* were also present in lesser abundances and dinoflagellates (*Protoperidinium* spp.) were observed, but in very low abundance. During the declining phase of the bloom, on the 27th of May, spores of *Thalassiosira* spp. were found (Figure 14), indicating that the spring bloom had reached the senescent phase (Arendt *et al.*, 2010; Krawczyk *et al.*, 2015).

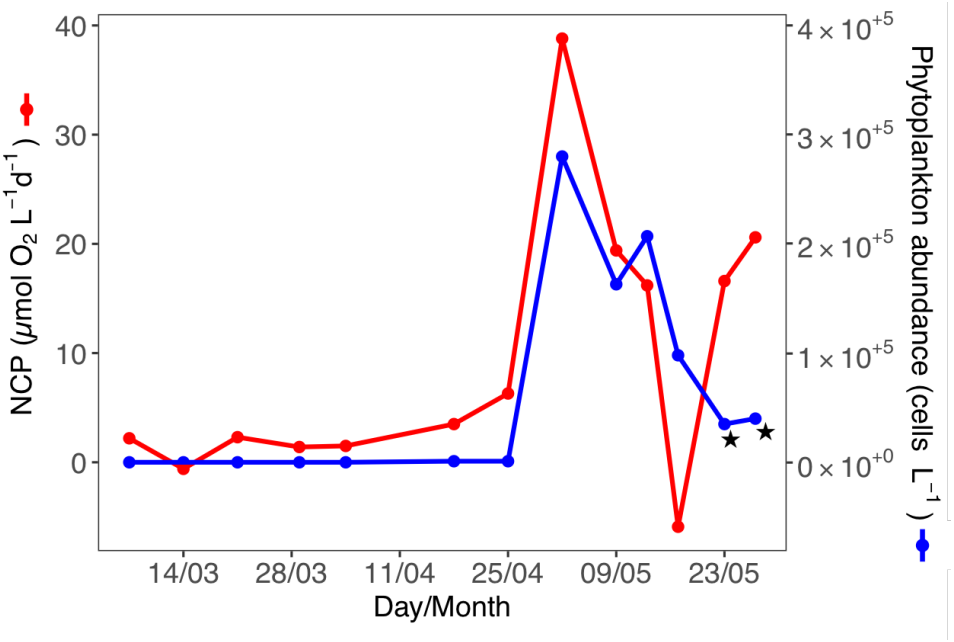

Figure 14: Net Community Production (NCP) and phytoplankton abundance at 5 m depth at station GF7 from March 7th to May 27th, 2016. Stars indicate the presence of spores of *Thalassiosira spp*.

During the winter and at the peak of the spring bloom, when pCO_2 was still relatively high (300 µatm), CO_2 additions did not enhance NCP of the surface plankton community, and sometimes even had a negative effect, (from February 29th to May 2nd, Figure 15). However, depletion of pCO_2 below 200 µatm with sustained high nutrient levels lead to a significant enhancement of the NCP with 52% by CO_2 additions on May 9th (CO_2 treatment 2, $p < 0.025$, Student t-test, Figure 15). Four days later, on May 13th, the NCP was stimulated by 17% with CO_2 additions (CO_2 treatment 1), with dissolved inorganic nutrients close to depletion (0.3 µmol N L^{-1}, 0 µmol P L^{-1} and 1 µmol Si L^{-1}, Figure 13). After four days more, on May 17th, CO_2 increased NCP by 176% (CO_2 treatment 2, $p < 0.025$, Student t-test),

from negative NCP at ambient pCO_2 to positive NCP at elevated CO_2, despite very low nutrient concentrations (0.1 µmol N L^{-1}, 0 µmol P L^{-1}, 1.2 µmol Si L^{-1}). In summary, the highest increase in NCP was found at the CO_2 treatment 2 after the peak bloom stage (from May 9th to 17th). Thus, CO_2 additions stimulated NCP for about 2 weeks following peak spring bloom development (Figure 15). After nutrient depletion, low pCO_2, increased temperature and low salinity, during the days from May 23rd to 27th, the dissolved inorganic nutrients increased slightly as well as pCO_2 (244 and 262 µatm, respectively) and salinity, whereas temperature decreased (from 1.9 to 1.6 °C). CO_2 additions resulted in a significant decline in NCP ($p < 0.025$, Figure 15), the highest decline was found at the CO_2 treatment 1 (Figure 15).

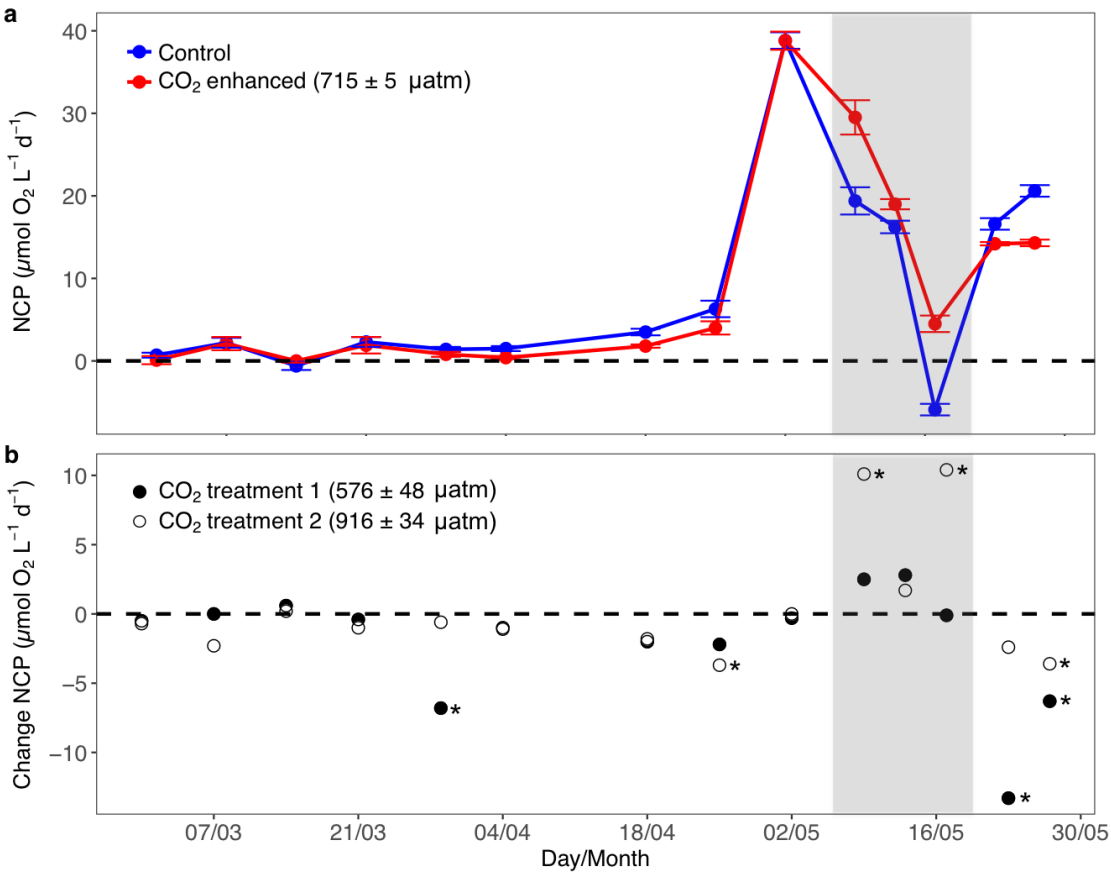

Figure 15: a) Net community production (NCP) in the control (in blue) and the maximum response of NCP to the CO_2 treatments (1 or 2, in red); b) the change in NCP between the control and the NCP response at CO_2 treatment 1 (mean ± SE) of CO_2 (in black) and at CO_2 treatment 2 (mean ± SE, in white) from February 28th to May 27th in 2016. The grey shadow indicates the 2-week period of CO_2 stimulation.

The spring bloom development, which lasted for three weeks at this subarctic locality in Greenland, led to a decline in pCO_2 and nutrient concentrations, resulting in a decline in pCO_2 of 56% to reach values around 170 µatm, potentially limiting to phytoplankton photosynthesis (Mercado & Gordillo, 2011). Similar

bloom conditions have previously been observed in this fjord system with peak NCP values in late May, at pCO_2 values that was also depleted to 56% of winter values (Sejr *et al.*, 2014; Meire *et al.*, 2015, 2016)

Experimental CO_2 addition in the two weeks following the peak spring bloom phase enhanced NCP by, on average, 7.4 μmol O_2 L^{-1} day^{-1} (Figure 14) supporting the hypothesis that CO_2 can limit NCP and, therefore, limit CO_2 removal at the late stages of the Arctic spring bloom. During this time window, nutrients and pCO_2 were declining and NCP was stimulated by CO_2 additions despite the low concentrations of nitrate, phosphate and silicic acid, probably producing carbon-overconsumption associated with nutrients-stressed communities (Sambrotto *et al.*, 1993; Hein & Sand-Jensen, 1997; Taucher *et al.*, 2015). After nutrient depletion and low pCO_2, pCO_2 increased (> 200 μatm) leading to non-limiting values that explain the negative effect of CO_2 addition in NCP (Figure 15).

Diatoms are generally considered to be unlikely to benefit from CO_2 enrichment (Kroeker *et al.*, 2010; Torstensson *et al.*, 2012) due to their efficient CCMs, which increase the CO_2 concentration at the site of carbon fixation (Rost *et al.*, 2008). However, the NCP of the plankton communities stimulated by CO_2 additions in the Arctic fjord examined here were completely dominated by diatoms, indicating that the diffusive entrance of CO_2 seems to be facilitated by higher CO_2 concentrations as suggested by other authors (Rost *et al.*, 2003). Several studies have demonstrated that the response of phytoplankton to increased CO_2 is species-specific due to the different sensitivities of CCMs (Tortell *et al.*, 2002; Rost *et al.*, 2003; Riebesell, 2004; Giordano *et al.*, 2005; Sobrino *et al.*, 2008; Reinfelder, 2010). However, most of the studies are based on single species of marine phytoplankton, and studies examining natural phytoplankton assemblages generally report enhanced photosynthetic rates and growth of Arctic natural plankton communities with elevated CO_2 (Engel *et al.*, 2013; Schulz *et al.*, 2013, 2017; Holding *et al.*, 2015), although this response seems to be temperature-dependent, restricted to the low temperatures characteristic of the spring period (Holding *et al.*, 2015) and low light irradiance (Hoppe *et al.*, 2017). However, reports of CO_2 limitation for the Arctic Ocean did not target specifically the spring bloom and, therefore, failed to resolve the phenology of CO_2 limitation of Arctic pelagic production.

In summary, we provided a seasonal assessment of the phenology of CO_2 limitation for Arctic pelagic production, demonstrating the existence of a short time window where NCP can be stimulated by CO_2 addition. This window existed after the peak production of the bloom when pCO_2 is < 200 μatm and nutrients are still available to support diatom growth and lasted nine days (from 9 to 17 May) of the 3-week long spring bloom (from 25 April to 17 May), with CO_2 addition potentially increasing NCP by 17% to 167% during this CO_2 limitation period. This period was also characterized by sinking of the diatom bloom, with maximum Chl *a*

concentration sinking progressively from 1 m down to 20 m depth during the CO_2-limited late phase of the spring bloom. In contrast, CO_2 additions either had no effect or reduced NCP in the pre- or post-bloom stages, possibly through indirect effects of CO_2 on pH-controlled processes, such as the speciation and toxicity of heavy metals (Millero *et al.*, 2009).

The Arctic Ocean is an important sink for atmospheric CO_2 (Bates & Mathis, 2009) and the strong drawdown of CO_2 with low pCO_2 due to the biological uptake and the input of sea ice melt and glacier waters during much of the productive season, is expected to affect Arctic primary production (Rysgaard *et al.*, 2009; Meire *et al.*, 2015). The NCP by the Arctic spring bloom is ultimately constrained by nutrient supply, but increased CO_2 supply may lead to a faster CO_2 removal and, potentially CO_2-overconsumption. It has been observed that at high CO_2 levels, carbon consumption increases whereas nutrient uptake remain the same, with a carbon relative to nitrogen drawdown in excess of the carbon:nitrogen ratio in the ocean (Riebesell *et al.*, 2007). Recent studies indicate that freshwater accumulation is reducing nutrient inventories and primary production in the euphotic zone of Arctic waters (Coupel *et al.*, 2015; Yun *et al.*, 2016) probably due the strong stratification produced by the freshening (McLaughlin & Carmack, 2010; Post *et al.*, 2013). Freshening decreases pCO_2 (Meire *et al.*, 2015) potentially increasing, CO_2 limitation. Modelling predictions indicate increases in primary production in the Eurasian perimeter, where less ice-cover implies less Arctic water and less stratification, while decreases are predicted North of Greenland and Canada (Slagstad *et al.*, 2015), but the CO_2 effect on Arctic primary production reported here was not included in these predictions. Increases in NCP as a consequence of increased CO_2 may increase the loss of organic carbon from the upper layer and stimulating vertical flux to the sea floor or below the sequestration horizon, thereby being sequestered through the biological pump, rather than be re-mineralized by microbial and grazer activity in the water column (Riebesell *et al.*, 2007; Passow & Carlson, 2012). In any case, the response of the Arctic ecosystem to the combined effects of increased CO_2 and freshening needs to be better understood for accurate predictions of future changes in NCP.

4.4 Long day length and increased CO_2 in subarctic macrophytes

Aim

Here we experimentally test the hypotheses that longer photoperiods (12:12, 15:9, 18:6, 21:3 and 24 light:dark hours) and increased CO_2 supply relative to the low ambient CO_2 levels of Arctic waters (200, 400 and 1000 ppm) increase photosynthesis of subarctic marine macrophytes, which would support the projected expansion of marine vegetation in the future Arctic. We use two macroalgae species (*A. nodosum* and *F. vesiculosus)* and one seagrass species (*Z. marina*) as test organisms that were alternately exposed to every photoperiod for 4 days.

Results

Rapid light curves (RLC) of *A. nodosum* (Figure A2),*F. vesiculosus* (Figure A3) and *Z. marina* (Figure A4) reflected the photosynthetic performance of the species at each photoperiod and CO_2 treatment. The RLC typically flattened out for all three species around 200 µmol photons m^{-2} s^{-1}, but light saturation, Ik, was reached at lower light levels for *F. vesiculosus* and *Z. marina* than *A. nodosum* (Figure A2, Figure A3 and Figure A4).

Photoinhibition was not detected. $rETR_{max}$ and saturating irradiance, Ik, varied significantly among photoperiods with the highest values recorded at 24 h-light photoperiod (Figure 16a, Figure 16c, Table 5), with the highest average values for *A. nodosum* among species (Figure 16g, Figure16i, Table 5). $rETR_{max}$ increased 15%, on average, from 200 ppm of pCO_2 to 1000 ppm (from 21.2 to 24.4 µmol electrons m^{-2} s^{-1}) although the effect of the CO_2 treatment was not significant (Figure 16c, Table 5).

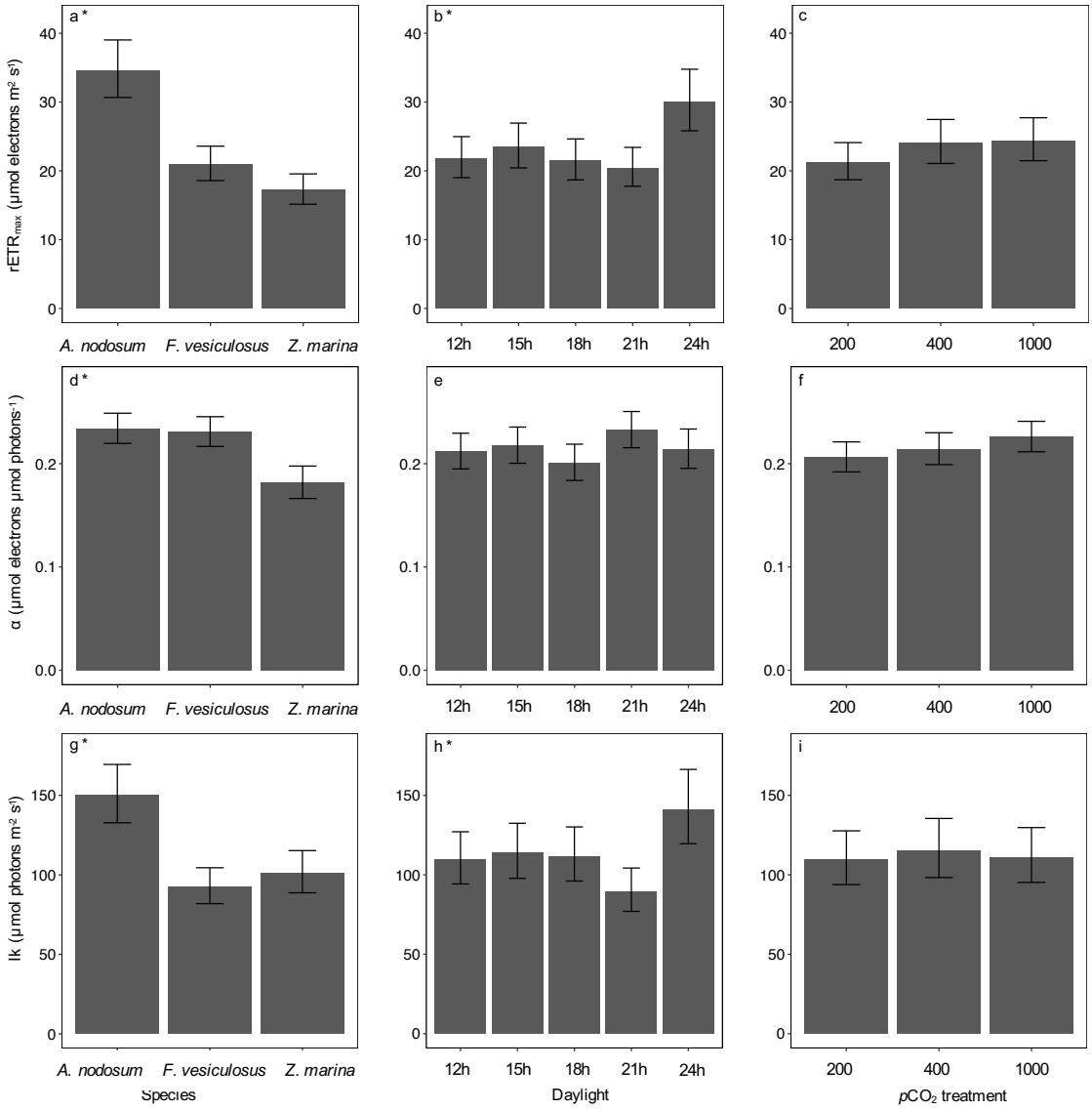

Figure 16: Estimated means of $rETR_{max}$ (a, b, c), α (d, e f,) and saturating irradiance, Ik (g, h, i) for different species (*A. nodosum*, *F. vesiculosus* and *Z. marina*), levels of daylight and pCO_2 treatments (200, 400 and 1000 ppm). Significant fixed factors are indicated with an asterisk ($p < 0.05$). Error bars mark standard errors of the means.

The photosynthetic efficiency, α, was significantly different between species with higher values for both macroalgae compared to *Z. marina* (Figure 16h, Table 5). The CO_2 effect on α was not significant but a gradual increase of 10% was observed from 200 to 1000 ppm (Figure 16f, Table 5), while Ik did not show an effect of CO_2.

Table 5: Statistical tests of the fixed effects for the three photosynthetic responses. Denominator degrees of freedom was calculated with Satterthwaite's approximation. Significant fixed factors are indicated with an asterisk ($p < 0.05$).

Parameter	Effect	Numerator Df	Denominator Df	F-value	p-value	
$rETR_{max}$	CO_2 treatment	2	9.0	1.4	0.30	
$rETR_{max}$	Photoperiod	4	14.6	4.6	0.01	*
$rETR_{max}$	Photoperiod*CO_2 treatment	8	14.2	0.7	0.72	
$rETR_{max}$	Species	2	8.6	34.9	7.7E-05	*
$rETR_{max}$	CO_2 treatment*Species	4	8.4	1.3	0.34	
$rETR_{max}$	Photoperiod*Species	8	87.5	1.3	0.27	
$rETR_{max}$	Photoperiod*CO_2 Treatment*Species	16	85.9	0.6	0.88	
α	CO_2 treatment	2	9.9	1.8	0.22	
α	Photoperiod	4	33.4	1.7	0.17	
α	Photoperiod*CO_2 treatment	8	32.7	0.7	0.68	
α	Species	2	9.8	14.1	1.3E-03	*
α	CO_2 treatment*Species	4	9.7	0.2	0.95	
α	Photoperiod*Species	8	32.8	3.8	2.9E-03	*
α	Photoperiod*CO_2 Treatment*Species	16	32.1	1.5	0.14	
Ik	CO_2 treatment	2	3.0	0.1	0.90	
Ik	Photoperiod	4	13.0	4.8	0.01	*
Ik	Photoperiod*CO_2 treatment	8	12.6	1.4	0.28	
Ik	Species	2	23.6	23.9	2.1E-06	*
Ik	CO_2 treatment*Species	4	23.1	1.0	0.41	
Ik	Photoperiod*Species	8	91.4	3.8	7.3E-04	*
Ik	Photoperiod*CO_2 Treatment*Species	16	90.2	1.1	0.38	

The interaction effect between the different photoperiods and the species was significant for α and Ik (Figure 17, Table 4). *Z. marina* showed the highest increase in $rETR_{max}$ on average from the photoperiod of 12 h to 24 h (10.7 µmol electrons m^{-2} s^{-1}); followed by *A. nodosum* (9.9 µmol electrons m^{-2} s^{-1}) and the lowest increase was observed in *F. vesiculosus* (3.2 µmol electrons m^{-2} s^{-1}, Figure 17a).

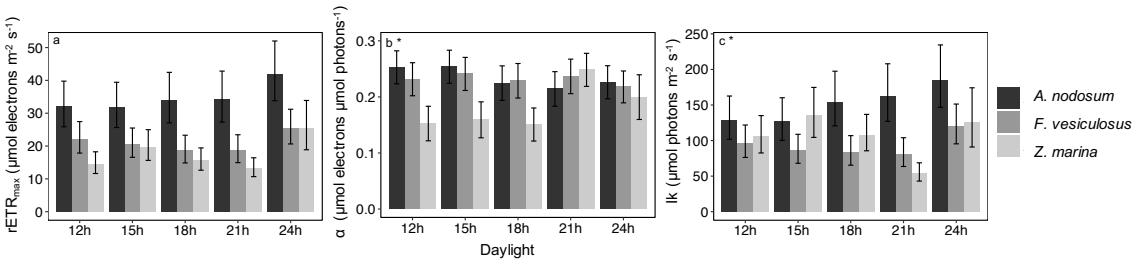

Figure 17: Estimated means of $rETR_{max}$, (a) α (b) and saturating irradiance, Ik (c) for different combinations of photoperiod and the species (*A. nodosum*, *F. vesiculosus* and *Z. marina*), i.e. $s_k \times p_j$ in the mixed model. Significance of the interaction is indicated with an asterisk ($p < 0.05$). Error bars mark standard errors of the means.

The interaction effect between CO_2 treatments and species was not significant for any of the photosynthetic responses, but *A. nodosum* showed the highest $rETR_{max}$ and Ik at 1000 ppm (Figure 18). The random effects for the three photosynthetic parameters showed significant residual variation while remaining random effects (aquarium and individual macrophyte specimen) were not significant.

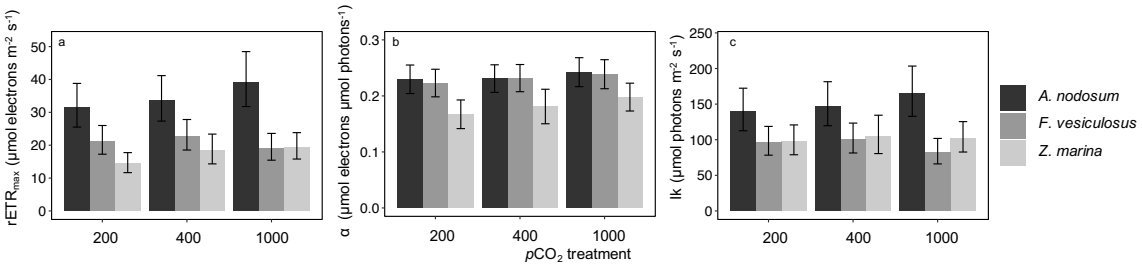

Figure 18: Estimated means of $rETR_{max}$ (a), α (b) and saturating irradiance, Ik (c) for different combinations of pCO_2 treatments and species, i.e. $s_k \times c_i$ in the mixed model. Significance of the interaction is indicated with an asterisk ($p < 0.05$) (none of them). Error bars mark standard errors of the means.

Our results showed a significant increase in photosynthetic activity ($rETR_{max}$, α and Ik) with longer photoperiods and a positive but non-significant CO_2-effect. The responses from 12 h to 24 h of photoperiod differed between species: *Z. marina* showed the highest increase in $rETR_{max}$ followed by *A. nodosum* and *F. vesiculosus* with increasing daylight hours. The photosynthetic efficiency, α, was similar among macroalgae but different from that of *Z. marina*. Estimates of photosynthetic activity at the physiological, individual leaf level has been adequately related with estimates of macrophytes productivity at community-level (Silva *et al.*, 2005).

Our results showed maximum $rETR_{max}$ at 24-h daylight for all three species, although *A. nodosum* and *Fucus serratus* from the North Sea and Norwegian Sea showed increased growth rates only up to 20 h of daylight (Strömgren, 1978). The small increase in $rETR_{max}$ of *F. vesiculosus* at continuous daylight is consistent with its current presence in the high-Arctic (Florczyk & Latala, 1989; Hansen & Haugen, 1989). Other species from the North Sea such as *Ulva lactuca* and *Porphyra umbilicalis* did not increase their growth at photoperiods greater than 16 h (Fortes and Lüning, 1980). Reduced photosynthetic rates from 21 to 24-h daylight in species from the North Sea and Norwegian Sea are likely produced by high photon flux rates leading to photoinhibition, light-induced reduction in the photosynthetic capacity of the macrophytes, to protect the photosynthetic apparatus, suggesting that macrophytes from different latitudes might regulate their photosynthetic rates differently. The Antarctic brown alga (*Adenoscystis utriculares*) showed faster photoinhibition than brown macroalgae of temperate zones (Hanelt, 1996). Nonetheless, the subarctic macroalgae tested in this study did not show

photoinhibition in their RLC at 24-h photoperiods (Figure A2, Figure A3).

$rETR_{max}$ and α increased somewhat in response to increasing CO_2, although, given the high variability, this was not significant. $rETR_{max}$ of *A. nodosum* and *Z. marina* tended to weakly increase with increasing CO_2 while *F. vesiculosus* did not show any trend. Previous analyses showed that *A. nodosum* was not CO_2-saturated at ambient levels and diffusive entry of CO_2 seemed to be required (Surif & Raven, 1989; Koch *et al.*, 2013), while *F. vesiculosus* was CO_2-saturated at ambient levels (Raven & Osmond, 1992; Koch *et al.*, 2013) and had high capacity for DIC uptake by non-diffusive mechanisms (Mercado *et al.*, 2009), which is in agreement with the responses to elevated CO_2 observed in our experiment. Our study suggests that increased CO_2 benefits subarctic *A. nodosum,* probably because it is not currently CO_2-saturated and the diffusive entry of CO_2 or CCMs based on HCO_3^- usage are required (Johnston & Raven, 1986; Surif & Raven, 1989; Koch *et al.*, 2013), while *F. vesiculosus* did not benefit from increased CO_2 probably due to its currently CO_2-saturated stage and its capacity for non-diffusive mechanisms (Raven & Osmond, 1992; Koch *et al.*, 2013). In conditions of severe CO_2 limitation, the high availability of HCO_3^- increases C acquisition, but it is energetically expensive and CO_2 remains preferable for photosynthesis as compared to HCO_3^- due to lower photosynthetic $K_{0.5}$ values for CO_2 than for HCO_3^- in seagrasses and macroalgae (Sand-Jensen & Gordon, 1984). The seagrass *Z. marina* can be either CO_2-saturated or -limited at ambient levels (Koch *et al.*, 2013). We observed a positive, though non-significant response of *Z. marina* to increased CO_2, in line with CO_2-stimulation of seagrass photosynthesis observed in other regions (Koch *et al.*, 2013).

Our results suggest that longer photoperiods allow subarctic macrophytes to increase photosynthetic activity. We observed that that the longest photoperiod (24 h), characteristic of Arctic summers, intensifies the photosynthetic performance of the Arctic macroalgae and subarctic seagrass species studied while a high-CO_2 environment may potentially stimulate photosynthesis further. The macroalgae and seagrass species tested here will, hence, benefit from increased day length during the Arctic summer as they migrate poleward with decreasing ice cover. Our results thereby support the forecasted poleward expansion of subarctic vegetation into the high-Arctic and the spread of existing Arctic macroalgae with climate change (Krause-Jensen and Duarte, 2014).

Image 5: Deployment of the equipment to measure pCO_2 in the water column aboard the Erissalikk boat in Godthåbsfjord, Greenland. Photo credit: F. Ugarte.

5. Discussion

5.1 General overview

The goals of this thesis are to evaluate the relationship between GPP estimates measured with three different methods in the Arctic Ocean and to assess the effects of increased CO_2 and long day length on planktonic communities and macrophytes, and I have developed the sections Results 4.1, 4.2, 4.3 & 4.4 to accomplish them. In Results 4.1 we found that during the growth season, from spring to late summer, the ^{14}C-PP estimates were on average 40 % lower than the O_2-based rates. However, due to marked seasonality of the Arctic Ocean, in May the ^{14}C-PP rates equate to less than half of the O_2-based rates, underestimating O_2–based GPP, and in August the ^{14}C-PP rates was higher than the O_2-based estimates. These results support the notion that the O_2-based methods approximate GPP while the ^{14}C method approximates NPP. Therefore, we recommended the use of the O_2-based methods during the productive period, given the C-based method's negative bias as a result of respiratory process, while during low productive periods, such as August, the use of both ^{14}C and O_2-based methods are adequate. These conclusions contribute to the field of Arctic oceanography and facilitate future studies on primary productivity in this region.

In Results 4.2, we observed that at highly productive periods such as spring bloom episodes and at low *in situ* pCO_2, high Chl *a* concentration, high GPP and in presence of dissolved inorganic nutrients, the experimental addition of CO_2 increased the GPP of Arctic planktonic communities from 32 to 72% on average. In Results 4.3, where the weekly development of a subarctic bloom with CO_2 experimental additions was researched, we identified a window of time of CO_2 limitation of about 2 weeks, during which NCP increased from 17 to 167% by CO_2 additions. The stimulation of the spring bloom at the later phase by increased CO_2 could result in a fertilization effect comparable to that recently demonstrated for terrestrial vegetation. During the pre-bloom and post-bloom phases, the experimental addition of CO_2 did not stimulate or supressed NCP due to probably the high pCO_2 in seawater.

In Results 4.4, we found that the photosynthetic activity of three subarctic macrophytes species (*A. nodosum*, *F. vesiculosus* and *Z. marina*) increased with increasing day length and the effect of increased CO_2 was positive but not significant. Thus, our results suggest that as subarctic macrophytes expand in the Arctic in response of the retracting sea ice, the long summer day will stimulate the photosynthesis of the tested species, while high-CO_2 environment might possible further benefit them. Although each Results section has its own discussion, there are some overarching themes within the thesis that can be discussed together along the next sections.

5.2 Primary production rates and photosynthetic activity

The relationship between C and O_2-based estimates of PP has been analysed in Results 4.1 but the exact relation between the fluorescence estimates of $rETR_{max}$, measured in Results 4.4, and primary productivity has not been addressed here. The physiological photosynthetic response of individual macrophytes, ETR, is theoretically an indicative of GPP (Beer *et al.*, 2014). The review of Beardall *et al.,* (2009) confirmed a good correlation between measurements of PP rates carried out using fluorescence estimates of ETR, C-assimilation and O_2-production in both plankton and macrophytes communities under low- and mid-levels of irradiance. However, stress conditions such as high light intensities, induce to reduced CO_2 fixation rates and limiting levels of DIC and nutrients can drive imbalances of electron transport (Beardall *et al.*, 2009).

When photosynthesis is light saturated, the fluorescence estimates of ETR may overestimate the O_2 production because ETR measurements can detect elevated electron flow possibly due to cyclic electron flow through PSII, since there is more light available than required for maximum photosynthesis (Franklin & Badger, 2001; Beardall *et al.*, 2009). Other critical processes such as photorespiration, dark respiration and the Mehler reaction already discussed, are alternative energy sinks that impede a straight conversion of fluorescence-measured ETR to GPP (Beardall *et al.*, 2009). High irradiance and low CO_2 concentrations lead to the necessity of CCMs, which are energetically expensive given the energy cost that requires the facilitation of the CO_2 entrance by diffusion and/or the $H_2CO_3^-$ uptake and its consequent conversion into CO_2 (Giordano *et al.*, 2005). CCMs can act as both sink of photosynthetic electrons and as a 'pump and leak' system of DIC (Sukeniw *et al.*, 1997; Beardall *et al.*, 2009), apparently increasing C fixation rates but producing the release of CO_2 and acting as a sink of electrons (Tchernov *et al.*, 1997; Beardall *et al.*, 2009). High irradiance is not expected in a changing Arctic, thus the linearity between ETR and GPP rates should be valid.

5.3 The CO_2 fertilization effect in Arctic and subarctic waters

Given the important role of Arctic and subarctic PP as CO_2 sinks (Bates & Mathis, 2009) and the large contribution of phytoplankton and benthic macrophytes (~76%) to PP rates of the near-shore areas in the high Arctic (Glud & Rysgaard, 2007), an increase of subarctic NCP for about nine days after the peak bloom stage (Results 4.2), the stimulation Arctic GPP at bloom conditions (Results 4.3) in a high CO_2 environment and the stimulation of subarctic macrophytes photosynthesis as they migrate poleward with the retreating of the ice (Results 4.4) should be taken into account to assess the response of the Arctic ecosystem to the current changes. Assuming linearity between ETR and GPP in macrophytes and given that the two

O_2-based methods applied in the CO_2 addition experiments were comparable and highly correlated (Results 4.1), hereafter the NCP rates and GPP-^{18}O estimates will be referred as PP.

Increases in PP in a high CO_2 environment might lead to changes in grazing, exudation of DOC and the production of detritus, altering the food web of the Arctic Ocean. An enhance of primary productivity might hypothetically strengthen the Arctic CO_2 sink, increase the vertical flux of organic matter to the sea floor and lead to a positive feed-back loop similar to the CO_2 fertilization effect on terrestrial vegetation (Denman *et al.*, 2007). The CO_2 fertilization effect on land vegetation has caused a pause in increasing global trends of atmospheric CO_2 and temperatures (Denman *et al.*, 2007; Leggett & Ball, 2015) in the last 10 years (Keenan *et al.*, 2016), although the existence of this pause is controverted (Cowtan & Way, 2014; Karl *et al.*, 2015). However, an increase of CO_2 in phytoplankton communities also had no or reduced effect on PP in the pre- or post-bloom stages in subarctic waters and no or reduced effect on Arctic PP in summer. The negative responses during these periods suggest that the CO_2 fertilization effect in Arctic and subarctic spring bloom production maybe offset by negative effects throughout the much longer recycling phase, two to three months, with potentially negatively affect the ecosystem. Whereas the mechanisms leading to enhanced PP in Arctic plankton when biological CO_2 demand exceed supply appear clear, the mechanisms leading to a prevalence of suppression of PP with CO_2 enrichment during summer and in the pre- and post-bloom stages need be resolved.

5.4 Long day length and increased CO_2 in Arctic and subarctic waters

Anthropogenic CO_2 emissions are directly related with Arctic sea-ice loss (Notz & Stroeve, 2017). While decreasing the habitat availability of ice associated species, ice loss during spring and summer also increases the availability of habitats for arctic biota in the high Artic, for both phytoplankton communities in the shelf and shelf-break given their drifting nature, and macrophyte communities in coastal shelf areas due to their ability to colonize new habitats. The Arctic region encompasses a large area. Day length increases up to 21 h in the subarctic region (~65°N) and 24 h in the high Arctic (~80°N) during summer. Despite decreasing the habitat availability of ice associated species, the current increase of free-ice habitat in the Arctic Ocean is highly relevant for benthic and pelagic ecosystems, since the growth of dense vegetation is often limited or even prevented by the presence of ice and the consequent reduction of submersed light penetration (Wulff *et al.*, 2009; Krause-Jensen *et al.*, 2012; Krause-Jensen & Duarte, 2014). In Results 4.4, the photosynthetic response of subarctic macrophytes, $rETR_{max}$,

increased with longer day length. Therefore, increased free-ice habitat in the high Arctic creates optimal conditions for marine vegetation (Krause-Jensen & Duarte, 2014; Krause-Jensen *et al.*, 2016). In spite of this, the macrophytes response to increased CO_2 was weak due to the lack of sufficient data, positive trends indicated that CO_2 additions may have also contributed to the increased $rETR_{max}$. In subarctic waters, planktonic NCP in the sea surface also increased with increasing daylight hours, reaching its maximum with 17 h of daylight and reduced pCO_2 levels at the beginning of May (Results 4.3). During the window of time of CO_2 limitation of about nine days, daylight hours increased from 17 h to 19.30 h of daylight, increasing the demand of C and the consumption of O_2 and playing an important role on increased productivity together with the experimental increases of CO_2.

5.5 Species – specific responses in a changing Arctic

The CO_2 fertilization effect has been attributed to species with low effective CCMs (Tortell *et al.*, 2002; Rost *et al.*, 2003; Riebesell, 2004; Giordano *et al.*, 2005; Sobrino *et al.*, 2008; Reinfelder, 2010). This is the case of *Phaeocystis sp*., an important Arctic haptophyte which dominated the CO_2-stimulated communities of Results 4.2. Other Arctic and subarctic species such as the picoeukaryotes *Micromonas spp.,* also has ineffective CCMs and benefited from CO_2 increases (Engel *et al.*, 2008; Hoppe *et al.*, 2017). On the other hand, diatoms are known to have efficient CCMs (Rost *et al.*, 2008) and no benefits has been observed at high CO_2 (Kroeker *et al.*, 2010; Torstensson *et al.*, 2012). However, communities dominated by the diatoms *Navicula pelagica*, *Thalassiosira* spp. and pennate diatoms were CO_2-stimulated in Results 4.2 & 4.3.

Although the response of macrophyte species to increased day length was positive in Results 4.4, the effect of increased CO_2 was not significant, despite the different responses between species. The macroalgae *F. vesiculosus* was not stimulated by elevated CO_2 probably because it was currently CO_2-saturated (Raven & Osmond, 1992; Koch *et al.*, 2013) and showed high capacity for non-diffusive mechanisms of DIC incorporation (Mercado *et al.*, 2009); *A. nodosum* showed higher stimulation probably because it is not CO_2-saturated (Johnston & Raven, 1986; Surif & Raven, 1989; Koch *et al.*, 2013) and the response of *Z. marina* also showed a positive but weak trend similar to seagrasses responses (Koch *et al.*, 2013) but its CO_2-saturation level is still unclear (Koch *et al.*, 2013).

5.6 Knowledge gaps and further research

In this thesis, we found that increased experimental CO_2 concentrations and increased day length stimulate the productivity of Arctic and subarctic phytoplankton after the peak bloom when *in situ* pCO_2 was low, while the photosynthetic activity of subarctic macrophytes is stimulated by increased day length and probably by increased CO_2 concentrations, which are relevant findings in the broad field of climate change ecology. However, further research on the CO_2 fertilization effect in the Arctic Ocean is needed as well as its interaction with increased temperatures (i.e. Holding *et al.*, 2015), increased irradiance (i.e. Hoppe *et al.*, 2017), ultraviolet radiation, increased stratification and the consequent changes in nutrients concentrations, increased freshening needs to be researched because changes in primary productivity will affect the ecosystem food web and the role of the Arctic Ocean as CO_2 sink, with probably global consequences.

Further research is also demanded on the respiratory processes such as photorespiration, the Mehler reaction, mitochondrial respiration and O_2 production in darkness, both at cellular and community level, to fully understand the underlying assumptions that can report biased estimates of PP based in O_2 and C methods during productive and unproductive periods.

The study of physiological responses at individual level coupled with the community level response is key to resolve the response of the ecosystem in a changing Arctic. Modelling and remote sensing have already shown that PP in the Arctic Ocean will increase despite regional contrasts (Arrigo *et al.*, 2008; Arrigo & van Dijken, 2015; Slagstad *et al.*, 2015), however additional research is required to include the driver of increased CO_2 to estimate the response of benthic and pelagic primary productivity in the Arctic Ocean.

Image 6: The marginal ice zone at the NW Svalbard shelf. Photo credit: M. Sanz-Martín.

6. Conclusions

1. Measurements of ^{14}C-based PP rates, with incubations of 24 h, are less than half of the O_2-based rates, underestimating the GPP of the European Arctic Ocean, although differences between methods are larger in spring than in summer.

2. Due to the marked seasonality of the Arctic, the use of O_2-based methods during productive periods such as spring is preferable. During low production periods, as in non-blooms conditions when recycling processes dominate, both C and O_2-based methods are adequate.

3. The gross productivity of Arctic is stimulated by experimental increases of CO_2 during highly productive periods, such as the spring blooms , when there is low *in situ* pCO_2, high biomass, high GPP and in presence of dissolved inorganic nutrients in seawater.

4. Shortly after the initiation of a subarctic spring bloom and after the peak phase, there is a window of time of CO_2 limitation that lasts about two weeks. During this time, experimental CO_2 increases have a fertilizing effect on planktonic NCP.

5. Arctic planktonic communities dominated by *Phaeocystis sp*., an important Arctic haptophyte, are stimulated by high CO_2 probably due to low efficacient CCMs.

6. Subarctic plankton communities dominated by the diatoms *Navicula pelagica*, *Thalassiosira* spp. and pennate diatoms are stimulated by increased CO_2, although the scientific literature reports that their CCMs are apparently effective.

7. Before a phytoplankton bloom starts, during the pre-bloom phase, at the end of the bloom and during summer, the productivity of subarctic and Arctic plankton communities are not affected or are suppressed by experimental CO_2 increases.

8. The longest photoperiod, characteristic of Arctic summers, intensifies the photosynthetic activity of the subarctic macroalgae *A. nodosum* and *F. vesiculosus* and the seagrass *Z. marina* and increased CO_2 may potentially stimulate the photosynthesis of *A. nodosum* and *Z. marina*.

9. Continuous daylight plays a major role in increasing photosynthetic activity of these three subarctic macrophyte species as they expand into the Arctic region with decreasing ice cover.

10. Increased CO_2 and day length stimulate the productivity of phytoplankton blooms in Arctic and subarctic waters, specifically after the peak phase, when the CO_2 concentrations are already low. Long day length also stimulates the photosynthetic activity of three macrophyte subarctic species and increased CO_2 might possible further benefit them.

Image 7: The ice edge at the NW Svalbard shelf aboard the R/V Helmer Hanssen. Photo credit: M. Cape.

7. References

ACIA (2004) *Impacts of a Warming Arctic: Arctic Climate Impact Assessment*,.

Arendt, K.E., Nielsen, T.G., Rysgaard, S. & Tönnesson, K. (2010) Differences in plankton community structure along the Godthåbsfjord, from the Greenland Ice Sheet to offshore waters. *Marine Ecology Progress Series*, **401**, 49–62.

Aristegui, J., Montero, M.F., Ballesteros, S., Basterretxea, G. & VanLenning, K. (1996) Planktonic primary production and microbial respiration measured by ^{14}C assimilation and dissolved oxygen changes in coastal waters of the Antarctic Peninsula during austral summer: Implications for carbon flux studies. *Marine Ecology-Progress Series*, **132**, 191–201.

Arrigo, K.R., van Dijken, G. & Pabi, S. (2008) Impact of a shrinking Arctic ice cover on marine primary production. *Geophysical Research Letters*, **35**, 1–6.

Arrigo, K.R. & van Dijken, G.L. (2015) Continued increases in Arctic Ocean primary production. *Progress in Oceanography*, **136**, 60–70.

Arrigo, K.R.R. (2007) *Chapter 7: Physical Control of Primary Productivity in Arctic and Antarctic Polynyas*. *Polynyas: Windows to the World*, pp. 223–238. Elsevier.

Assmy, P., Fernández-Méndez, M., Duarte, P., Meyer, A., Randelhoff, A., Mundy, C.J., Olsen, L.M., Kauko, H.M., Bailey, A., Chierici, M., Cohen, L., Doulgeris, A.P., Ehn, J.K., Fransson, A., Gerland, S., Hop, H., Hudson, S.R., Hughes, N., Itkin, P., Johnsen, G., King, J.A., Koch, B.P., Koenig, Z., Kwasniewski, S., Laney, S.R., Nicolaus, M., Pavlov, A.K., Polashenski, C.M., Provost, C., Rösel, A., Sandbu, M., Spreen, G., Smedsrud, L.H., Sundfjord, A., Taskjelle, T., Tatarek, A., Wiktor, J., Wagner, P.M., Wold, A., Steen, H. & Granskog, M.A. (2017) Leads in Arctic pack ice enable early phytoplankton blooms below snow-covered sea ice. *Scientific reports*, 1–9.

Badger, M.R., Andrews, T.J., Whitney, S.M., Ludwig, M., Yellowlees, D.C., Leggat, W. & Price, G.D. (1998) The diversity and coevolution of Rubisco, plastids, pyrenoids, and chloroplast-based CO_2-concentrating mechanisms in algae. *Canadian Journal of Botany*, **76**, 1052–1071.

Badger, M.R., Kaplan, A. & Berry, J.A. (1980) Internal inorganic carbon pool of Chiamydomonas reinhardtii. *Plant physiology*, **66**, 407–413.

Bakker, D.C.E., Pfeil, B., Landa, C.S., Metzl, N., O'Brien, K.M., Olsen, A., Smith, K., Cosca, C., Harasawa, S., Jones, S.D., Nakaoka, S., Nojiri, Y., Schuster, U., Steinhoff, T., Sweeney, C., Takahashi, T., Tilbrook, B., Wada, C., Wanninkhof, R., Alin, S.R., Balestrini, C.F., Barbero, L., Bates, N.R., Bianchi, A.A., Bonou, F., Boutin, J., Bozec, Y., Burger, E.F., Cai, W.-J., Castle, R.D., Chen, L., Chierici, M., Currie, K., Evans, W., Featherstone, C., Feely, R.A., Fransson, A., Goyet, C., Greenwood, N., Gregor, L., Hankin, S., Hardman-Mountford, N.J., Harlay, J., Hauck, J., Hoppema, M., Humphreys, M.P., Hunt, C.W., Huss, B., Ibánhez, J.S.P., Johannessen, T., Keeling, R., Kitidis, V., Körtzinger, A., Kozyr, A., Krasakopoulou, E., Kuwata, A., Landschützer, P., Lauvset, S.K., Lefèvre, N., Lo Monaco, C., Manke, A., Mathis, J.T., Merlivat, L., Millero, F.J., Monteiro, P.M.S., Munro, D.R., Murata, A., Newberger, T., Omar, A.M., Ono, T., Paterson, K.,

Pearce, D., Pierrot, D., Robbins, L.L., Saito, S., Salisbury, J., Schlitzer, R., Schneider, B., Schweitzer, R., Sieger, R., Skjelvan, I., Sullivan, K.F., Sutherland, S.C., Sutton, A.J., Tadokoro, K., Telszewski, M., Tuma, M., Van Heuven, S.M.A.C., Vandemark, D., Ward, B., Watson, A.J. & Xu, S. (2016) A multi-decade record of high quality fCO_2 data in version 3 of the Surface Ocean CO_2 Atlas (SOCAT). *Earth System Science Data Discussions*, **8**, 383–413.

Ballantyne, A.P., Alden, C.B., Miller, J.B., Tans, P.P. & White, J.W.C. (2012) Increase in observed net carbon dioxide uptake by land and oceans during the past 50 years. *Nature*, **488**, 70–72.

Banse, K. (1993) On the dark bottle in the ^{14}C method for measuring marine phytoplankton production. *ICES Journal of Marine Science*, **197**, 132–140.

Banse, K. (1994) Uptake of inorganic carbon and nitrate by marine plankton and the Redfield Ratio. *Global Biogeochemical Cycles*, **8**, 81–84.

Bates, N.R. & Mathis, J.T. (2009) The Arctic Ocean marine carbon cycle: evaluation of air-sea CO_2 exchanges, ocean acidification impacts and potential feedbacks. *Biogeosciences*, **6**, 2433–2459.

Bates, N.R., Moran, S.B., Hansell, D.A. & Mathis, J.T. (2006) An increasing CO_2 sink in the Arctic Ocean due to sea-ice loss. *Geophysical Research Letters*, **33**, 1–7.

Beardall, J., Ihnken, S. & Quigg, A. (2009) Gross and net primary production: closing the gap between concepts and measurements. *Aquatic Microbial Ecology*.

Beer, S., Björk, M. & Beardall, J. (2014) *Photosynthesis in the marine environment*, John Wiley & Sons.

Bender, M., Grande, K., Johnson, K., Marra, J., LeB, P.J., Sieburth, J., Pilson, M., Langdon, C., Hitchcock, G., Orchardo, J. & others (1987) A comparison of four methods for determining planktonic community production. *Limnology and Oceanography*, **32**, 1085–1098.

Bender, M.L., Orchardo, J., Dickson, M.L., Barber, R. & Lindley, S. (1999) *In vitro* O_2 fluxes compared with ^{14}C production and other rate terms during the JGOFS Equatorial Pacific experiment. *Deep-Sea Research Part I*, **46**, 637–654.

Bender, M.L., Taylor, E., Tans, P., Francey, R. & Lowe, D. (1996) Variability in the O_2/N_2 ratio of southern hemisphere air, 1991-1994: Implications for the carbon cycle. *Global Biogeochemical Cycles*, **10**, 9–21.

Berreville, O.F., Vézina, a F., Thompson, K.R. & Klein, B. (2008) Exploratory data analysis of the interactions among physics, food web structure, and function in two Arctic polynyas. *Canadian Journal of Fisheries and Aquatic Sciences*, **65**, 1036–1046.

Bowes, G. & Salvuci, M.E. (1989) Plasticity in the photosynthetic carbon metabolism of submersed aquatic macrophytes. *Aquat Bot*, **34**, 233–266.

Canadell, J.G., Le Quéré, C., Raupach, M.R., Field, C.B., Buitenhuis, E.T., Ciais, P.,

Conway, T.J., Gillett, N.P., Houghton, R. a & Marland, G. (2007) Contributions to accelerating atmospheric CO_2 growth from economic activity, carbon intensity, and efficiency of natural sinks. *Proceedings of the National Academy of Sciences of the United States of America*, **104**, 18866–70.

Carpenter, J. (1995) The accuracy of the Winkler method for dissolved oxyen analysis. *The Johns Hopkins University, Baltimore, Maryland*, 135–140.

Carritt, D.E. & Carpenter, J.H. (1966) Comparison and evaluation of currently employed modifications of the Winkler method for determining dissolved oxygen in seawater. *Journal of Marine Research*, **24**, 286–318.

Chierici, M., Fransson, A., Lansard, B., Miller, L.A., Mucci, A., Shadwick, E., Thomas, H., Tremblay, J.E. & Papakyriakou, T.N. (2011) Impact of biogeochemical processes and environmental factors on the calcium carbonate saturation state in the Circumpolar Flaw Lead in the Amundsen Gulf, Arctic Ocean. *Journal of Geophysical Research: Oceans*, **116**, 1–12.

Clarke, M.R.B. (1980) The reduced major axis of a bivariate sample. *Biometrika*, **67**, 441–446.

Coello-Camba, A., Agustí, S., Holding, J. & Arrieta, J.M. (2014) Interactive effect of temperature and CO_2 increase in Arctic phytoplankton. *Frontiers in Marine Science*, **1**, 1–10.

Coupel, P., Ruiz-Pino, D., Sicre, M.A., Chen, J.F., Lee, S.H., Schiffrine, N., Li, H.L. & Gascard, J.C. (2015) The impact of freshening on phytoplankton production in the Pacific Arctic Ocean. *Progress in Oceanography*, **131**, 113–125.

Cowtan, K. & Way, R.G. (2014) Coverage bias in the HadCRUT4 temperature series and its impact on recent temperature trends. *Quarterly Journal of the Royal Meteorological Society*, **140**, 1935–1944.

Denman, K.L., Brasseur, G.P., Chidthaisong, A., Ciais, P., Cox, P.M., Dickinson, R.E., Hauglustaine, D.A., Heinze, C., Holland, E.A. & Jacob, D.J. (2007) *Couplings Between Changes in the Climate System and Biogeochemistry*. *Climate Change 2007: The Physical Science Basis*, Cambridge University Press.

Dickson, A.G., Sabine, C.L. & Christian, J.R. (2007) Guide to best practices for ocean CO_2 measurements.

Dickson, M.L., Orchardo, J., Barber, R.T., Marra, J., McCarthy, J.J. & Sambrotto, R.N. (2001) Production and respiration rates in the Arabian Sea during the 1995 Northeast and Southwest Monsoons. *Deep-Sea Research Part II*, **48**, 1199–1230.

Duarte, C.M., Agustí, S. & Regaudie-de-Gioux, A. (2011) *The role of marine biota in the metabolism of the biosphere*. *The Role of Marine Biota in the Functioning of the Biosphere*, pp. 38–53.

Duarte, C.M., Agustí, S., Wassmann, P., Arrieta, J.M., Alcaraz, M., Coello, A., Marbà, N., Hendriks, I.E., Holding, J., García-Zarandona, I., Kritzberg, E. & Vaqué, D. (2012a) Tipping elements in the Arctic marine ecosystem. *Ambio*, **41**, 44–55.

Duarte, C.M. & Cebrián, J. (1996) The fate of marine autotrophic production. *Limnology and Oceanography*, **41**, 1758–1766.

Duarte, C.M., Lenton, T.M., Wadhams, P. & Wassmann, P. (2012b) Abrupt climate change in the Arctic. *Nature Climate Change*, **2**, 60–62.

Engel, A., Borchard, C., Piontek, J., Schulz, K.G., Riebesell, U. & Bellerby, R. (2013) CO_2 increases ^{14}C primary production in an Arctic plankton community. *Biogeosciences*, **10**, 1291–1308.

Engel, A., Piontek, J., Grossart, H.P., Riebesell, U., Schulz, K.G. & Sperling, M. (2014) Impact of CO_2 enrichment on organic matter dynamics during nutrient induced coastal phytoplankton blooms. *Journal of Plankton Research*, **36**, 641–657.

Engel, A., Schulz, K.G., Riebesell, U., Bellerby, R., Delille, B. & Schartau, M. (2008) Effects of CO_2 on particle size distribution and phytoplankton abundance during a mesocosm bloom experiment (PeECE II). *Biogeosciences*, **5**, 509–521.

Falkowski, P.G. & Raven, J.A. (2013) *Aquatic photosynthesis*, (ed. by Array) Princeton University Press.

Falkowski, P.G. & Raven, J.A. (1997) *Aquatic Photosynthesis*, Blackwell Science, Paris.

Fernández-Méndez, M., Katlein, C., Rabe, B., Nicolaus, M., Peeken, I., Bakker, K., Flores, H. & Boetius, A. (2015) Photosynthetic production in the central Arctic Ocean during the record sea-ice minimum in 2012. *Biogeosciences*, **12**, 3525–3549.

Florczyk, I. & Latala, A. (1989) The phytobenthos of the Hornsund fiord, SW Spitsbergen. *Polar Research*, **7**, 29–41.

Fortes, M.D. & Lüning, K. (1980) Growth rates of North Sea macroalgae in relation to temperature, irradiance and photoperiod. *Helgoländer Meeresuntersuchungen*, **34**, 15–29.

Franklin, L. a & Badger, M.R. (2001) A comparison of photosynthetic electron transport rates in macroalgae measured by pulse amplitude modulated chloropyll fluorometry and mass specrtometry. *J. Phycol.*, **37**, 756–767.

Fransson, A., Chierici, M., Anderson, L.G., Bussman, I., Kattner, G., Jones, E.P. & Swift, J.H. (2001) The importance of shelf processes for the modification of chemical constituents in the waters of the Eurasian Arctic Ocean: implication for carbon fluxe. *Continental Shelf Research*, **21**, 225–242.

Fransson, A., Chierici, M. & Nojiri, Y. (2009) New insights into the spatial variability of the surface water carbon dioxide in varying sea ice conditions in the Arctic Ocean. *Continental Shelf Research*, **29**, 1317–1328.

Fransson, A., Chierici, M., Skjelvan, I., Olsen, A., Assmy, P., Peterson, A.K., Spreen, G. & Ward, B. (2017) Effects of sea-ice and biogeochemical processes and storms on under-ice water fCO_2 during the winter-spring transition in the high Arctic

Ocean: implications for sea-air CO_2 fluxes. *Journal of Geophysical Research: Oceans*, **122**, 5566–5587.

Gazeau, F., Middelburg, J.J., Loijens, M., Vanderborgh, J.-P., Pizay, M.-D. & Gattuso, J.-P. (2007) Planktonic primary production in estuaries: comparison of ^{14}C, O_2 and ^{18}O methods. *Aquatic Microbial Ecology*, **46**, 95–106.

Giordano, M., Beardall, J. & Raven, J.A. (2005) CO_2 concentrating mechanisms in algae: mechanisms, environmental modulation, and evolution. *Annual review of plant biology*, **56**, 99–131.

Del Giorgio, P.A. & Duarte, C.M. (2002) Respiration in the open ocean. *Nature*, **420**, 379–384.

Glud, R.N. & Rysgaard, S. (2007) The annual organic carbon budget of Young Sound, NE Greenland. *Wollaston Forland*, 194.

Gordillo, F.J.L., Niell, F.X. & Figueroa, F.L. (2001) Non-photosynthetic enhancement of growth by high CO_2 level in the nitrophilic seawed *Ulva rigida* C. Agardh (Chlorophyta). *Biomedical and life sciences*, **213**, 64–70.

Gosselin, M., Levasseur, M., Wheeler, P.A., Horner, R.A. & Booth, B.C. (1997) New measurements of phytoplankton and ice algal production in the Arctic Ocean. *Deep-Sea Research Part II: Topical Studies in Oceanography*, **44**, 1623–1644.

Grande, K.D., Marra, J., Langdon, C., Heinemann, K. & Bender, M.L. (1989a) Rates of respiration in the light measurement in marine phytoplankton using an ^{18}O isotope-labeling technique. *Journal of Experimental Marine Biology and Ecology*, **129**, 95–120.

Grande, K.D., Williams, P.J.L., Marra, J., Purdie, D.A., Heinemann, K., Eppley, R.W. & Bender, M.L. (1989b) Primary Production in the North Pacific gyre: a comparison of rates determined by the ^{14}C, O_2 concentration and ^{18}O methods. *Deep-Sea Research*, **36**, 1621–1634.

Grebmeier, J.M. & Mcroy, C.P. (1989) Food Supply and Carbon Cycling. **53**, 79–91.

Grebmeier, J.M., Overland, J.E., Moore, S.E., Farley, E. V, Carmack, E.C., Cooper, L.W., Frey, K.E., Helle, J.H., Mclaughlin, F.A. & Mcnutt, S.L. (2006) A Major Ecosystem Shift in the Northern Bering Sea. *Science*, **311**, 1461–1464.

Grebmeier, J.M., Smith, W.O. & Conover, R.J. (2013) Biological processes on Arctic continental shelves: Ice-ocean-biotic interactions. *Arctic Oceanography: Marginal Ice Zones and Continental Shelves*, 231–261.

Hanelt, D. (1996) Photoinhibition of photosynthesis in marine macroalgae. *Scientia Marina*, **60**, 243–248.

Hansen, H.P. & Koroleff, E. (1999) Determination of nutrients. *Methods of Seawater Analysis*, 159–228.

Hansen, J.R. & Haugen, I. (1989) Some observations of intertidal communities on

Spitsbergen (79°N), Norwegian Arctic. *Polar Research*, **7**, 23–27.

Harrison, W.G. & Platt, T. (1986) Photosynthesis-irradiance relationship in polar and temperate phytoplankton populations. *Polar Biology*, **5**, 153–164.

Hedges, L. V., Gurevitch, J. & Curtis, P.S. (1999) The meta-analysis of response ratios in experimental ecology. *Ecology*, **80**, 1150–1156.

Hein, M. & Sand-Jensen, K. (1997) CO_2 increases oceanic primary production. *Nature*, **388**, 526–527.

Hendriks, I.E., Duarte, C.M., Marbà, N. & Krause-Jensen, D. (2017) pH gradients in the diffusive boundary layer of subarctic macrophytes. *Polar Biology*, 1–6.

Hodal, H., Falk-Petersen, S., Hop, H., Kristiansen, S. & Reigstad, M. (2012) Spring bloom dynamics in Kongsfjorden, Svalbard: Nutrients, phytoplankton, protozoans and primary production. *Polar Biology*, **35**, 191–203.

Holbrook, G.P., Beer, S., Spencer, W.E., Reiskind, J.B., Davis, J.S. & Bowes, G. (1987) Photosynthesis in marine macroalgae: evidence for carbon limitation. *Canadian Journal of Botany*, **66**, 577–582.

Holding, J.M., Duarte, C.M., Arrieta, J.M., Vaquer-Suyner, R., Coello-Camba, a., Wassmann, P. & Agustí, S. (2013) Experimentally determined temperature thresholds for Arctic plankton community metabolism. *Biogeosciences*, **10**, 357–370.

Holding, J.M., Duarte, C.M., Sanz-Martín, M., Mesa, E., Arrieta, J.M., Chierici, M., Hendriks, I.E., García-Corral, L.S., Regaudie-de-Gioux, A., Delgado, A., Reigstad, M., Wassmann, P. & Agustí, S. (2015) Temperature dependence of CO_2-enhanced primary production in the European Arctic Ocean. *Nature Climate Change*, 8–11.

Hoppe, J.C.M., Schuback, N., Semeniuk, D.M., Maldonado, M.T. & Rost, B. (2017) Functional Redundancy Facilitates Resilience of Subarctic Phytoplankton Assemblages toward Ocean Acidification and High High Irradiance. *Frontiers in Marine Science*, **4**, 1–14.

Hurd, C.L., Hepburn, C.D., Currie, K.I., Raven, J.A. & Hunter, K.A. (2009) Testing the effects of ocean acidification on algal metabolism: Considerations for experimental designs. *Journal of Phycology*, **45**, 1236–1251.

IPCC (2014) *Climate Change 2014: Synthesis Report. Contribution of Working Groups I, II and III to the Fifth Assessment Report of the Intergovernmental Panel on Climate Change*,.

IPCC Panel (2014) *Climate Change 2014: Synthesis Report*,.

Johnston, A.M. & Raven, J.A. (1986) The utilization of bicarbonate ions by the macroalga *Ascophyllum nodosum* (L.) Le Jolis. *Plant, Cell & Environment*, **9**, 175–184.

Juul-Pedersen, T., Arendt, K.E., Mortensen, J., Blicher, M.E., Søgaard, D.H. &

Rysgaard, S. (2015) Seasonal and interannual phytoplankton production in a sub-Arctic tidewater outlet glacier fjord, SW Greenland. *Marine Ecology Progress Series*, **524**, 27–38.

Kaltin;, S., Anderson;, L.G., Olsson;, K., Fransson;, A. & Chierici, M. (2002) Uptake of atmospheric carbon dioxide in the Barents Sea. *Journal of Marine Systems*, **38**, 31–45.

Kaltin, S. & Anderson, L.G. (2005) Uptake of atmospheric carbon dioxide in Arctic shelf seas: Evaluation of the relative importance of processes that influence pCO_2 in water transported over the Bering-Chukchi Sea shelf. *Marine Chemistry*, **94**, 67–79.

Kaplan, A., Badger, M.R. & Berry, J.A. (1980) Photosynthesis and the intracellular inorganic carbon pool in the bluegreen alga *Anabaena variabilis*: Response to External CO_2 concentration. *Planta*, **149**, 219–226.

Karl, T.R., Arguez, A., Huang, B., Lawrimore, J.H., McMahon, J.R., Menne, M.J., Peterson, T.C., Vose, R.S. & Zhang, H.-M. (2015) Possible artifacts of data biases in the recent global surface warming hiatus. *Science*, **348**, 1469–1472.

Keenan, T.F.T.F., Prentice, I.C., Canadell, J.G., Williams, C.A., Wang, H., Raupach, M.R. & Collatz, G.J. (2016) Recent pause in the growth rate of atmospheric CO_2 due to enhanced terrestrial carbon uptake. *Nature Communications*, **7**, 1.

Kjesbu, O.S., Bogstad, B., Devine, J.A., Gjøsæter, H., Howell, D., Ingvaldsen, R.B., Nash, R.D.M. & Skjæraasen, J.E. (2014) Synergies between climate and management for Atlantic cod fisheries at high latitudes. *Proceedings of the National Academy of Sciences*, **111**, 3478–3483.

Koch, M., Bowes, G., Ross, C. & Zhang, X.H. (2013) Climate change and ocean acidification effects on seagrasses and marine macroalgae. *Global Change Biology*, **19**, 103–132.

Krause-Jensen, D. & Duarte, C.M. (2014) Expansion of vegetated coastal ecosystems in the future Arctic. *Frontiers in Marine Science*, **1**, 1–10.

Krause-Jensen, D., Marbà, N., Olesen, B., Sejr, M.K., Christensen, P.B., Rodrigues, J., Renaud, P.E., Balsby, T.J.S. & Rysgaard, S. (2012) Seasonal sea ice cover as principal driver of spatial and temporal variation in depth extension and annual production of kelp in Greenland. *Global Change Biology*, **18**, 2981–2994.

Krause-Jensen, D., Marbà, N., Sanz-Martín, M., Hendriks, I.E., Thyrring, J., Carstensen, J., Sejr, M.K. & Duarte, C.M. (2016) Long photoperiods sustain high pH in Arctic kelp forests. *Science Advances*, **2**, 1–8.

Krawczyk, D.W., Witkowski, A., Juul-Pedersen, T., Arendt, K.E., Mortensen, J. & Rysgaard, S. (2015) Microplankton succession in a SW Greenland tidewater glacial fjord influenced by coastal inflows and run-off from the Greenland Ice Sheet. *Polar Biology*, **38**, 1515–1533.

Kroeker, K.J., Kordas, R.L., Crim, R.N. & Singh, G.G. (2010) Meta-analysis reveals

negative yet variable effects of ocean acidification on marine organisms. *Ecology Letters*, **13**, 1419–1434.

Lasternas, S. & Agustí, S. (2010) Phytoplankton community structure during the record Arctic ice-melting of summer 2007. *Polar Biology*, **33**, 1709–1717.

Laws, E.A., Landry, M.R., Barber, R.T., Campbell, L., Dickson, M.L. & Marra, J. (2000) Carbon cycling in primary production bottle incubations: Inferences from grazing experiments and photosynthetic studies using ^{14}C and ^{18}O in the Arabian Sea. *Deep-Sea Research II*, **47**, 1339–1352.

Legendre, P. (2014) lmodel2: Model II Regression. R package version 1.7-2.

Legendre, P. & Legendre, L. (1998) Numerical ecology: second English edition. *Developments in environmental modelling*, **20**.

Leggett, L.M.W. & Ball, D.A. (2015) Granger causality from changes in level of atmospheric CO_2 to global surface temperature and the El Niño – Southern Oscillation, and a candidate mechanism in global photosynthesis. *Atmospheric Chemistry and Physics Discussions*, **15**, 11571–11592.

Maberly, S.C. & Gontero, B. (2017) Ecological imperatives for aquatic carbon dioxide-concentrating mechanisms.

Marra, J. (2002) *Approaches to the measurement of plankton production. Phytoplankton Productivity: Carbon Assimilation in Marine and Freshwater* (ed. by C.S. Williams, P.J.leB., Thomas, D.N. and Reynolds), Oxford UK: BlackwellScience.

Marra, J. (2009) Net and gross productivity: weighing in with ^{14}C. *Aquatic Ecosystem Health & Management*, **56**, 123–131.

Maslanik, J.A., Fowler, C., Stroeve, J., Drobot, S., Zwally, J., Yi, D. & Emery, W. (2007) A younger, thinner Arctic ice cover: Increased potential for rapid, extensive sea-ice loss. *Geophysical Research Letters*, **34**, 2004–2008.

Matrai, P.A., Olson, E., Suttles, S., Hill, V., Codispoti, L.A., Light, B. & Steele, M. (2013) Synthesis of primary production in the Arctic Ocean: I. Surface waters, 1954 – 2007. *Progress in Oceanography*, **110**, 93–106.

McArdle, B.H. (1988) The structural relationship: regression in biology. *Canadian Journal of Zoology*, **66**, 2329–2339.

McLaughlin, F.A. & Carmack, E.C. (2010) Deepening of the nutricline and chlorophyll maximum in the Canada Basin interior, 2003-2009. *Geophysical Research Letters*, **37**, 1–5.

Meire, L., Mortensen, J., Rysgaard, S., Bendtsen, J., Boone, W., Meire, P. & Meysman, F.J.R. (2016) Spring bloom dynamics in a subarctic fjord influenced by tidewater outlet glaciers (Godthåbsfjord, SW Greenland). *Journal of Geophysical Research: Biogeosciences*, **121**, 1581–1592.

Meire, L., Søgaard, D.H., Mortensen, J., Meysman, F.J.R., Soetaert, K., Arendt, K.E.,

Juul-Pedersen, T., Blicher, M.E. & Rysgaard, S. (2015) Glacial meltwater and primary production are drivers of strong CO_2 uptake in fjord and coastal waters adjacent to the Greenland Ice Sheet. *Biogeosciences*, **12**, 2347–2363.

Mercado, J.M. & Gordillo, F.J.L. (2011) Inorganic carbon acquisition in algal communities: are the laboratory data relevant to the natural ecosystems? *Photosynthesis research*, **109**, 257–67.

Mercado, J.M., de los Santos, C.B., Lucas Pérez-Llorens, J. & Vergara, J.J. (2009) Carbon isotopic fractionation in macroalgae from Cádiz Bay (Southern Spain): Comparison with other bio-geographic regions. *Estuarine, Coastal and Shelf Science*, **85**, 449–458.

Mesa, E., Delgado-Huertas, A., Carrillo-De-Albornoz, P., García-Corral, L.S., Sanz-Martín, M., Wassmann, P., Reigstad, M., Sejr, M., Dalsgaard, T. & Duarte, C.M. (2017) Continuous daylight in the high-Arctic summer supports high plankton respiration rates compared to those supported in the dark. *Scientific Reports*, **1**, 1–8.

Mikkelsen, D.M., Rysgaard, S. & Glud, R.N. (2008) Microalgal composition and primary production in Arctic sea ice: A seasonal study from Kobbefjord (Kangerluarsunnguaq), West Greenland. *Marine Ecology Progress Series*, **368**, 65–74.

Millero, F., Woosley, R., DiTrolio, B. & Waters, J. (2009) Effect of Ocean Acidification on the Speciation of Metals in Seawater. *Oceanography*, **22**, 72–85.

Mortensen, J., Bendtsen, J., Motyka, R.J., Lennert, K., Truffer, M., Fahnestock, M. & Rysgaard, S. (2013) On the seasonal freshwater stratification in the proximity of fast-flowing tidewater outlet glaciers in a sub-Arctic sill fjord. *Journal of Geophysical Research: Oceans*, **118**, 1382–1395.

Mortensen, J., Lennert, K., Bendtsen, J. & Rysgaard, S. (2011) Heat sources for glacial melt in a sub-Arctic fjord (Godth??bsfjord) in contact with the Greenland Ice Sheet. *Journal of Geophysical Research: Oceans*, **116**.

Nguyen, D., Maranger, R., Tremblay, J.É. & Gosselin, M. (2012) Respiration and bacterial carbon dynamics in the Amundsen Gulf, western Canadian Arctic. *Journal of Geophysical Research: Oceans*, **117**, 1–12.

Niebauer, H.J. (1991) Bio-physical oceanographic interactions at the edge of the Arctic ice pack. *Journal of Marine Systems*, **2**, 209–232.

Notz, D. & Stroeve, J. (2017) Observed Arctic sea-ice loss directly follows anthropogenic CO_2 emission. *Science*, **354**, 747–750.

Olesen, B., Krause-Jensen, D., Marbà, N. & Christensen, P.B. (2015) Eelgrass *Zostera marina* in subarctic Greenland: Dense meadows with slow biomass turnover in cold waters. *Marine Ecology Progress Series*, **518**, 107–121.

Oudot, C., Gerard, R., Morin, P. & Gningue, I. (1988) Precise shipboard determination of dissolved oxygen (Winkler procedure) for productivity studies with a

commercial system. *Limnology and Oceanography*, **33**, 146–150.

Pabi, S., van Dijken, G.L. & Arrigo, K.R. (2008) Primary production in the Arctic Ocean, 1998-2006. *Journal of Geophysical Research: Oceans*, **113**, 1998–2006.

Parsons, T.R., Maita, Y. & Lalli, C.M. (1984) *A manual of biological and chemical methods for seawater analysis*, Publ. Pergamon Press, Oxford.

Passow, U. & Carlson, C.A. (2012) The biological pump in a high CO_2 world. **470**, 249–271.

Peterson, B.J. (1980) Aquatic primary productivity and the ^{14}C-CO_2: A history of the productivity problem. *Annual Reviews Inc*, **11**, 359–385.

Pierrot, D., Lewis, E. & Wallace, D.W.R. (2006) MS excel program developed for CO_2 system calculations.

Platt, T., Bird, D.F. & Sathyendranath, S. (1991) Critical Depth and Marine Primary Production. *Proceedings: Biological Sciences*, **246**, 205–217.

Platt, T., Harrison, G., Irwin, B., Horne, E.P. & Gallegos, C.L. (1982) Photosynthesis and photoadaptation of marine phytoplankton in the Arctic. *Deep Sea Research*, **29**, 1159–1170.

Post, E., Bhatt, U.S., Bitz, C.M., Brodie, J.F., Fulton, T.L., Hebblewhite, M., Kerby, J., Kutz, S.J., Stirling, I. & Walker, D.A. (2013) Ecological consequences of sea-ice decline. *Science*, **341**, 519–525.

Ralph, P.J. & Gademann, R. (2005) Rapid light curves: A powerful tool to assess photosynthetic activity. *Aquatic Botany*, **82**, 222–237.

Randelhoff, A., Fer, I. & Sundfjord, A. (2017) Turbulent Upper-Ocean Mixing Affected by Meltwater Layers during Arctic Summer. *Journal of Physical Oceanography*, **47**, 835–853.

Randelhoff, A., Fer, I., Sundfjord, A., Tremblay, J.-E. & Reigstad, M. (2016) Vertical fluxes of nitrate in the seasonal nitracline of the Atlantic sector of the Arctic Ocean. *Journal of Geophysical Research: Oceans*, **121**, 3372–3380.

Raven, J.A. (1991) Physiology of inorganic C acquisition and implications for resource use efficiency by marine phytoplankton: relation to increased CO_2 and temperature. *Plant, Cell & Environment*, **14**, 779–794.

Raven, J.A., Johnston, A.M., Kübler, J.E., Korb, R., McInroy, S.G., Handley, L.L., Scrimgeour, C.M., Walker, D.I., Beardall, J., Clayton, M.N., Vanderklift, M., Fredriksen, S. & Dunton, K.H. (2002) Seaweeds in cold seas: Evolution and carbon acquisition. *Annals of Botany*, **90**, 525–536.

Raven, J.A. & Osmond, C.B. (1992) Inorganic C acquisition processes and their ecological significance in inter- and sub-tidal macroalgae of North Carolina. *Functional Ecology*, **6**, 41–47.

Raven, J. a., Giordano, M., Beardall, J. & Maberly, S.C. (2011) Algal and aquatic plant carbon concentrating mechanisms in relation to environmental change. *Photosynthesis Research*, **109**, 281–296.

Raven, J. a, Ball, L. a, Beardall, J., Giordano, M. & Maberly, S.C. (2005) Algae lacking carbon-concentrating mechanisms. *Canadian Journal of Botany*, **83**, 879–890.

Raven, J. a & Beardall, J. (2014) CO_2 concentrating mechanisms and environmental change. *Aquatic Botany*, **118**, 24–37.

Regaudie-de-Gioux, A., Lasternas, S.S., Agustí-, S., Duarte, C.M., Agustí, S. & Duarte, C.M. (2014) Comparing marine primary production estimates through different methods and development of conversion equations. *Frontiers in Marine Science*, **1**, 1–14.

Reigstad, M., Wassmann, P., Wexels Riser, C., Øygarden, S. & Rey, F. (2002) Variations in hydrography, nutrients and chlorophyll a in the marginal ice-zone and the central Barents Sea. *Journal of Marine Systems*, **38**, 9–29.

Reinfelder, J.R. (2010) Carbon concentrating mechanisms in eukaryotic marine phytoplankton. *Annual review of marine science*, **3**, 291–315.

Riebesell, U. (2004) Effects of CO_2 enrichment on marine phytoplankton. *Journal of Oceanography*, **60**, 719–729.

Riebesell, U., Schulz, K.G., Bellerby, R.G.J., Botros, M., Fritsche, P., Meyerhöfer, M., Neill, C., Nondal, G., Oschlies, A., Wohlers, J. & Zöllner, E. (2007) Enhanced biological carbon consumption in a high CO_2 ocean. *Nature*, **450**, 545–548.

Robinson, C., Archer, S.D. & Williams, P.J. le B. (1999) Microbial dynamics in coastal waters of East Antarctica : plankton production and respiration. *Marine Ecology Progress Series*, **180**, 23–36.

Robinson, C., Tilstone, G.H., Rees, A.P., Smyth, T.J., Fishwick, J.R., Tarran, G.A., Luz, B., Barkan, E. & David, E. (2009) Comparison of *in vitro* and *in situ* plankton production determinations. *Aquatic Microbial Ecology*, **54**, 13–34.

Rost, B., Riebesell, U., Burkhardt, S. & Sültemeyer, D. (2003) Carbon acquisition of bloom-forming marine phytoplankton. *Limnology and Oceanography*, **48**, 55–67.

Rost, B., Riebesell, U. & Sültemeyer, D. (2006) Carbon acquisition of marine phytoplankton: Effect of photoperiod length. *Limnology and Oceanography*, **51**, 12–20.

Rost, B., Zondervan, I. & Wolf-Gladrow, D. (2008) Sensitivity of phytoplankton to future changes in ocean carbonate chemistry: Current knowledge, contradictions and research directions. *Marine Ecology Progress Series*, **373**, 227–237.

Rudels, B., Anderson, L.G. & Jones, E.P. (1996) Formation and evolution of the surface mixed layer and halocline of the Arctic Ocean. *Journal of Geophysical Research*, **101**, 8807.

Rudels, B., Meyer, R., Fahrbach, E., Ivanov, V. V., Østerhus, S., Quadfasel, D., Schauer, U., Tverberg, V. & Woodgate, R.A. (2000) Water mass distribution in Fram Strait and over the Yermak Plateau in summer 1997. *Annales Geophysicae*, **18**, 0687–0705.

Rysgaard, S., Bendtsen, J., Pedersen, L.T., Ramløv, H. & Glud, R.N. (2009) Increased CO_2 uptake due to sea ice growth and decay in the Nordic Seas. *Journal of Geophysical Research*, **114**, C09011.

Rysgaard, S., Nielsen, T.G. & Hansen, B.W. (1999) Seasonal variation in nutrients, pelagic primary production and grazing in a high-Arctic coastal marine ecosystem, Young Sound, Northeast Greenland. *Marine Ecology Progress Series*, **179**, 13–25.

Saito, M.A. & Goepfert, T.J. (2008) Zinc-cobalt colimitation of Phaeocystis antarctica. *Limnology and Oceanography*, **53**, 266–275.

Sakshaug, E., Johnsen, G.H. & Kovacs, K.M. (2009) *Ecosystem Barents Sea*, Tapir Academic Press.

Sakshaug, E. & Skjoldal, H.R. (1989) Life at the ice edge. *AMBIO*, **18**.

Sambrotto, R.N., Savidge, G., Robinson, C., Boyd, P., Takahashi, T., Karl, D.M., Langdon, C., Chipman, D., Marra, J. & Codispoti, L. (1993) Elevated consumption of carbon relative to nitrogen in the surface ocean. *Nature*, **363**.

Sand-Jensen, K. & Gordon, D.M. (1984) Differential ability of marine and freshwater macrophytes to utilize HCO_3^- and CO_2. *Marine Biology*, **80**, 247–253.

Sarmiento, J.L. & Gruber, N. (2004) *Ocean Biogeochemical Dynamics*,.

Sarmiento, J.L., Slater, R., Barber, R., Bopp, L., Doney, S.C., Hirst, A.C., Kleypas, J., Matear, R., Mikolajewicz, U., Monfray, P., Soldatov, V., Spall, S.A. & Stouffer, R. (2004) Response of ocean ecosystems to climate warming. *Global Biogeochemical Cycles*, **18**.

Schulz, K.G., Bach, L.T., Bellerby, R., Bermudez, R., Boxhammer, T., Czerny, J., Engel, A., Ludwig, A., Larsen, A., Paul, A., Sswat, M. & Riebesell, U. (2017) Phytoplankton blooms at increasing levels of atmospheric carbon dioxide: experimental evidence for negative effects on prymnesiophytes and positive on small picoeukaryotes. *Frontiers in Marine Science*, **4**, 64.

Schulz, K.G., Bellerby, R.G.J., Brussaard, C.P.D., Büdenbender, J., Czerny, J., Engel, a., Fischer, M., Koch-Klavsen, S., Krug, S.A., Lischka, S., Ludwig, A., Meyerhöfer, M., Nondal, G., Silyakova, a., Stuhr, A. & Riebesell, U. (2013) Temporal biomass dynamics of an Arctic plankton bloom in response to increasing levels of atmospheric carbon dioxide. *Biogeosciences*, **10**, 161–180.

Sejr, M.K., Krause-jensen, D., Dalsgaard, T., Ruiz-halpern, S., Duarte, C.M., Middelboe, M., Glud, R.N., Bendtsen, J., Balsby, T.J.S. & Rysgaard, S. (2014) Seasonal dynamics of autotrophic and heterotrophic plankton metabolism and pCO_2 in a subarctic Greenland fjord. *Limnology and Oceanography*, **59**, 1764–1778.

Seuthe, L. (2011) Planktonic food webs in the Arctic Ocean. *Univesity of Tromso*.

Shi, D., Xu, Y., Hopkinson, B.M. & Morel, F.M.M. (2010) Effect of ocean acidification on iron availability to marine phytoplankton. *Science (New York, N.Y.)*, **327**, 676–679.

Silva, J., Santos, R., Calleja, M.L. & Duarte, C.M. (2005) Submerged versus air-exposed intertidal macrophyte productivity: from physiological to community-level assessments. *Journal of Experimental Marine Biology and Ecology*, **317**, 87–95.

Slagstad, D., Wassmann, P.F.J. & Ellingsen, I. (2015) Physical constrains and productivity in the future Arctic Ocean. *Frontiers in Marine Science*, **2**, 1–23.

Sobrino, C., Neale, P.J., Phillips-kress, J.D., Moeller, R.E. & Porter, J.A. (2009) Elevated CO_2 increases sensitivity to ultraviolet radiation in lacustrine phytoplankton assemblages. *Limnology and Oceanography*, **54**, 2448–2459.

Sobrino, C., Ward, M.L. & Neale, P.J. (2008) Acclimation to elevated carbon dioxide and ultraviolet radiation in the diatom *Thalassiosira pseudonana*: Effects on growth, photosynthesis, and spectral sensitivity of photoinhibition. *Limnology and Oceanography*, **53**, 494–505.

Spielhagen, R.F., Werner, K., Sørensen, S.A., Zamelczyk, K., Kandiano, E., Budeus, G., Husum, K., Marchitto, T.M. & Hald, M. (2011) Enhanced Modern Heat Transfer to the Arctic by Warm Atlantic Water. *Science*, **331**, 450–453.

Spilling, K. (2007) Dense sub-ice bloom of dinoflagellates in the Baltic Sea, potentially limited by high pH. *Journal of Plankton Research*, **29**, 895–901.

Steemann-Nielsen, C. (1952) The use of radiactive carbon (^{14}C) for measuring organic production in the sea. *J Cons Perm Int Explor Mer*, **18**, 117–140.

Strömgren, T. (1978) The effect of photoperiod on the length growth of five species of intertidal fucales. *Sarsia*, **63**, 155–157.

Sukeniw, A., Tchernov, D., Kaptan, A. & Livne, A. (1997) Uptake, efflux, and photosynthetic utilization. **974**, 969–974.

Sundfjord, A., Ellingsen, I., Slagstad, D. & Svendsen, H. (2008) Vertical mixing in the marginal ice zone of the northern Barents Sea—Results from numerical model experiments. *Deep Sea Research Part II: Topical Studies in Oceanography*, **55**, 2154–2168.

Surif, M.B. & Raven, J.A. (1989) Exogenous inorganic carbon sources for photosynthesis in seawater by members of the Fucales and the Laminariales (Phaeophyta): ecological and taxonomic implications. *Oecologia*, **78**, 97–105.

Takahashi, T., Sutherland, S.C., Wanninkhof, R., Sweeney, C., Feely, R.A., Chipman, D.W., Hales, B., Friederich, G., Chavez, F., Sabine, C., Watson, A., Bakker, D.C.E., Schuster, U., Metzl, N., Yoshikawa-Inoue, H., Ishii, M., Midorikawa, T., Nojiri, Y., Körtzinger, A., Steinhoff, T., Hoppema, M., Olafsson, J., Arnarson,

T.S., Tilbrook, B., Johannessen, T., Olsen, A., Bellerby, R., Wong, C.S., Delille, B., Bates, N.R. & de Baar, H.J.W. (2009) Climatological mean and decadal change in surface ocean pCO_2, and net sea-air CO_2 flux over the global oceans. *Deep-Sea Research Part II: Topical Studies in Oceanography*, **56**, 554–577.

Taraldsvik, M. & Myklestad, S.M. (2000) The effect of pH on growth rate, biochemical composition and extracellular carbohydrate production of the marine diatom Skeletonema costatum. *European Journal of Phycology*, **35**, 189–194.

Taucher, J., Jones, J., James, A., Brzezinski, M. a., Carlson, C.A., Riebesell, U. & Passow, U. (2015) Combined effects of CO_2 and temperature on carbon uptake and partitioning by the marine diatoms *Thalassiosira weissflogii* and *Dactyliosolen fragilissimus*. *Limnology and Oceanography*, **0**, 1–19.

Taucher, J., Schulz, K.G., Dittmar, T., Sommer, U., Oschlies, A. & Riebesell, U. (2012) Enhanced carbon overconsumption in response to increasing temperatures during a mesocosm experiment. *Biogeosciences*, **9**, 3531–3545.

Tchernov, D., Hassidim, M., Luz, B., Sukenik, A., Reinhold, L. & Kaplan, A. (1997) Sustained net CO_2 evolution during photosynthesis by marine microorganisms. *Current Biology*, **7**, 723–728.

Torstensson, A., Chierici, M. & Wulff, A. (2012) The influence of increased temperature and carbon dioxide levels on the benthic/sea ice diatom *Navicula directa*. *Polar Biology*, **35**, 205–214.

Tortell, P.D., DiTullio, G.R., Sigman, D.M. & Morel, F.M.M. (2002) CO_2 effects on taxonomic composition and nutrient utilization in an Equatorial Pacific phytoplankton assemblage. *Marine Ecology Progress Series*, **236**, 37–43.

Tremblay, J.-E., Michel, C., Hobson, K.A., Gosselin, M., Price, N.M., Michel, C., Hobson, K.A., Gosselin, M. & Price, N.M. (2006) Bloom dynamics in early opening waters of the Arctic Ocean. *Limnology and Oceanography*, **51**, 900–912.

Tremblay, J.E., Anderson, L.G., Matrai, P., Coupel, P., Bélanger, S., Michel, C. & Reigstad, M. (2015) Global and regional drivers of nutrient supply, primary production and CO_2 drawdown in the changing Arctic Ocean. *Progress in Oceanography*, **139**, 171–196.

Tremblay, J.E., Gratton, Y., Fauchot, J. & Price, N.M. (2002) Climatic and oceanic forcing of new, net, and diatom production in the North Water. *Deep-Sea Research Part II: Topical Studies in Oceanography*, **49**, 4927–4946.

Trenberth, K.E., Jones, P.D., Ambenje, P., Bojariu, R., Easterling, D., Tank, A.K., Parker, D., Rahimzadeh, F., Renwick, J.A., Rusticucci, M., Soden, P. & Zhai, B. (2007) *Climate Change 2007: The Physical Science Basis.*,.

Vaquer-Sunyer, R., Duarte, C.M., Regaudie-De-Gioux, a., Holding, J., García-Corral, L.S., Reigstad, M. & Wassmann, P. (2013) Seasonal patterns in Arctic planktonic metabolism (Fram Strait - Svalbard region). *Biogeosciences*, **10**, 1451–1469.

Vaughan, D.G., Comiso, J.C., Allison, I., Carrasco, J., Kaser, G., Kwok, R., Mote, P.,

Murray, T., Paul, F., Ren, J., Rignot, E., Solomina, O., Steffen, K.S. & Zhang, T. (2013) *Observations: Cryosphere*. *Climate Change 2013: The Physical Science Basis. Contribution of Working Group I to the Fifth Assessment Report of the Intergovernmental Panel on Climate Change*, Cambridge, United Kingdom and New York.

Vernet, M., Matrai, P. a. & Andreassen, I. (1998) Synthesis of particulate and extracellular carbon by phytoplankton at the marginal ice zone in the Barents Sea. *Journal of Geophysical Research*, **103**, 1023.

Viechtbauer, W. (2010) Conducting Meta-Analyses in R with the metafor Package. *Journal of Statistical Software*, **36**, 1–16.

Wang, M. & Overland, J.E. (2009) A sea ice free summer Arctic within 30 years ? **36**, 2–6.

Wanninkhof, R. & McGillis, W.R. (1999) A cubic relationship between air-sea CO_2 exchange and wind speed. *Geophysical Research Letters*, **26**, 1889–1892.

Wassmann, P. (2011) Arctic marine ecosystems in an era of rapid climate change. *Progress in Oceanography*, **90**, 1–17.

Wassmann, P., Ratkova, T., Andreassen, I., Vernet, M., Pedersen, G. & Rey, F. (1999) Spring bloom development in the marginal ice zone and the central Barents Sea. *Marine Ecology*, **20**, 321–346.

Wassmann, P.F. (2008) *Impacts of Global Warming on Polar Ecosystems*. *Impacts of Global Warming on Polar Ecosystems* (ed. by C.M. Duarte), pp. 111–138. Fundación BBVA.

Weiss, R.F. (1974) Carbon dioxide in water and seawater: the solubility of a non-ideal gas. *Marine chemistry*, **2**, 203–215.

Wilce, R.T. & Dunton, K.H. (2014) The boulder Patch (North Alaska, Beaufort Sea) and its benthic algal flora. *Arctic*, **67**, 43–56.

Williams, P.J.B., Raine, R.C.T. & Bryan, J.R. (1979) Agreement between the ^{14}C and oxygen methods of measuring phytoplankton production: reassessment of the photosynthetic quotient. *Oceanologica Acta*, **2**, 411–416.

Winkler, L.S. (1988) The determination of dissolved oxygen. *Ber. Dtsche. Chem. Ges.*, **21**, 2843–2855.

Wolf-Gladrow, D. a., Zeebe, R.E., Klaas, C., Körtzinger, A. & Dickson, A.G. (2007) Total alkalinity: The explicit conservative expression and its application to biogeochemical processes. *Marine Chemistry*, **106**, 287–300.

Wolf-Gladrow, D., Riebesell, U., Burkhardt, S. & Bijma, J. (1999) Direct effects of CO_2 concentration on growth and isotopic composition of marine plankton. *Tellus*, **51**, 461–476.

Woodward, F.I. (2007) Global primary production. *Current Biology*, **17**, R269–R273.

Wulff, A., Iken, K., Quartino, M.L., Al-Handal, A., Wiencke, C. & Clayton, M.N. (2009) Biodiversity, biogeography and zonation of marine benthic micro- and macroalgae in the Arctic and Antarctic. *Botanica Marina*, **52**, 491–507.

Xu, Y., Shi, D., Aristilde, L. & Morel, F. (2012) The effect of pH on the uptake of zinc and cadmium in marine phytoplankton: Possible role of weak complexes. *Limnology and Oceanography*, **57**, 293–304.

Xu, Z., Zou, D. & Gao, K. (2010) Effects of elevated CO_2 and phosphorus supply on growth, photosynthesis and nutrient uptake in the marine macroalga *Gracilaria lemaneiformis* (Rhodophyta). *Botanica Marina*, **53**, 123–129.

Yasunaka, S., Murata, A., Watanabe, E., Chierici, M., Fransson, A., van Heuven, S., Hoppema, M., Ishii, M., Johannessen, T., Kosugi, N., Lauvset, S.K., Mathis, J.T., Nishino, S., Omar, A.M., Olsen, A., Sasano, D., Takahashi, T. & Wanninkhof, R. (2016) Mapping of the air-sea CO_2 flux in the Arctic Ocean and its adjacent seas: Basin-wide distribution and seasonal to interannual variability. *Polar Science*, **10**, 323–334.

Yun, M.S., Whitledge, T.E., Stockwell, D., Son, S.H., Lee, J.H., Park, J.W., Lee, D.B., Park, J. & Lee, S.H. (2016) Primary production in the Chukchi Sea with potential effects of freshwater content. *Biogeosciences*, **13**, 737–749.

Zeebe, R.E. (2012) History of Seawater Carbonate Chemistry, Atmospheric CO_2, and Ocean Acidification Richard. *Annual Review of Earth and Planetary Sciences*, **40**, 141–165.

Zou, D. & Gao, K. (2009) Effects of elevated CO_2 on the red seaweed *Gracilaria lemaneiformis* (Gigartinales, Rhodophyta) grown at different irradiance levels. *Phycologia*, **48**, 510–517.

Zou, D., Gao, K. & Luo, H. (2011) Short- and long-term effects of elevated CO_2 on photosynthesis and respiration in the marine macroalga *Hizikia Fusiformis* (Sargassaceae, Phaeophyta) grown at low and high N supplies. *Journal of Phycology*, **47**, 87–97.

8. List of manuscripts

Submitted

Sanz-Martín, M., Vernet, M., Mesa, E., Cape, M., Delgado-Huertas, A., Reigstad, M., Wassmann, P.F., and Duarte, C. M. Multi-method assessment of primary production at the NW Svalbard shelf in the Arctic Ocean. *Submitted to Marine Ecology Progress Series.* Included in the thesis as Results 4.1

Sanz-Martín, M., Chierici, M., Mesa, E., Carrillo-de-Albornoz, P., Delgado-Huertas, A., Agustí, S., Reigstad, M., Kristiansen, S., Wassmann, P.F., and Duarte, C. M. Episodic Arctic CO_2 limitation at the W Svalbard shelf. *Submitted to Frontiers in Marine Sciences.* Included in the thesis as Results 4.2

Sanz-Martín, M., Hendriks, I. E., Carstensen, J., Marbà, N., Krause-Jensen, D., Sejr, M. and Duarte, C. M. Continuous daylight stimulates the photosynthetic response of sub-Arctic macrophytes with CO_2 supply. *Submitted to Aquatic Botany*. Included in the thesis as Results 4.3

In preparation

Sanz-Martín, M., Meire, L., Sejr M. K., Agustí, S., Juul-Pedersen, T., and Duarte, C.M. CO_2 limits Arctic spring bloom. *It will be submitted to Nature Geosciences*. Included in the thesis as Results 4.4

Published

Mesa, E., Delgado-Huertas, A., Carrillo-De-Albornoz, P., García-Corral, L. S., **Sanz-Martín, M**., Wassmann, P., Reigstad, M., Sejr, M., Dalsgaard, T. and Duarte, C. M.: Continuous daylight in the high-Arctic summer supports high plankton respiration rates compared to those supported in the dark, *Scientific Reports*, 1(1), 1–8, doi:10.1038/s41598-017-01203-7, 2017.

Sanz-Martín, M., Pitt, K. A., Condon, R. H., Lucas, C. H., Novaes de Santana, C. and Duarte, C. M.: Flawed citation practices facilitate the unsubstantiated perception of a global trend toward increased jellyfish blooms, *Global Ecology and Biogeography*, 25(9), 1039–1049, doi:10.1111/geb.12474, 2016.

Krause-Jensen, D., Marbà, N., **Sanz-Martín, M.,** Hendriks, I. E., Thyrring, J., Carstensen, J., Sejr, M. K. and Duarte, C. M.: Long photoperiods sustain high pH in Arctic kelp forests, *Science Advances*, 2, 1–8, doi:10.1126/sciadv.1501938, 2016.

Holding, J. M., Duarte, C. M., **Sanz-Martín, M.**, Mesa, E., Arrieta, J. M., Chierici, M., Hendriks, I. E., García-Corral, L. S., Regaudie-de-Gioux, A., Delgado, A., Reigstad, M., Wassmann, P. and Agustí, S.: Temperature dependence of CO_2-enhanced primary production in the European Arctic Ocean, *Nature Climate Change*, August, 8–11, doi:10.1038/nclimate2768, 2015.

Cózar, A., **Sanz-Martín, M**., Martí, E., González-Gordillo, J. I., Ubeda, B., Gálvez, J. Á., Irigoien, X. and Duarte, C. M.: Plastic Accumulation in the Mediterranean Sea, *PloS One*, 10, e0121762, doi:10.1371/journal.pone.0121762, 2015.

9. Lists of symbols, figures, tables and images

List of symbols and abbreviations

α: photosynthetic efficiency

°K: degrees Kelvin

°C: degrees Celsius

^{14}C-DOC: incorporation of inorganic carbon into dissolved organic carbon

^{14}C-POC: incorporation of inorganic carbon into particulate organic carbon

^{14}C-TOC: incorporation of inorganic carbon into total organic carbon

^{14}C, ^{13}C: 14 and 13-carbon isotope respectively

^{18}O: 18-oxygen isotope

ACIA: Arctic Climate Impact Assessment

ANOVA: analysis of variance

ASE: air-sea exchange

C: carbon

$CaCO_3$: calcium carbonate

CCMs: carbon concentrating mechanisms

CH_4: methane

Chl *a*: chlorophyll *a*

CO_2: carbon dioxide

CO_2^{-3}: carbonate

CR and R: community respiration

CSIC: Consejo Superior de Investigaciones Científicas

CTD: conductivity, temperature, and depth recorder

d: days

DCM: deep chlorophyll maximum layer

DIC: dissolved inorganic carbon

DOC: dissolved organic carbon

DPM: units of disintegration per minute

e.g.: *exempli gratia*, a Latin phrase meaning "for example"

EF: effect size

ETR: electron transport rate

F: statistic from F-test

g: grams

GHGs: greenhouse gases

GLMM: Generalized Linear Mixed Model

GLMs: Generalized Linear Models

GPP-^{18}O: gross photosynthetic production of ^{18}O from ^{18}O-labelled water additions

GPP-DO: gross primary production of dissolved oxygen

GPP: gross primary production

GPP_C: gross primary production in the control treatment

GPP_E: gross primary production in the experimental treatment

Gt: gigatons

h: hours

H_2O: water

HCO_3^-: bicarbonate

$HgCl_2$: mercury chloride

i.e.: *id est*, a Latin phrase meaning "that is" or "in other words"

Ik: saturating irradiance

IMEDEA: Instituto Mediterráneo de Estudios Avanzados

IPCC: Intergovernmental Panel on Climate Change

Kg: kilograms

Km: kilimeters

L: liters

LN: natural logarithm

m: meters

mg: miligrams

mL: millilitres

mm: millimeters

mmol: millimoles

mol: mol

N: nitrogen

N: North

n.d.: no data

n(N): number

N_2O: nitrous oxide

NCP: net community production

nM: nanoMolar

NO_2^-: nitrite

NO_3^-: nitrate

NOAA: National Oceanic and Atmospheric Administration, USA

NPP: net primary production

NW: Northwest

O_2: oxygen

p: p-value from statistical test

P: phosphorus

PAR: photosynthetically active radiation

pCO_2: partial pressure of carbon dioxide

PO_4^{3-}: phosphate

POC: particulate organic carbon

PP: primary production

ppm: parts per million

PQ: photosynthetic quotient

PS: photosystem

R/V: research vessel

R^2: coefficient of determination

$rETR_{max}$: maximum relative electron transport rate

RLCS: rapid light curves

RMA: Reduced Major Axis

Rubisco: enzyme ribulosa-1, 5-biphosphate carboxylase/oxygenase

SD: standard deviation

SE: standard error

Si: silicon

SiO_4^{4-}: silicate

SST: sea surface temperature

TA: total alkalinity

TOC: total organic carbon

UB: University of Barcelona

UNIS: University Center in Svalbard

UV: Ultraviolet

UVA/B: Ultraviolet A and B

V-SMOW: Vienna Standard Mean Ocean Water

W: West

WSC: West Spitsbergen Current

Yr: years

$\delta^{13}C$: delta notation for quantifying the ratio of the 13-carbon isotope to 12-carbon

µatm: micro atmospheres

µg: micrograms

µL: microliters

µM: micromolar

µmol: micromoles

List of figures

List of tables

List of images

10. Appendices

Appendices of Results 4.2

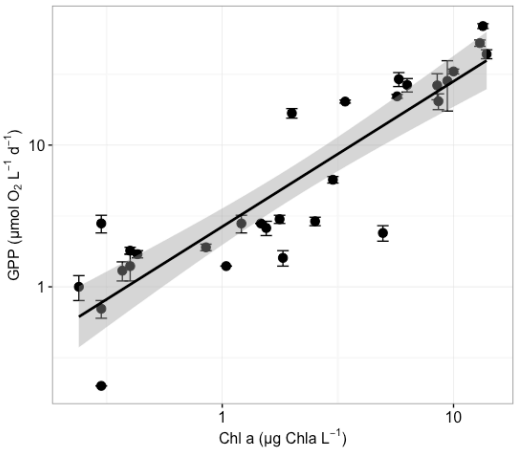

Figure A1: a) Relationship between log-log transformed gross primary production as the change in dissolved O_2 (GPP-O_2) (mean ± SE) and Chlorophyll a concentration (Chl *a*) at different depths ($p < 0.0001$, $R^2 = 0.86$, df = 35); The grey shadow represents the confidence interval.

Table A1: pCO_2 and CO_2 concentration at which the plankton communities of the Control and treatments of every experiments, as well as CO_2 removal rates, GPP response and the standard errors (SE), the averaged change in GPP, the Ln effect size of GPP (LN ES GPP ± SE) and the averaged Ln effect size of GPP from each experiment.

Experiment	CO_2 Treatment	pCO_2 µatm	CO_2 umol L^{-1}	CO_2 removal umol L^{-1} d^{-1}	GPP ± SE µmolO_2 L^{-1} d^{-1}	Avg. GPP change with %	Ln Effect Size GPP ± SE µmolO_2 L^{-1} d^{-1}	Avg. LN ES GPP µmolO2 L-1 d-1
	Control - *in situ*	142.5	9.3	-0.1	6.2 ± 0.1			
	Treatment 1	225.1	14.7	1	13.1 ± 0.5		0.7 ± 0.0	
May2014-1	Treatment 2	341.3	22.2	1.3	10.2 ± 0.8	72.2	0.5 ± 0.0	0.5
	Treatment 3	570.1	37.1	3.6	6.8 ± 0.6		0.1 ± 0.0	
	Treatment 4	1096.5	71.4	6	12.6 ± 1.2		0.7 ± 0.0	
	Control - *in situ*	127.9	8.5	0.2	5.8 ± 0.6			
	Treatment 1	178.5	11.8	0.6	5.5 ± 0.1		-0.1 ± 0.1	
May2014-2	Treatment 2	255.7	16.9	1	3.9 ± 0.1	-33.2	-0.4 ± 0.1	-0.5
	Treatment 3	460.0	30.4	6.3	4.0 ± 0.4		-0.6 ± 0.1	
	Treatment 4	680.8	45.0	4.4	2.5 ± 0.1		-0.8 ± 0.1	
	Control - *in situ*	281.2	13.6	2.3	1.4 ± 0.1			
	Treatment 1	319.1	15.5	-0.5	0.1 ± 0.1		-2.2 ± 0.1	
Aug2014-1	Treatment 2	454.1	22.0	2.3	0.5 ± 0.1	-75.0	-1.1 ± 0.1	-1.5
	Treatment 3	556.7	27.0	4.2	0.2 ± 0.1		-1.9 ± 0.2	
	Treatment 4	615.9	29.9	1	0.6 ± 0.1		-0.9 ± 0.1	
	Control - *in situ*	170.8	11.1	-0.1	0.4 ± 0.0			
	Treatment 1	223.9	14.5	-0.1	0.3 ± 0.0		-0.1 ± 0.1	
Aug2014-2	Treatment 2	300.5	19.5	0.9	0.2 ± 0.0	-33.3	-0.3 ± 0.1	-0.1
	Treatment 3	416.0	27.0	0.4	0.3 ± 0.0		-0.2 ± 0.1	
	Treatment 4	637.7	41.4	2.6	0.4 ± 0.0		0.1 ± 0.1	
	Control - *in situ*	185.7	11.9	0.6	0.8 ± 0.1			
	Treatment 1	243.3	15.6	0.1	0.6 ± 0.0		-0.3 ± 0.1	
Aug2014-3	Treatment 2	353.1	22.6	0.9	0.5 ± 0.1	-58.3	-0.5 ± 0.1	-0.6
	Treatment 3	463.1	29.7	-3	0.4 ± 0.0		-0.6 ± 0.1	
	Treatment 4	732.1	46.9	4.2	0.3 ± 0.0		-1.0 ± 0.1	
	Control - *in situ*	167.5	11.0	2.1	46.0 ± 6.0			
May2015-1	Treatment 1	247.8	16.2	4	61.3 ± 1.8	32.3	0.3 ± 0.1	0.3
	Treatment 2	341.7	22.4	5.4	60.4 ± 5.5		0.3 ± 0.1	
	Control - *in situ*	192.5	12.8	2	82.4 ± 11.4			
May2015-2	Treatment 1	233.5	15.5	3.5	79.3 ± 6.5	31.9	0.0 ± 0.1	0.2
	Treatment 2	273.5	18.1	3.6	138.1 ± 17.3		0.5 ± 0.1	

Appendices of Results 4.3

Table A2: *In situ* conditions at 5 m depth and results of the CO_2 supply experiments

Experiment	Date	Daylight (h)	Chl *a* (µg L^{-1})	Pytoplankton abundance (cell L^{-1})	$NO_2 + NO_3$ (µmol L^{-1})	PO_4 (µmol L^{-1})	SiO_4 (µmol L^{-1})	Air-sea exchange (µmol C m^{-2} d^{-1})	CO_2 Treatment	pCO_2 (ppm)	NCP ± SE (µmol O_2 L^{-1} d^{-1})	DIC removal ± SE (µmol C L^{-1} d^{-1})
									Control	370	0.7 ± 0.3	nd
A	29/2/16	9.50	0.05	420	nd	nd	nd		Level 1	661	0.1 ± 0.5	nd
									Level 2	813	-0.1 ± 0.2	nd
									Control	378	2.2 ± 0.6	25.2 ± 13.7
B	7/3/16	10.25	0.04	180	10.4	0.8	5.7	-1178.4	Level 1	529	2.1 ± 0.8	9.4 ± 0.8
									Level 2	743	-0.1 ± 0.7	-6.4 ± 1.4
									Control	365	-0.6 ± 0.5	65.2 ± 3.9
C	14/3/16	12.00	0.11	360	10.4	0.8	5.8	-5314.0	Level 1	622	0 ± 0.2	6.0 ± 3.2
									Level 2	749	-0.4 ± 0.4	-61.3 ± 6.1
									Control	365	2.3 ± 0.6	-1.2 ± 6.7
D	21/3/16	12.75	0.06	80	10.4	0.8	6.2	-4352.3	Level 1	645	1.9 ± 1	9.6 ± 3.0
									Level 2	841	1.3 ± 0.7	3.2 ± 1.8
									Control	364	1.4 ± 0.3	0.9 ± 3.2
E	29/3/16	13.50	0.13	380	10.3	0.8	6.1	-117.3	Level 1	562	-5.4 ± 0.3	5.6 ± 1.7
									Level 2	822	0.8 ± 0.3	5.7 ± 3.4
									Control	355	1.5 ± 0.3	nd
F	4/4/16	14.25	0.22	220	10.2	0.8	6.2	-16334.9	Level 1	503	0.4 ± 0.2	62.7 ± 8.5
									Level 2	729	0.3 ± 0.4	-52.1 ± 2.5
									Control	370	3.5 ± 0.4	-11.7 ± 1.5
G	18/4/16	15.75	0.17	760	9.5	0.8	6	-943.9	Level 1	479	1.5 ± 0.6	-10.1 ± 2.1
									Level 2	844	1.8 ± 0.2	1.3 ± 1.4
									Control	383	6.3 ± 1	1.5 ± 3.4
H	25/4/16	16.50	0.28	500	9.6	0.8	6	-1934.3	Level 1	524	4 ± 0.8	-4.2 ± 4.0
									Level 2	915	2.6 ± 1.4	-6.9 ± 4.4
									Control	303	38.8 ± 1	-30.8 ± 0.7
I	2/5/16	17.25	6.49	279940	2.5	0.3	3.7	-5160.7	Level 1	451	38.5 ± 0.7	-42.6 ± 5.9
									Level 2	944	38.8 ± 1.1	-29.8 ± 1.9
									Control	190	19.4 ± 1.7	-24.3 ± 4.1
J	9/5/16	18.00	4.09	162803	5.6	0.5	4	-147740.6	Level 1	451	21.9 ± 2.4	-20.0 ± 1.5
									Level 2	944	29.5 ± 2.1	-22.9 ± 2.9
									Control	191	16.2 ± 0.8	-11.1 ± 1.3
K	13/5/16	18.75	5.05	207356	0.3	0	1	-6546.8	Level 1	594	19 ± 0.6	-20.9 ± 6.2
									Level 2	747	18 ± 0.5	-16.9 ± 4.6
									Control	177	-5.9 ± 0.7	4.1 ± 5.5
L	17/5/16	19.5	1.50	98016	0.1	0	1.2	-19736.0	Level 1	400	-6 ± 0.4	-1.8 ± 3.6
									Level 2	700	4.5 ± 1	-10.8 ± 8.0
									Control	244	16.6 ± 0.7	-19.5 ± 5.9
M	23/5/16	20.25	2.87	34700	2.1	0.2	2.2	-7339.1	Level 1	605	3.3 ± 1	65.4 ± 24.6
									Level 2	985	14.2 ± 0.2	12.0 ± 8.4
									Control	262	20.6 ± 0.7	-15.2 ± 9.0
N	27/5/16	21	2.76	40060	1.9	0.2	2.3	-1415.0	Level 1	606	14.3 ± 0.4	-21.3 ± 1.4
									Level 2	903	10.7 ± 0.9	-11.5 ± 1.0

Appendices of Results 4.4

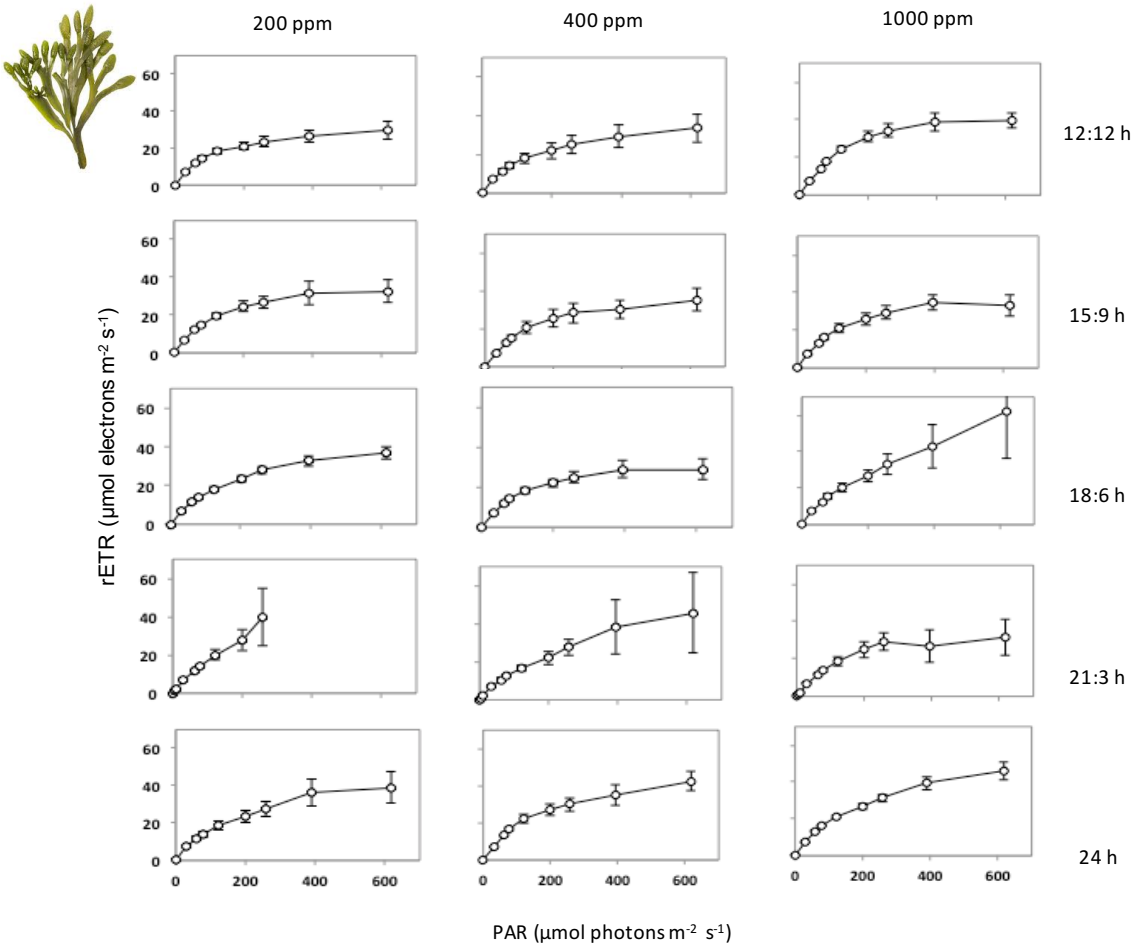

Figure A2: Rapid light curves (RLCs) on *A. nodosum* at different photoperiods and pCO_2 treatment (n = 4). The photosynthetic parameters were obtained by fitting the non-linear model of Eq. 6 to the RLCs.

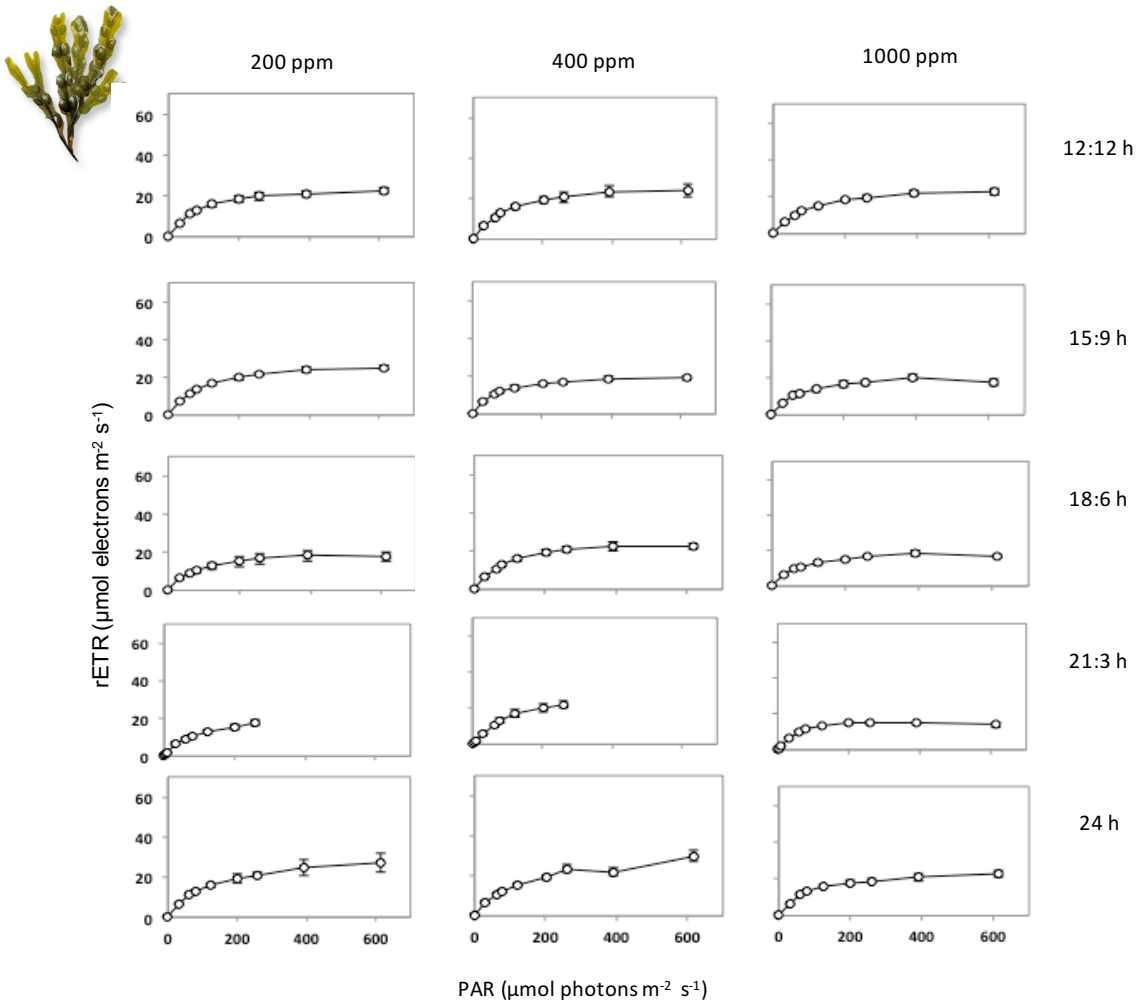

Figure A3: Rapid light curves (RLC) on *F. vesiculosus* at different photoperiods and pCO_2 treatment (n = 4). The photosynthetic parameters were obtained by fitting the non-linear model of Eq. 6 to the RLCs.

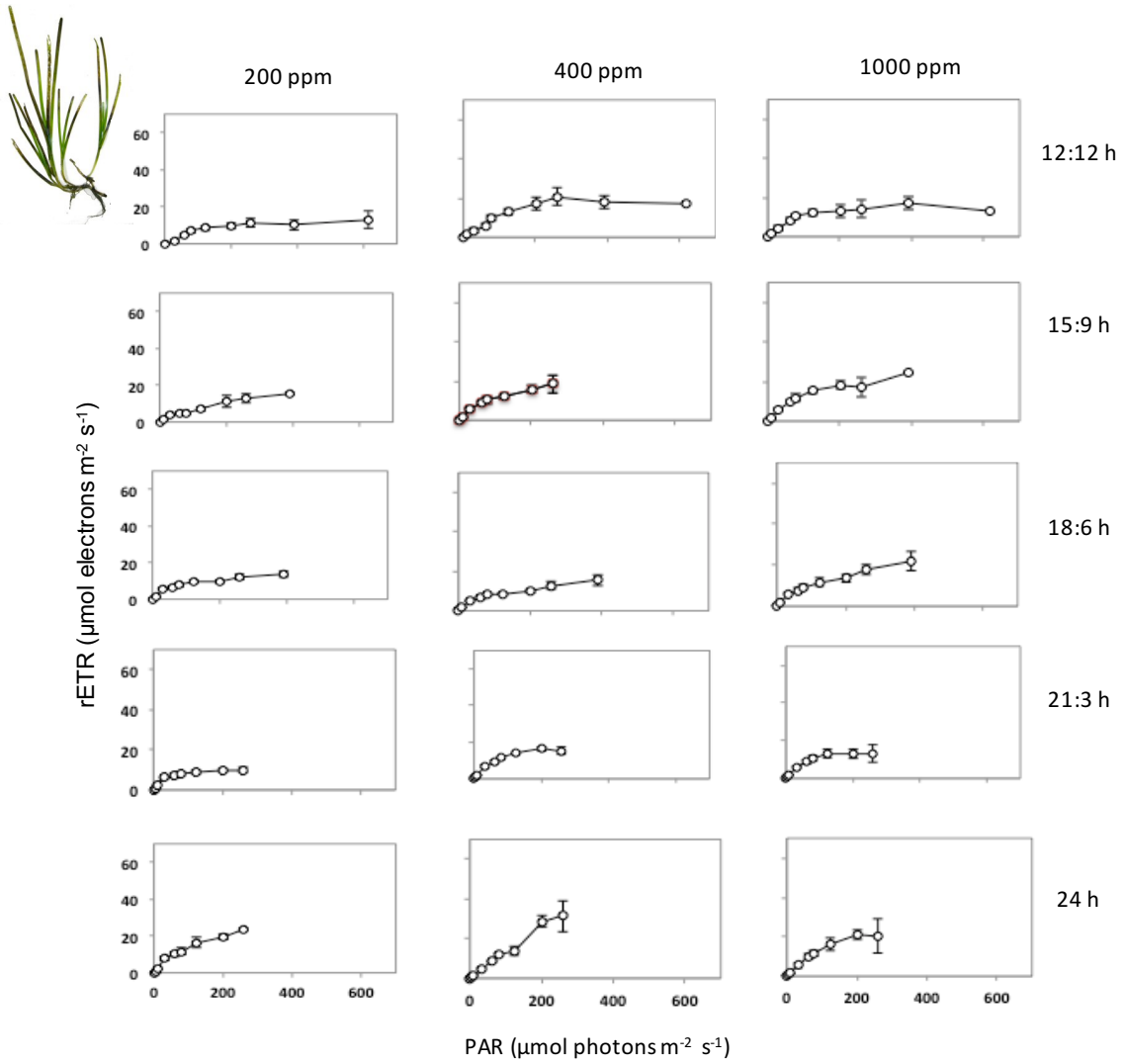

Figure A4: Rapid light curves (RLC) on *Z. marina* at different photoperiods and pCO_2 treatment (n = 4). The photosynthetic parameters were obtained by fitting the non-linear model of Eq. 6 to the RLCs.

Acknowledgements - Agradecimientos

I thank Fundación La Caixa for granting my Ph. D. thesis and the contribution of the Carbon Bridge (RCN-226415) project funded by the Norwegian Research Council to Results 4.1 & 4.2, the 'Efecte del canvi global sobre els ecosistemes marins' project funded by the University of Balearic Islands to Results 4.3, and the Danish Environmental Protection Agency within the Danish Cooperation for Environment in the Arctic program to Results 4.4. I would like also thank the King Abdullah University of Science and Technology for funding my visits.

I would like to thank my thesis director, Carlos M. Duarte, for the time he has dedicated to my thesis, with a more than tight agenda, for the corrections and the advices, for the many challenges I faced. Thanks Carlos for redirecting me when I needed, and for giving me the tools to become more critical. Thanks for giving me the great opportunity to travel and collaborate with very good researchers from all the world. Thanks also for facilitating my life in KAUST, it meant a lot for me. Thanks to my co-director Paul F. Wassmann, from The Arctic University of Norway, in Tromsø for his honesty and wise advices. Thanks to my tutor of the University of Barcelona, Miquel Canals, for commenting my proposals and helpful advices and the Follow-up Commission of University of Barcelona for their positive reports. Thanks to Núria Marbà for her time. Thanks also to all my co-authors for their contributions, thanks to Maria Vernet & Mattias Cape for their encouraging words and always be willing to contribute positively, thanks to Marit Reigstad & Mikael Sejr for being always kind.

I would like to greatly thank the accompaniment of my colleague and friend Johnna Holding during this travel. Thanks for your support, for your advices, for all your time, for your patience, for your corrections & comments, for always being there to discuss. Thanks for appreciating my curiosity. Your confidence made me strong. Iris Hendriks and Aurore Regaudie-de-Gioux, thank you for your altruistic help. Thanks for your time, for solving my doubts, for our discussions, for your advices. Thanks for helping me to find the alternative ways. I really appreciate your presence. Ana Payo, thanks for your constant pragmatism and for always giving me your best advices to finish this project.

I thank the presence of the people of the Carbon Bridge project, my cruise mates and friends Maria and Achim, Maria thanks for your cuddles and Achim for making every day easier on board. Marit, Lena, Birgit & Elisabeth, thanks for such a great organization, Geràld Darnis thanks for saving me in the cold and dark Polar night. Paloma, I really learnt a lot from you. I'm better in the lab thanks to your help. Thank you so much for being there as a colleague and a friend. Samal, thanks for your help on board and your smiles. Max, thanks for our time in Longyearbyen and Mallorca. From Nuuk, I would like specially thank the Biologist station people, who

cooked and feed me every night I arrived late at home: Andreas, Wieter & Isabeau. Lorenz, thanks for all your help at the Natur Institute. Fernando, thanks for making me feel at home, for your support, for your love. Many thanks to the people from KAUST, Paloma, Neus, Rubén, María, Verónica, Juan, Ima for taking me in there and share your time with me, for the trips and all the fun; thanks to Carlos and Susana for take us to dinner coral fishes in nice and interesting places.

I spent many hours in IMEDEA working on data. I would like to thank Amparo Lázaro, Gema Escribano, Raquel Vaquer, Ana P. and Carlos Díaz for the time they spent solving my doubts in R. Germán Martín, for being there when I needed stats discussions. Thanks to Paqui García and Angel López-Urrutia for their plotting help. Luis Cayuela for his valuable stats notes. Thanks to the Green Team, for making my lunch breaks easy and fun: Guillem, Eva, Fra, Eugenio, thanks to my beloved Julia for understanding my silence needs and for your friendship, David thanks for the Catalan lessons. Thanks to whom has already gone but were there when I needed: Inés and Eviña. Thanks Celia for being still there, far but there. Thanks Noe for being part of my life. Thanks Marc, Albert, Paula, Josep, Ana, Noe & Jaume for being part of my life, I still want you close. Gema & Carlos thanks for your supporting advices. And thanks to all those IMEDEICOS for time we spent in the Ágora: Fran, Edu, Sara, Javi, Juanma, Chema, Julia; Ana Sanz for being always kind; Ramona, Cati and Inés for keeping our lives full of smiles; and thanks to the IT department for their help.

My people from Barcelona, Paulo for your encouragement since we met, Lali thanks for your love and cares, for keeping me fit and well fed, for taking care of me despite the distance. And Virgi, thanks for your charm. Llanos, thanks for being always there, I do not imagine my life without you. Lucas, thanks for living outside of the box. My beloved girls Ana O. and Ana P., thanks for this new life. I love to share my life with you. Thanks to Juana & Tiza, Jaume and Mary, with whom my life was always better. Gracias a Olga, gràcies Uri, por ser un soplo de aire fresco en esta última etapa. A la gent del Jardí d'Epicur, perque la lluita continua. A Laura, porque enseñarme que otra vida también es posible. Gracias a mis amig*s de Albacete, Carlos, Ángela, Kike, Paco, Elena y Teté; a mis chicas Gaby, Rosa y Cris; a mi gran familia de Albacete, y también a la Cuenca: gracias por vuestro constante apoyo y vuestro esfuerzo por mantenernos unid*s. A mi Abuelita Encarnita por seguir en su línea y quererme tanto, a mi Abuela Maruchy por su alegría y sus ganas de viajar, porque su independencia ha sido siempre un ejemplo. A mi hermano Guille, gracias por tu apoyo, por quererme en las buenas y en las malas, nos echo de menos. Gracias Mamá y Papa, por vuestra permanente confianza y por todo vuestro cariño, por hacerme sentir querida y valorada a pesar de las pequeñas diferencias ¡y gracias también por el apoyo económico cuando ha sido necesario!

Esporles, 13 de Noviembre de 2017 Marina

Re-thinking my refs

Let me tell you a story about the authors I have cited within this thesis. During these years, I have read many articles and I have cited the work of researchers that I did not personally meet such as Grande, Hein, Bakker, Le-Quéré, Yasunaka and Wulff, among others. One day, I realized the surname Grande was accompained by the name of Karen, and Hein, by the name of Mette. That surprised me. I was upset. In spite of having worked and collaborated with many great women scientists, my unbconcious mind was still full of male scientists.

I made small numbers with the help of Francesca. And I found the answer. Researchers identified as women are only 23% of the first-authors cited in my dissertation, while citations to researchers identified as men reach 70%, and 7% are indeterminate or not identified. Unfortunately, the leaky pipeline in academia is more than evident in our lives and in our numbers.

I am grateful for the presence and the work of the women in science. Thanks to Karen Grande, Mette Hein, Anja Engel, Elena García-Martín, Corinne Le Quéré, Dorothee Bakker, Jacqueline Grebmeier, Sayaka Yasunaka, Marguerite Koch, Kristine Arendt, Helene Hodal, Elena Mesa, Francisca García, Ingrid Ellingsen, Clara Hoppe, Concepción Íñiguez, Agnetta Fransson, Angela Wulff, Susana Agustí, Ireneusz Florczyk, Alexia Coello-Camba, Melissa Chiericci, Cristina Sobrino, Maria L. Paulsen, Merit Reigstad, Maria Vernet, Patti Matrai, Raquel Vaquer-Sunyer, Lena Seuthe, Lara García-Corral, Mar Fernández-Méndez, Aurore Regaudie-de-Gioux, Dorte Krause-Jensen, Mary-Lynn Dickson, Iris Hendriks, Johnna Holding and Núria Marbà. Thanks for staying here despite all the hardships and being part of my References. Thanks to you I know that there is place for women in STEM, even though the way is hard.

Repensando mis referencias

Dejadme que os cuente una historia sobre las referencias en las que he basado mi trabajo. Durante estos años he leído muchos artículos y he citado estudios de personas que no conocía, como Grande, Hein, Bakker, Le-Quéré, Yasunaka, Wulff y entre otros. Un día me dí cuenta de que el apellido Grande iba acompañado del nombre de Karen, y Hein iba precedido de Mette. Aquello me sorpendió. Estaba enfadada. A pesar de haber trabajado con un montón de grandes científicas, mi imaginario seguía lleno de científicos.

Hice unos pequeños cálculos con la ayuda de Francesca. Y hallé la respuesta. Solo el 23% de los primeros autores son investigadoras identificadas como mujeres, mientras que las citas a investigadores identificados como hombres asciencende al 70% junto con un 7% de referencias indeterminadas o no identificables. Tristemente la falta de mujeres en ciencia sigue siendo más que evidente, en nuestras vidas y en nuestros números.

Quiero agradecer expresamente la presencia y el trabajo de las mujeres en ciencia. Gracias a Karen Grande, Mette Hein, Anja Engel, Elena García-Martín, Corinne Le Quéré, Dorothee Bakker, Jacqueline Grebmeier, Sayaka Yasunaka, Marguerite Koch, Kristine Arendt, Helene Hodal, Elena Mesa, Francisca García, Ingrid Ellingsen, Clara Hoppe, Concepción Íñiguez, Agnetta Fransson, Angela Wulff, Susana Agustí, Ireneusz Florczyk, Alexia Coello-Camba, Melissa Chiericci, Cristina Sobrino, Maria L. Paulsen, Merit Reigstad, Maria Vernet, Patti Matrai, Raquel Vaquer-Sunyer, Lena Seuthe, Lara García-Corral, Mar Fernández-Méndez, Aurore Regaudie-de-Gioux, Dorte Krause-Jensen, Mary-Lynn Dickson, Iris Hendriks, Johnna Holding y Núria Marbà. Gracias por seguir ahí a pesar de todo y dar luz a mis referencias. Gracias a vosotras sé que hay un lugar en la ciencia para las mujeres, aunque el camino sea duro.